

# **The interplay between thylakoid biogenesis and plastid vesicle transport in *Arabidopsis thaliana***

Dissertation der Fakultät für Biologie  
der Ludwig-Maximilians-Universität München

vorgelegt von  
**Annabel Mechela**

München, 2021

**“The greatest obstacle to discovery is not ignorance - it is the illusion of knowledge.”**

**Prof. Dr. Stephen Hawking**

Diese Dissertation wurde unter der Leitung von Prof. Dr. Jürgen Soll und PD Dr. Serena Schwenkert an der Fakultät für Biologie der Ludwig-Maximilians-Universität München angefertigt.

Erstgutachter: Prof. Dr. Jürgen Soll

Zweitgutachter: Prof. Dr. Christof Osman

Tag der Abgabe: 23.03.2021

Tag der mündlichen Prüfung: 24.06.2021

### **Eidesstattliche Versicherung**

Ich versichere hiermit an Eides statt, dass meine Dissertation selbstständig und ohne unerlaubte Hilfsmittel angefertigt worden ist.

Die vorliegende Dissertation wurde weder ganz noch teilweise bei einer anderen Prüfungskommission vorgelegt. Ich habe noch zu keinem früheren Zeitpunkt versucht, eine Dissertation einzureichen oder an einer Doktorprüfung teilzunehmen.

Planegg-Martinsried, 17.07.2021

---

Annabel Mechela

## Table of contents

List of figures .....	IV
List of tables .....	V
Publications .....	VI
Summary .....	VII
Zusammenfassung.....	IX
Abbreviations .....	XI
1. Introduction .....	1
1.1 The thylakoid membrane: a very fascinating green network.....	1
1.1.1 Origins and structure of the thylakoid membrane .....	1
1.1.2 Chloroplast development and composition of the thylakoid membrane.....	3
1.1.3 The big mystery of thylakoid biogenesis.....	6
1.2 Plastid vesicle transport: the idea of green shuttles .....	8
1.2.1 The secretory pathway: vesicle transport in the cytosol .....	8
1.2.2 First experimental insights into chloroplast vesicle formation.....	10
1.2.3 Design of a working model for a plastid vesicle transport system .....	14
1.3 Putative new players in plastid vesicle transport.....	16
1.3.1 Putative vesicle transport SNARE-associated protein (SNARE AP) .....	16
1.3.2 Synaptotagmin- like protein 5.2 (SYTL5.2/AtNTMC2T5.2).....	16
1.3.3 Embryo defective 1303 (EMB1303) .....	17
1.3.4 Plastid nucleoid-associated protein of 45 kDa (ptNAP45) .....	18
1.4 Aims of this study .....	19
2. Material and Methods.....	21
2.1 Material .....	21
2.1.1 Chemicals, beads and membranes.....	21
2.1.2 Enzymes and Kits.....	21
2.1.3 Molecular weight site marker and DNA standard.....	21
2.1.4 Plant material .....	22
2.1.5 Bacterial strains.....	22
2.1.6 Accession numbers.....	22
2.1.7 Vectors and clones .....	24
2.1.8 Oligonucleotides.....	25
2.1.9 Antisera .....	28
2.1.10 Computational analysis and software.....	28

2.2	Plant methods .....	29
2.2.1	Growth conditions for <i>Arabidopsis thaliana</i> , <i>Nicotiana benthamiana</i> and <i>Pisum sativum</i> .....	29
2.2.2	Isolation of genomic DNA from <i>Arabidopsis thaliana</i> .....	29
2.2.3	RNA extraction from <i>Arabidopsis thaliana</i> leaves .....	30
2.2.4	RNA extraction from <i>Arabidopsis thaliana</i> seeds .....	30
2.2.5	<i>Agrobacterium</i> -mediated transient expression of fluorescent proteins in <i>Nicotiana benthamiana</i> .....	30
2.2.6	<i>Agrobacterium</i> -mediated stable expression of fluorescent proteins in <i>Arabidopsis thaliana</i> .....	31
2.2.7	Greening and chlorophyll measurement .....	31
2.2.8	Confocal microscopy .....	31
2.2.9	Analysis of chloroplast ultrastructure .....	32
2.3	Molecular biological methods .....	32
2.3.1	Growth conditions for <i>Escherichia coli</i> and <i>Agrobacterium tumefaciens</i> .....	32
2.3.2	Cloning strategies .....	33
2.3.2.1	Traditional cloning by restriction enzyme digest and ligation .....	33
2.3.2.2	Gateway® Technology based cloning .....	33
2.3.2.3	Golden Gate® based cloning .....	33
2.3.3	Sequencing .....	33
2.3.4	Amplification of DNA fragments by Polymerase chain reaction .....	34
2.3.5	cDNA synthesis, RT-PCR and qPCR analysis .....	34
2.3.6	Transformation of <i>Escherichia coli</i> .....	34
2.3.7	Transformation of <i>Agrobacterium tumefaciens</i> .....	34
2.3.8	Purification of plasmid DNA from <i>Escherichia coli</i> .....	35
2.4	Biochemical methods .....	35
2.4.1	Overexpression of recombinant proteins in <i>Escherichia coli</i> .....	35
2.4.2	Mass spectrometry .....	35
2.4.3	Isolation of total proteins .....	35
2.4.4	Isolation of soluble and membrane proteins from leaves .....	35
2.4.5	Determination of protein content by Bradford .....	36
2.4.6	Chloroplast isolation from <i>Arabidopsis thaliana</i> .....	36
2.4.7	Isolation of plastid sub-compartments from <i>Arabidopsis thaliana</i> chloroplasts .....	36
2.4.8	Thylakoid membrane association .....	37
2.4.9	Chloroplast isolation from <i>Pisum sativum</i> .....	37
2.4.10	<i>In vitro</i> transcription and translation .....	37
2.4.11	<i>In vitro</i> import into chloroplasts of <i>Pisum sativum</i> .....	37

2.4.12	Detection of radiolabelled proteins .....	38
2.4.13	Isolation of plastid sub-compartments from <i>Pisum sativum</i> chloroplasts .....	38
2.4.14	Size exclusion chromatography (SEC) of native pea stroma .....	38
2.4.15	SDS-Polyacrylamide gel electrophoresis and immunoblotting.....	39
2.4.15.1	SDS-Polyacrylamide gel electrophoreses .....	39
2.4.15.2	2 <sup>nd</sup> dimension SDS-Polyacrylamide gel electrophoreses.....	39
2.4.15.3	Coomassie staining .....	39
2.4.15.4	Semi-dry western blot .....	39
2.4.15.5	Immunodetection.....	40
2.4.16	Blue native (BN) polyacrylamide gel electrophoresis .....	40
2.4.17	Northern blot .....	40
3.	Results .....	42
3.1	SNARE AP .....	42
3.2	SYTL5.2/AtNTMC2T5.2 .....	45
3.3	EMB1303 .....	47
3.4	ptNAP45.....	53
4.	Discussion.....	68
4.1	SNARE AP & SYTL5.2 .....	68
4.2	EMB1303 .....	69
4.3	ptNAP45.....	70
4.4	Now, what's the deal with plastid vesicles?.....	73
	Supplement .....	75
	References.....	76
	Acknowledgements .....	88

## List of figures

<b>Figure 1:</b> Thylakoid structure in cyanobacteria, green algae and land plants .....	2
<b>Figure 2:</b> Chloroplast ultrastructure and the three-dimensional network of the thylakoid membrane.	3
<b>Figure 3:</b> Chloroplast development from a proplastid towards a mature organelle .....	4
<b>Figure 4:</b> Model of three possible ways of thylakoid biogenesis in higher plants .....	7
<b>Figure 5:</b> Plastid vesicles occur in the stroma of young pea chloroplasts.....	10
<b>Figure 6:</b> Suggestion of processes contributing to thylakoid biogenesis in chloroplasts of land plants .....	15
<b>Figure 7:</b> Characterization of two <i>snare ap</i> T-DNA insertion lines.....	42
<b>Figure 8:</b> Complementation of a <i>snare ap</i> T-DNA insertion line .....	43
<b>Figure 9:</b> Chloroplast ultrastructure and greening of WT and <i>snare ap</i> mutant plants .....	44
<b>Figure 10:</b> Characterization of two <i>syt15.2</i> T-DNA insertion lines .....	45
<b>Figure 11:</b> Chloroplast ultrastructure and greening of WT and <i>syt15.2</i> mutant plants.....	46
<b>Figure 12:</b> Characterization and complementation of an <i>emb1303</i> T-DNA insertion line .....	47
<b>Figure 13:</b> Chloroplast ultrastructure of WT and <i>emb1303</i> mutant plants .....	49
<b>Figure 14:</b> Greening of WT and <i>emb1303</i> under continuous low light.....	50
<b>Figure 15:</b> <i>In vitro</i> import into chloroplasts and sub-localization of EMB1303. ....	50
<b>Figure 16:</b> Complex involvement of EMB1303 in the chloroplast inner envelope .....	52
<b>Figure 17:</b> ptNAP45 loss-of-function phenotype in <i>Arabidopsis thaliana</i> .....	53
<b>Figure 18:</b> Anthocyanin phenotype of <i>ptnap45</i> lines under stress conditions .....	54
<b>Figure 19:</b> Chloroplast ultrastructure of WT and <i>ptnap45</i> .....	55
<b>Figure 20:</b> Thylakoid composition in <i>ptnap45</i> RNAi lines .....	56
<b>Figure 21:</b> Chloroplast localization and developmental expression of ptNAP45.....	57
<b>Figure 22:</b> Nucleoid localization of ptNAP45 .....	58
<b>Figure 23:</b> Localisation of ptNAP45 without its transit peptide.....	59
<b>Figure 24:</b> Transcriptional defects in <i>ptnap45</i> .....	60
<b>Figure 25:</b> ptNAP45 is part of an RNA containing complex.....	62
<b>Figure 26:</b> Comparison of leaf variegation between <i>ptnap45</i> and <i>var2-5</i> .....	64
<b>Figure 27:</b> ptNAP45 is present in etiolated seedlings .....	65
<b>Figure 28:</b> Phylogenetic tree based on degrees of homology between protein sequences of ptNAP45 and ptNAP45-like from green algae to higher plants.....	66
<b>Figure 29:</b> Localisation of ptNAP45-like .....	67

## Supplement

<b>Figure S1:</b> <i>In vitro</i> import of ptNAP45 into chloroplasts .....	75
<b>Figure S2:</b> Translational defects in <i>ptnap45</i> .....	75

## List of tables

<b>Table 1:</b> Accession numbers of proteins and their respective species .....	22
<b>Table 2:</b> Clones with respective genes, vectors, sequence description, restriction sites and purpose.	24
<b>Table 3:</b> Oligonucleotides with their respective sequence and purpose.....	25
<b>Table 4:</b> Antibiotics used for selection with their respective concentrations .....	32

## Publications

**Parts of this study have been published in the following research articles:**

**Mechela, A., Schwenkert, S., & Soll, J.** (2019). A brief history of thylakoid biogenesis. *Royal Society Open Biology*, 9(1), 180237. <http://dx.doi.org/10.1098/rsob.180237>

© 2019 The Authors

Published by the Royal Society under the terms of the Creative Commons Attribution

The article is licensed under the Creative Commons Attribution 4.0 International license (<http://creativecommons.org/licenses/by/4.0/>), which permits unrestricted use, provided the original author and source are credited. Text passages (section 1.1 and 1.2) and figures therein have been reused for this thesis (Fig. 6) or were partially modified or rearranged (Fig. 1, 2, 3, 4, 5).

**Mechela, A., Espinoza-Corral, R., Szulc, B., Scheibenbogen, T., Seydel, Ch., Klingl, A., Soll, J. & Schwenkert, S.** (2021). Plastid nucleoid-associated protein 45 (ptNAP45) is essential for plastid translation and chloroplast biogenesis. *In preparation for resubmission*.

© 2021 The Authors

At the time of the final submission of this thesis, the manuscript of the paper was in preparation for resubmission. Text passages (section 1.3.4, 3.4, 4.3) and figures therein have been reused for this thesis (Fig. 17, 19, 20, 22, 25, 27, 28) or were partially modified or rearranged (Fig. 21, 24, Fig. S1, Fig. S2).

A.M. performed most of the experiments, analysed data, participated in designing experiments, generated figures and wrote the manuscripts including all text sections that were incorporated into this thesis in exact or almost exact wording. This is hereby confirmed on behalf of all co-authors.

The publisher's copyrights are protected by the fact that the present dissertation is an academic, non-commercial publication and the corresponding original articles are duly cited.

## Summary

The biogenesis of plant organelles is a highly regulated and dynamic process that is still poorly understood. In particular, the differentiation of proplastids to chloroplasts is an essential process, since it produces the energy production centres of the plant cell. Inside the chloroplast is the thylakoid membrane, a dynamic, adaptable and highly specialised biomembrane. Embedded in these are high-molecular weight protein complexes that allow photosynthesis. Over the past few decades, advances in molecular biology and biochemistry have made it possible to better understand the mechanisms of photosynthesis at the molecular level. However, it is not yet clear which factors are involved in the formation of the thylakoid membrane and how this process is initiated and regulated. Since both lipids and many plastid proteins are imported across the inner envelope membrane, it is reasonable to assume a connection between both membrane systems. Frequent observations of vesicular structures suggest that a vesicle transport system similar to that found in the endomembrane system of the cell is responsible.

In this work, several candidate proteins were investigated for a possible role in plastid vesicle transport. The first candidate, a putative SNARE-associated protein, is an evolutionarily conserved plastid protein whose bacterial homologs appear to play a role in membrane formation. It was found in a bioinformatics screen and may in theory assist SNARE proteins on the thylakoid membrane in the vesicle fusion process. SYTL5.2 belongs to the family of plant synaptotagmins. It is known from animal cells that these proteins induce membrane curvature and, with the help of their specific C2 domain, assist SNAREs in docking and fusion of incoming vesicles. A similar function would also be conceivable within the chloroplast. However, since plants lacking SNARE AP or SYTL5.2 did not show any phenotype under any conditions tested, nor did they exhibit altered chloroplasts, both proteins do not appear to be essential and were therefore not investigated further.

EMB1303 is a plastid protein that has been previously studied in relation to plant growth and chloroplast development. EMB1303 is essential for thylakoid membrane formation, as mutants not only exhibit an albino phenotype but also abnormally shaped chloroplasts lacking the typical thylakoid membrane structure. In addition, it was shown that EMB1303 is located in the inner envelope membrane of chloroplasts, where, however, it doesn't seem to be present in any complex. Based on its phenotype, structure and localisation, EMB1303 could be a SNARE protein in the chloroplast. However, this needs to be proven by further experiments.

ptNAP45 is a newly identified protein of unknown function that was found in fractions of very young chloroplasts and was thus considered a candidate for proteins involved in early chloroplast development. It was found that ptNAP45 is localised in the chloroplast stroma. Knockout of ptNAP45 resulted in a seedling lethal albino phenotype with severely disturbed chloroplast morphology without

proper thylakoid membranes. Furthermore, ptNAP45 was found to be associated with plastid nucleoids and additionally showed the same dynamic movement from the inner envelope in young chloroplasts towards the thylakoids in mature chloroplasts like nucleoids. It was also shown that ptNAP45 is essential for proper plastid ribosome accumulation and consequently translation. Strikingly, ptNAP45 was found in a high molecular weight RNase sensitive complex, co-migrating with 50S ribosome particles. Since ptNAP45 does not seem to be able to bind RNA by itself and rRNA maturation is not affected in the mutant, it can be concluded that ptNAP45 functions as an rRNA-independent plastid ribosome biogenesis factor. Taken together, ptNAP45 proved to be an essential protein for chloroplast development as well as thylakoid biogenesis, probably by promoting chloroplast ribosome assembly.

Although the deeper analysis of these four candidate proteins did not demonstrate direct involvement of these in a plastid vesicle transport system, two proteins essential for chloroplast development and thylakoid biogenesis were found. The precise molecular functions of the proteins described here require further research, as does the elucidation of vesicle transport in the chloroplast.

## Zusammenfassung

Die Biogenese pflanzlicher Organellen ist ein hochregulierter und dynamischer Prozess, der zum jetzigen Zeitpunkt noch unzureichend verstanden ist. Insbesondere die Ausdifferenzierung von Proplastiden zu Chloroplasten ist ein essentieller Vorgang, da dabei die Energieproduktionszentren der Pflanzenzelle entstehen. Die Umwandlung von Lichtenergie in chemische Energie ermöglicht nicht nur Pflanzen eine photoautotrophe Lebensweise, sondern dient durch die gekoppelte Produktion von Biomasse als Grundlage jeglicher weiteren Lebensformen. Innerhalb des Chloroplasten befindet sich die Thylakoidmembran, eine dynamische, anpassungsfähige und hochspezialisierte Biomembran. In diese eingebettet sind hochmolekulare Proteinkomplexe, welche die Photosynthese ermöglichen. Im Laufe der letzten Jahrzehnte ist es durch Fortschritte in der Molekularbiologie und Biochemie gelungen, die Mechanismen der Photosynthese auf molekularer Ebene immer besser zu verstehen. Jedoch ist bislang nicht klar, welche Faktoren an der Entstehung der Thylakoidmembran beteiligt sind und wie dieser Vorgang initiiert und reguliert wird. Da sowohl Lipide an der inneren Hüllmembran gebildet werden als auch die meisten plastidären Proteine über diese Membran in den Chloroplasten eintreten, ist eine Verbindung zwischen beiden Membransystemen naheliegend. Häufige Beobachtungen von vesikulären Strukturen legen die Vermutung nahe, dass ein Vesikeltransportsystem, ähnlich wie es im Endomembransystem der Zelle vorzufinden ist, dafür verantwortlich ist.

In dieser Arbeit wurden vier verschiedene Kandidatenproteine auf eine mögliche Rolle im plastidären Vesikeltransport hin untersucht. Diese Proteine sind SNARE AP, SYTL5.2, EMB1303 und ptNAP45. Das erste Kandidatenprotein, ein mögliches SNARE-assoziiertes Protein, ist ein evolutionär konserviertes Protein, dessen bakterielle Vertreter eine Rolle in der Formierung von Membranen zu spielen scheinen. Es wurde in einem bioinformatischen Screen gefunden und könnte in der Theorie SNARE Proteine auf der Thylakoidmembran beim Fusionsprozess der Vesikel unterstützen. SYTL5.2 gehört zur Familie pflanzlicher Synaptotagmine. Aus tierischen Zellen ist bekannt, dass diese Proteine die Krümmung von Membranen induzieren und mithilfe ihrer spezifischen C2 Domäne SNAREs beim Andocken und Fusionieren der ankommenden Vesikel unterstützen. Eine ähnliche Funktion wäre auch innerhalb des Chloroplasten denkbar. Da Pflanzen, denen SNARE AP oder SYTL5.2 fehlten, jedoch unter keiner der getesteten Bedingungen einen Phänotyp zeigten noch veränderte Chloroplasten aufwiesen, scheinen beide Proteine nicht essentiell zu sein und wurden daher nicht weitergehend untersucht.

EMB1303 ist ein plastidäres Protein, welches bereits in Bezug auf pflanzliches Wachstum und Chloroplastenentwicklung untersucht wurde. EMB1303 ist essentiell für die Bildung der Thylakoidmembran, da Mutanten nicht nur einen albinotischen Phänotyp, sondern auch abnormal geformte Chloroplasten ohne die typische Thylakoidmembranstruktur aufweisen. Zusätzlich konnte gezeigt werden, dass sich EMB1303 in der inneren Hüllmembran der Chloroplasten befindet, wo es

allerdings in keinem größeren Komplex vorkommt. Aufgrund seiner Struktur könnte EMB1303 ein SNARE Protein im Chloroplasten sein. Dies muss jedoch mittels weiterer Experimente bewiesen werden.

ptNAP45 ist ein bisher unbekanntes Protein, das in Fraktionen von sehr jungen Chloroplasten gefunden wurde und somit als Kandidat für Proteine, die an der frühen Chloroplastenentwicklung beteiligt sind, gilt. ptNAP45 befindet sich im Stroma des Chloroplasten. Der Knockout von ptNAP45 führte zu einem letalen Albino-Phänotyp des Keimlings mit stark gestörter Chloroplastenmorphologie ohne richtige Thylakoidmembranen. Darüber hinaus wurde festgestellt, dass ptNAP45 mit plastidären Nukleoiden assoziiert ist. Zusätzlich zeigte ptNAP45 die gleiche dynamische Bewegung von der inneren Hülle in jungen Chloroplasten in Richtung der Thylakoide in voll entwickelten Chloroplasten wie die Nukleoide. Weiterhin zeigte sich, dass ptNAP45 essentiell für die korrekte plastidäre Ribosomenassemblierung und damit für die Translation ist. Auffallend ist, dass ptNAP45 in einem hochmolekularen RNase-sensitiven Komplex gefunden wurde, der mit 50S-Ribosomen-Partikeln komigriert. Da ptNAP45 nicht in der Lage zu sein scheint, selbst RNA zu binden und die rRNA-Prozessierung in der Mutante nicht beeinträchtigt ist, kann gefolgert werden, dass ptNAP45 als ein rRNA-unabhängiger plastidärer Ribosomen-Biogenese-Faktor fungiert. Zusammengenommen erwies sich ptNAP45 als essentielles Protein für die Chloroplastenentwicklung sowie die Thylakoidbiogenese, wahrscheinlich durch dessen Funktion während der Assemblierung plastidärer Ribosomen.

Auch wenn durch die tieferegehende Analyse der vier Kandidatenproteine keine direkte Beteiligung dieser in einem plastidären Vesikeltransportsystem nachgewiesen werden konnte, so wurden doch zwei für die Chloroplastenentwicklung und Thylakoidbiogenese essentielle Proteine gefunden. Die genauen molekularen Funktionen der hier beschriebenen Proteine bedarf ebenso weiterer Forschung wie die Aufklärung des Vesikeltransportes im Chloroplasten.

## Abbreviations

aa	amino acid(s)
ADP/ ATP	Adenosine-5'-diphosphate/ triphosphate
APS	Ammonium persulfate
AS1	Asymmetric Leaves 1
ATPase	ATP synthase
BASTA®	Trade name of glufosinolate
bp	Base pairs
BSA	Bovine serum albumin
CBB	Coomassie-Brilliant-Blue
cDNA	Complementary DNA
CFP	Cyan fluorescent protein
Col-0	<i>Arabidopsis thaliana</i> ecotype Columbia
COP	Coat protein
cp	Chloroplast
C-terminus	Carboxy-terminus
Da	Dalton
ddH <sub>2</sub> O	Double-distilled water
DGDG	Dinogalactosyl diacylglycerol
DMSO	Dimethyl sulfoxide
DNA	Deoxyribonucleic acid
dNTP	Deoxynucleotide triphosphate
DTT	1,4-dithiothreitol
ECL	Enhanced chemiluminescence

EDTA	Ethylenediaminetetraacetic acid
EGTA	Ethylene-glycol-bis( $\beta$ -aminoethyl ether)-N,N,N',N'-tetraacetic acid
ER	Endoplasmic reticulum
g	Earth's gravitational acceleration
gDNA	Genomic DNA
GDP/GTP	Guanosine-5'-diphosphate/ triphosphate
GFP	Green fluorescent protein
h	hour(s)
HEPES	4-(2-hydroxyethyl)-1-piperazineethanesulfonic acid
IE	Inner chloroplast envelope
LB	Lysogeny broth
LDM	Light-dense membranes
LDS	Lithium dodecylsulphate
LHC	Light harvesting complex
LMW	Low molecular weight
LPOR	protochlorophyllide oxidoreductase
MES	2-(N-morpholino)-ethanesulphonic acid
MGDG	Monogalactosyl diacylglycerol
MgOAc	magnesium acetate
min	minutes
MOPS	3-(N-morpholino)propanesulphonic acid
mRNA	Messenger RNA
MS	Murashige-Skoog
NADPH	Nicotinamide adenine dinucleotide phosphate
NEP	Nuclear-encoded RNA polymerase

N-terminus	Amino-terminus
OD	Optical density
OE	Outer chloroplast envelope
OPR	Octotricopeptide repeat
PA	Phosphatidic acid
PAGE	Polyacrylamide gel electrophoresis
PC	Phosphatidylcholine
PCR	Polymerase chain reaction
PDM	PratA-defined membrane
PEG	Polyethylene glycol
PEP	Plastid-encoded RNA polymerase
PG	Phosphatidylglycerol
PIP	Phosphatidylinositol phosphate
PLB	Prolamellar body
PMSF	Phenylmethanesulphonyl fluoride
PR	Plastid reticulum
PS	Photosystem
ptNAP	Plastid nucleoid associated protein
PVDF	Polyvinylidene difluoride
PVP-40	Polyvinylpyrrolidone, average molecular weight: 40,000
RNAi	RNA interference
rpm	Rounds per minute
rRNA	Ribosomal ribonucleic acid
RT-PCR	Polymerase chain reaction based on reverse transcription
RuBisCO	Ribulose-1,5-bisphosphate carboxylase/oxygenase

s	Second(s)
SAM	Shoot apical meristem
SDS	Sodium dodecyl sulphate
SNARE	Soluble N-ethylmaleimide-sensitive-factor attachment receptor
TAE	Tris-acetate-EDTA buffer
TBS	Tris-buffered saline
TBS-T	Tris-buffered saline with Tween20
T-DNA	Transferred DNA
TEM	Transmission electron microscopy
TEMED	Tetramethylethylenediamine
TIC	Translocase of the inner chloroplast envelope
TMD	Transmembrane domain
TOC	Translocase of the outer chloroplast envelope
TPR	Tetratricopeptide repeat
Tris	Tris(hydroxymethyl)aminomethane
Tween 20	Polysorbate 20
UTR	Untranslated region
v/v	Volume per volume
w/v	Weight per volume
WT	Wild-type
YFP	Yellow fluorescent protein

## 1. Introduction

### 1.1 The thylakoid membrane: a very fascinating green network

Life on Earth largely depends on atmospheric oxygen that is produced by photosynthetic cyanobacteria and plants. Oxygenic photosynthesis is estimated to have evolved 3 to 3.5 billion years ago, thereby enriching the Earth's atmosphere with oxygen (Buick, 2008, Dyall et al., 2004). Alongside the emergence of photosynthesis and aerobic respiration, mitochondria as the primary site for respiration and chloroplasts as the place of photosynthesis were established as new cell organelles. Both originated independently from a primary endosymbiotic event during which a prokaryote was engulfed into the cytoplasm of a host cell (Margulis, 1970). In case of chloroplasts, a eukaryotic host that already contained mitochondria took up an ancestor of today's living cyanobacteria which massively transferred parts of its genome to the host nucleus to eventually become a cell organelle still containing own plastid DNA (Dyall et al., 2004, Keeling, 2010, Martin et al., 1998, Martin et al., 2015, McFadden, 2001).

Owing to their endosymbiotic origin, chloroplasts are surrounded by two envelope membranes, both of which are of prokaryotic origin. In addition, chloroplasts possess an internal membrane network lying in the aqueous stroma called the thylakoids which are the place of the light-dependent reactions of oxygenic photosynthesis. Due to the unique composition and structure of the thylakoid membrane, solar energy is efficiently converted into chemical energy with the help of major protein complexes. Chlorophyll pigments in the multi-subunit protein complexes of photosystem II (PSII) and photosystem I (PSI) are excited by light and initiate electron flow between the complexes. This process generates chemical energy in form of ATP and reducing equivalents such as NADPH that later are used in the light-regulated reactions of the Calvin-Benson cycle located in the stroma. There, CO<sub>2</sub> is fixed by the abundant enzyme ribulose-1,5-bisphosphate carboxylase/oxygenase (RuBisCO) to supply the cell with carbohydrates (Vothknecht and Westhoff, 2001, Waters and Langdale, 2009).

#### 1.1.1 Origins and structure of the thylakoid membrane

The thylakoid membrane is a unique feature of organisms that perform oxygenic photosynthesis. In contrast to prokaryotes performing anoxygenic photosynthesis, where the internal membranes are continuous with the plasma membrane (Dierstein et al., 1981, Drews and Golecki, 1995), thylakoids in mature chloroplasts as well as in cyanobacteria and green algae no longer seem to be connected to the inner envelope or the plasma membrane, respectively.

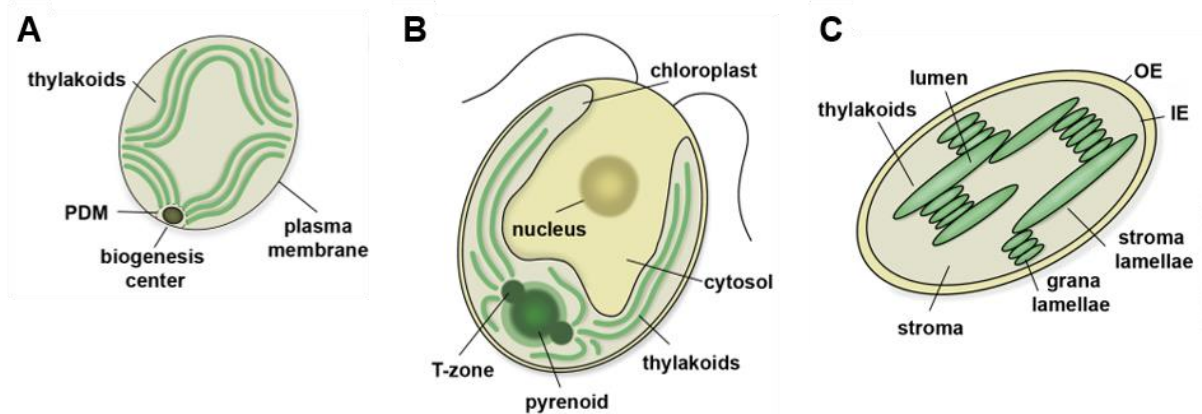


**Figure 1: Thylakoid structure in cyanobacteria, green algae and land plants.** Thylakoids of cyanobacteria and green algae are less complex than those of land plants. **A** Cyanobacterial thylakoids consist of single lamellae. Specialised membrane regions are believed to function as thylakoid biogenesis centres. These PratA-defined membranes (PDMs) appear at convergence zones of the thylakoid and the plasma membrane (Nickelsen and Zerges, 2013). **B** Green algae contain only one single chloroplast with concentric thylakoids. The pyrenoid, a plastid microcompartment, supports with the fixation of CO<sub>2</sub>. Around the pyrenoid, the translation zone (T-zone) is also believed to function in thylakoid biogenesis (Nickelsen and Zerges, 2013, Uniacke and Zerges, 2007). **C** Chloroplasts of land plants differ from those of cyanobacteria and green algae as they build an intertwined network of stroma lamellae and grana lamellae. Figure partially taken from Mechela et al. (2019).

In general, the thylakoid structure in mature chloroplasts is more complex than in cyanobacteria and many algae, which mainly contain single layers of long lamellae (Fig. 1A/B). In chloroplasts from land plants, thylakoids appear as an intertwined network of stroma lamellae and densely packed interconnected grana stacks providing a huge surface for metabolic processes (Fig. 1C) (Vothknecht and Westhoff, 2001).

Different models were proposed for the unique architecture of the thylakoid membrane. In 1970, Paolillo suggested the helical fretwork model in which the stroma lamellae, here referred to as frets, are helically arranged around the cylindrical grana stacks. In contrast to previous viewpoints, this model stated the continuity of the thylakoids as multiple frets that were thought to wind around each granum creating a highly interconnected fretwork. Furthermore, it was found that all present helices are wound around the grana stacks as multiple, right-handed helices (Paolillo, 1970). Junctional connections between the spiralling frets and the grana thylakoids appear as slits in the grana margins and can vary in size. This led to the assumption that junctional slits may participate in the functional regulation of thylakoid activities (Austin and Staehelin, 2011). Experiments that used three-dimensional reconstitution to gain insights into the formation and structure of the thylakoids also considered the grana membranes to be associated with stroma thylakoids in a helical way (Kowalewska et al., 2016).

An alternative model known as the forked membrane model was suggested. Here, a single continuous membrane is thought to be at the origin of thylakoid formation. Complexity of grana regions is gained

through folding and stacking of bifurcated stroma lamellae which fuse within the granum body (Andersson and Anderson, 1980, Arvidsson and Sundby, 1999). With that, grana are built of repeating units that are rotated in a relative manner to each other around the axis of the granal cylinder. Also here, all parts are directly connected to neighbouring membranes resulting again in an interconnected morphology (Shimoni et al., 2005). A current view on chloroplast ultrastructure and internal organization is given in Fig. 2A and 2B.

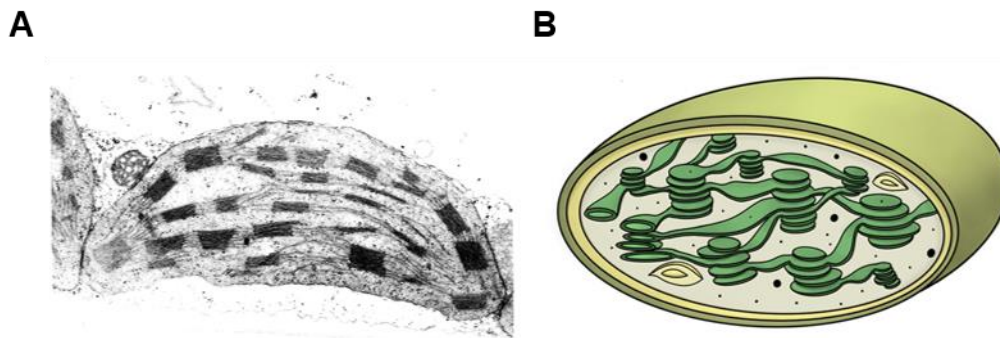


**Figure 2: Chloroplast ultrastructure and the three-dimensional network of the thylakoid membrane.** **A** Modern electron micrographs provide insights into the actual arrangement of the grana stacks. **B** The complex internal organization of a chloroplast with thylakoids forming a highly interconnected fretwork. Figure partially taken from Mechela et al. (2019).

It was stated for a long time that lateral heterogeneity of photosynthetic protein complexes as well as the three-dimensional structure of the thylakoids essentially contributed to a balanced distribution of excitation energy. By now, it is rather assumed that redox balance is mainly achieved by reversible phosphorylation of PSII-LHCII supercomplexes, by slowing down the electron transport and by thermal dissipation of excess energy (Tikkanen et al., 2012). Nevertheless, the unique and complex intertwined structure of the thylakoid membrane is strongly interconnected with its proper function. Still, many gaps remain to be filled when it comes to elucidating the three-dimensional structure of this unique membrane system. To date, the three-dimensional structure is still debated, but a helical model is favoured.

### 1.1.2 Chloroplast development and composition of the thylakoid membrane

Investigation of thylakoid biogenesis and structure is closely related to the light-dependent differentiation process from proplastids to mature chloroplasts. In angiosperms, plastids start developing from a simple undeveloped progenitor called proplastid as soon as light is available.

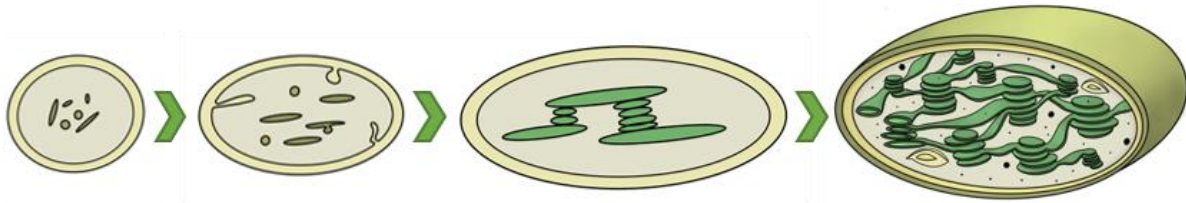


**Figure 3: Chloroplast development from a proplastid towards a mature organelle.** Differentiation towards mature chloroplasts happens from a progenitor called proplastid via invaginations of the inner envelope. Proplastids contain only few internal membranes and vesicles that finally assemble the thylakoid membrane network in the presence of light. Figure partially taken from Mechela et al. (2019), modified.

Proplastids are non-photosynthetic small round shaped organelles that are present in meristematic tissues of the shoot as well as the root apex (Adam et al., 2011). They contain only few internal membranes mostly in the form of vesicles or small saccular structures that sometimes are in contact with the inner envelope (Mühlethaler and Frey-Wyssling, 1959, Strugger, 1950, von Wettstein, 1959). The maturation process starts with the formation of long lamellae inside the proplastid. Later, these lamellae are transformed into disc-shaped structures that assemble into grana stacks. Eventually, the complex and intertwined thylakoid membrane network arises in mature chloroplasts (Fig. 3) (Vothknecht and Westhoff, 2001).

However, in the absence of light, proplastids are not able to form chloroplasts but instead turn into etioplasts. These organelles contain a spherical and paracrystalline structure of about 1-2  $\mu\text{m}$  in diameter called the prolamellar body (PLB) which consists of plastid lipids, the chlorophyll *a* precursor protochlorophyllide and the NADPH- and light-dependent enzyme protochlorophyllide oxidoreductase (LPOR) (Grzyb et al., 2013, Ryberg and Sundqvist, 1988). The function of PLBs is not fully understood to date, but they could act as a storage place for lipids and proteins that are needed for the synthesis of the photosynthetic apparatus as light becomes available (Grzyb et al., 2013, Solymosi and Schoefs, 2010). From the crystal-like centre of the PLB, perforated tubular lamellae reach out into the stroma or even connect to the inner envelope. These structures are named prothylakoids as they strongly resemble unstacked stroma lamellae (Grzyb et al., 2013).

Light induces the transition from the etioplast stage to a mature chloroplast via dispersion of the PLB (Gunning, 1965, von Wettstein, 1959). Upon illumination, the PLB disintegrates rapidly and simultaneously with the photochemical reduction of protochlorophyllide to chlorophyllide. It was observed that the PLB first enlarges in size before it disperses into small spherical vesicles (Grzyb et al., 2013). Moreover it was suggested, that these vesicles would then arrange in primary layers to eventually fuse into discs to form grana (Eriksson et al., 1961, Klein et al., 1964). Interestingly, a new PLB will form upon re-darkening of chloroplasts (Mühlethaler, 1971).

In contrast to this view, tubular structures of bean PLBs were shown to transform directly into flat slats without dispersing into vesicles. These slats then continuously formed first stacked grana structures through overlapping of neighbouring membranes. Thylakoid formation furthermore coincided with the observation of the appearance of the first chlorophyll-protein complexes. This indicated protein complex arrangement and membrane formation as a crucial interplay for chloroplast biogenesis (Kowalewska et al., 2016).

Photomorphogenesis in general is a highly coordinated process that requires numerous cellular changes. Light perception via photoreceptor proteins like phytochromes and cryptochromes initiate chloroplast biogenesis via alteration of gene expression, import of nuclear-encoded proteins, increase of chlorophyll content and finally the establishment of a thylakoid network. In angiosperms, photomorphogenesis of proplastids towards mature chloroplasts takes place at the vegetative shoot apex meristem (SAM). This region can therefore be considered as the initiation site for thylakoid biogenesis. For a long time, it was thought that the SAM would only harbour proplastids while primordial leaves would already contain mature chloroplasts. A developmental gradient was thus predicted to exist between the two regions of the shoot apex. In contrast to these beliefs it could be shown that the SAM was not at all uniform regarding chloroplast differentiation (Charuvi et al., 2012). Not only in the SAM, but also in growing leaves chloroplasts show clear developmental gradients. These gradients can not only be observed between leaves of different age, but also within a given single leaf. Leaves at the tip of the shoot are the first to complete the differentiation process while leaves at the lamina base are the youngest. However, an age gradient not only exists from top to base but also from the leaf margin to the midrib (Gügel and Soll, 2017). Taking this into account, chloroplast differentiation in dicotyledonous plants is not as homogenous as in monocots that exhibit a gradient along the leaf blade. Grasses for example show a gradual development of plastids from the leaf base, the location of the meristem, to the leaf tip where mature chloroplasts reside. In dicots, this process seems to be more complex as it is not only dependent on the leaf part but additionally on the organ, tissue and developmental stage of the plant (Pogson et al., 2015).

Not only is chloroplast differentiation and the formation of the thylakoid network a fascinating process, but also the exact composition of this membrane system is stunning. Today it is known that the thylakoid lipid bilayer shows a unique composition. It is estimated to contain about 30 % lipids of which 70-80 % are galactosyl diglycerides in form of monogalactosyl diacylglycerols (MGDGs) and digalactosyl diacylglycerols (DGDGs). Interestingly, MGDG as the main galactolipid of the thylakoids is a non-bilayer forming lipid due to its two highly unsaturated fatty acyl chains while DGDG is a bilayer-forming lipid. In addition to galactosyl diacylglycerides, the thylakoid membrane also contains around 10 % sulfoquinovosyl diacylglycerols (SQDGs) and little amounts of phosphatidylglycerol (PG) and phosphatidylcholine (PC) all of which also contribute to bilayer formation. These lipids are thought to

be unevenly distributed between the stromal and the luminal leaflet of the thylakoids (Joyard et al., 1998, Vothknecht and Westhoff, 2001). As previously assumed, the same is true for the dominant protein complexes of the thylakoids which are PSI (Chitnis, 2001) and PSII (Hankamer et al., 1997) with their respective associated light harvesting antenna, the cytochrome  $b_6/f$  complex (Berry et al., 2000) and the chloroplast ATP synthase (Groth and Strotmann, 1999). While PSII is more prominent in the grana-stacks, PSI and the ATP synthase dominate in the stroma lamellae (Albertsson, 1995).

The thylakoid membrane is characterised by a unique composition of proteins, lipids, pigments and multiple cofactors. As MGDG as one of the major membrane lipids is a non-bilayer forming lipid, the interplay of lipids and proteins seems to be important for thylakoid formation. Another feature is the lateral heterogeneity of the major photosynthetic protein complexes as they are asymmetrically distributed among the thylakoid membrane.

### 1.1.3 The big mystery of thylakoid biogenesis

Besides its structure, the exact mechanisms by which the thylakoid membrane itself is formed largely remains elusive to date. In general, thylakoids are very dynamic as they must adapt rapidly to environmental changes and stresses by changing their lipid and protein content (Pribil et al., 2014). But stunningly, little is known about how and where the numerous protein subunits as well as hundreds of cofactors are assembled to eventually build functional complexes during thylakoid biogenesis.

In cyanobacteria and green algae, there is evidence for specialised membranous compartments involved in the synthesis and assembly of photosynthetic compartments. In the cyanobacterium *Synechocystis*, so-called "PratA-defined membranes" (PDM) were identified as distinct regions at zones where thylakoids and plasma membrane converge. PratA has been described as a tetratricopeptide repeat (TPR) protein responsible for the binding and delivery of  $Mn^{2+}$  ions to PSII pre-complexes. It is assumed that PDM resemble biogenesis centres that function as nucleation points where PSII proteins are preloaded with  $Mn^{2+}$  while the final assembly is accomplished after transfer to the developing thylakoid lamellae (Fig. 1A) (Nickelsen and Zerges, 2013, Stengel et al., 2012).

As chloroplasts started as primary endosymbionts including a massive reorganization of gene regulation and coordination, thylakoid biogenesis in plastid-containing organisms is logistically more complex than in cyanobacteria. Green algae like *Chlamydomonas reinhardtii* contain only one single chloroplast with concentric thylakoids. Inside this chloroplast, a subcellular microcompartment called the pyrenoid helps with fixing  $CO_2$ . Around the pyrenoid, a specific cytological region named "translation (T)-zone" was detected where PSII subunit-encoding mRNAs and ribosomes co-localise in distinct foci. The T-zone is therefore believed to also represent a specialised localization of PSII subunit synthesis and assembly (Fig. 1B) (Nickelsen and Zerges, 2013, Uniacke and Zerges, 2007).

Chloroplasts of land plants contain a more complex and intertwined thylakoid network (Fig. 1C/2B). It is known, that many of the needed components of the thylakoid membrane such as lipids or pigments originate from the inner envelope (Vothknecht and Westhoff, 2001, Kelly and Dormann, 2004), especially galactolipids like MGDG and DGDG are essential for thylakoid formation (Kobayashi et al., 2007). Both lipids are produced at the envelope membranes. DGDG assembly takes place in the outer envelope while MGDG is assembled in the inner envelope, where also its main producing synthase MGD 1 is located. Considering that the inner envelope produces lipids for the thylakoids, it is not surprising that both membranes share a similar lipid composition (Andersson and Dörmann, 2008). Furthermore, it was hypothesised that the apoproteins of LHCII bind to pigments in the inner envelope. This process is thought to stabilise initial intermediates and to promote assembly of LHCs within the chloroplast envelope (Eggink et al., 1999, Hooper and Eggink, 2001). With that, the question arises how these hydrophobic components bridge the aqueous stroma in order to reach the thylakoid membrane. In principle, there are three possible ways how lipids, proteins and small organic molecules could be trafficking from the inner plastid envelope membrane to the thylakoids (Fig. 4) (Adam et al., 2011, Rast et al., 2015b).

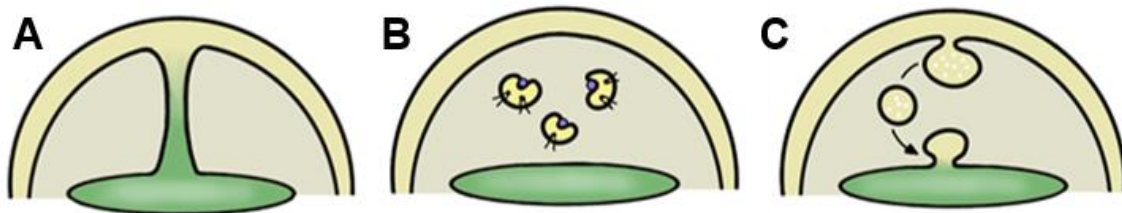


**Figure 4: Model of three possible ways of thylakoid biogenesis in higher plants.** As it is known that many important building blocks for the thylakoids derive from the inner envelope, three ideas exist on how this transfer could happen. **A** Components could either bridge the stroma via invaginations from the inner envelope. **B** Alternatively, they could be shuttled by soluble transfer proteins (proteins and lipids attached to a cargo protein are shown) **C** They could also travel as cargo of plastid vesicles (Rast et al., 2015a). Figure partially taken from Mechela et al. (2019).

First, components could reach their target through stable connections that would form lateral fusions between the two membranes. As already shown, invaginations of the inner envelope have been observed very early and were thought to contribute to the formation of prothylakoids in differentiating proplastids (Fig. 4A) (Mühlethaler and Frey-Wyssling, 1959). Even though sometimes a continuum between the inner envelope and the developing internal membrane system in the early stages of plastid differentiation can be observed, mature chloroplasts as well as cyanobacteria show no connection between the inner envelope or the plasma membrane and the thylakoids, respectively (Rast et al., 2015b). While early formation of thylakoids might be achieved by invaginations of the inner envelope, this is unlikely to happen in later stages (Vothknecht and Westhoff, 2001). Second, soluble

transfer proteins inside the stroma could function as a shuttle for thylakoid building blocks (Fig. 4B). So far, there is no clear evidence for the existence of such transfer proteins inside chloroplasts as no putative proteins could be identified yet (Lindquist and Aronsson, 2018). A third idea assumes the existence of a vesicle transport system inside the chloroplast (Fig. 4C). The suggested vesicle transfer could be similar to the ones observed in the cytosol such as the secretory pathway or endocytosis, neural transmission and vacuole formation (Waters and Langdale, 2009).

## 1.2 Plastid vesicle transport: the idea of green shuttles

In today's definition, vesicles are large structures with a lipid bilayer that enclose an interior space. Within the cell, vesicles are needed to transport specific cargo between different membrane systems. They are formed via induced curvature of the membrane and loaded with cargo. After budding off the membrane, vesicles "travel" along the cytoskeleton towards their target membrane where they get tethered by specific proteins. As the vesicles fuse with the target membrane, their cargo is released and can be used precisely where it is subsequently needed.

### 1.2.1 The secretory pathway: vesicle transport in the cytosol

The classical vesicle transport process called the secretory pathway is found in both animal and plant cells in the cytosol. The secretory pathway forms an extensive endomembrane system that branches throughout the cell. Every protein that is synthesised on ribosomes attached to the endoplasmic reticulum (ER) is transported via this system. Vesicle trafficking between a donor and an acceptor membrane consists of several steps, namely vesicle assembly, budding, fission, translocation, tethering, docking and fusion. Each of these steps is mediated by specific regulator proteins and cofactors (Bonifacino and Glick, 2004).

In plants, the secretory pathway includes the ER, the Golgi apparatus and various *post*-Golgi intermediate compartments, the vacuoles, the lysosomes and the plasma membrane. Between all these individual compartments, many steps are cyclic and therefore comprise anterograde and retrograde transport (Foresti and Denecke, 2008). The initial vesicle budding can be mediated by three different kinds of coat protein complexes (COP), namely COPI, COPII and clathrin. These coats are supramolecular assemblies of proteins that initiate membrane deformation and participate in cargo selection. Clathrin coats are needed in *post*-Golgi locations whereas COPI is involved in *intra*-Golgi transport and retrograde transport from the Golgi apparatus back to the ER. COPII protein coats mediate the export from the ER to the Golgi complex. Regulation of the coat proteins is achieved by small GTPases such as the ADP ribosylation factor (ARF) for COPI-coated vesicles or the secretion-associated RAS-related protein 1 (Sar1) for COPII-coated vesicles. Fission of clathrin coated vesicles requires the large GTPase dynamin. After the vesicles detach from the donor membrane, they shed

their coat proteins and migrate along the cytoskeleton toward the respective acceptor membrane. Once there, vesicle targeting and fusion is mediated by membrane-spanning soluble N-ethylmaleimide-sensitive factor attachment receptor (SNARE) proteins and regulated by RAB GTPases (Bonifacino and Glick, 2004). SNAREs are located on the vesicle membrane (v-SNAREs) as well as on the target membrane (t-SNAREs) where they support the fusion process and the delivery of the cargo protein by forming a *trans*- and a *cis*-complex. More accurately, SNAREs can also be divided into R-SNAREs containing conserved arginine residues and Q-SNAREs with conserved glutamine residues. Q-SNAREs are further classified into Qa-, Qb- and Qc-SNAREs based on their respective amino acid composition. SNAREs play an important role during docking of vesicles by forming parallel four-helix-bundles requiring one each of the Qa-, Qb- and Qc-SNAREs and R-SNAREs that assist vesicle fusion at the acceptor membrane. Beside tethering factors, SNAREs are also assisted by so-called SNARE-associated proteins, that are believed to support the fusion process by assisting the formation of the *trans*-complex between v- and t-SNAREs (Jahn and Scheller, 2006, Khan et al., 2013). Eventually, vesicles fuse with the acceptor membrane to deliver their respective cargo.

In addition to the secretory pathway in the cytosol of eukaryotes, vesicular structures could also be observed over and over again in organelles of prokaryotic origin such as chloroplasts. Besides, no such vesicle system could be found in cyanobacteria (Westphal et al., 2001). Taken this into account, it is very likely that the chloroplast vesicle system is of eukaryotic origin and that the cytosolic system was transferred into the organelle. Evolutionary it could be shown that such a trafficking system does not exist in any lineage of algae. It was exclusively found in organisms belonging to the embryophytes comprising bryophytes (mosses and liverworts), pteridophytes (ferns, horsetails and lycophytes) and spermatophytes (seed plants). Interestingly, embryophytes evolved simultaneously with the challenging transition to a life outside the water which correlated with the development of extensive tissue organization as well as a complex thylakoid structure. The colonization of this new habitat most likely required enormous adaptation and maintenance of the photosynthetic apparatus and might therefore be one of the reasons for the establishment of a vesicle transport system (Westphal et al., 2003). But as detailed prove of involved proteins is lacking, it can't be excluded that also prokaryotic traits are important for plastid vesicle transport. The same has been described for the import machinery found in the envelope membranes. These hetero-oligomeric protein complexes consists of both eukaryotic and prokaryotic derived components (Vothknecht and Soll, 2005). Taken this into account, it is conceivable that the eukaryotic system was acquired by plastids in the first instance to then be transformed into a unique and new trafficking system by altering and adapting the function of prokaryotic proteins.

### 1.2.2 First experimental insights into chloroplast vesicle formation

Even though the presence of vesicles in chloroplasts has often been observed, a deeper understanding of the mechanism and proteins involved is still lacking today. It was already known that vesicles would accumulate in the chloroplast stroma after exposure to stress (Cran and Possingham, 1974) or low temperature treatment (Morré et al., 1991). Upon incubation at 12°C it could be shown in pea that vesicles occurred within the stroma between the inner envelope and the thylakoid membrane. The formation of these temperature dependent vesicles had previously also been observed in the cytosol of animal cells (Morré et al., 1989). Based on this it was estimated that vesicle fusion with the target membrane was hindered by cold treatment in both cases. Simultaneously with the appearance of stromal vesicles, also invaginations that were continuous with the inner envelope could be captured in electron microscopy (Morré et al., 1991). Furthermore, it was shown that the use of established eukaryotic inhibitors and competitors such as protein phosphatase inhibitors, calmodulin inhibitors or calcium antagonists would also lead to the accumulation of stromal vesicles by preventing fusion. Hence, vesicle formation at the donor membrane could be inhibited by a non-hydrolysable GTP which led to the assumption that budding could be controlled by a GTPase similar to the eukaryotic secretory pathway of the endosomal vesicle trafficking system (Westphal et al., 2001).

Another vesicular phenomenon that can especially be observed in C4 plants is the peripheral or plastid reticulum (PR) that is found in chloroplasts (Soll, 2016). Early on, the PR was described as tubular double membranes continuous with the inner envelope as well as the thylakoids putatively facilitating the movement of materials from one membrane to another (Rosado-Alberio et al., 1968). Between the inner envelope and the thylakoid membrane, the PR appears as a dense layer of vesicles. If a PR also exists in C3 plants is currently debated. Its physiological role is still completely unknown.

Vesicles have most often been observed either in proplastids or in developing chloroplasts (Fig. 5).

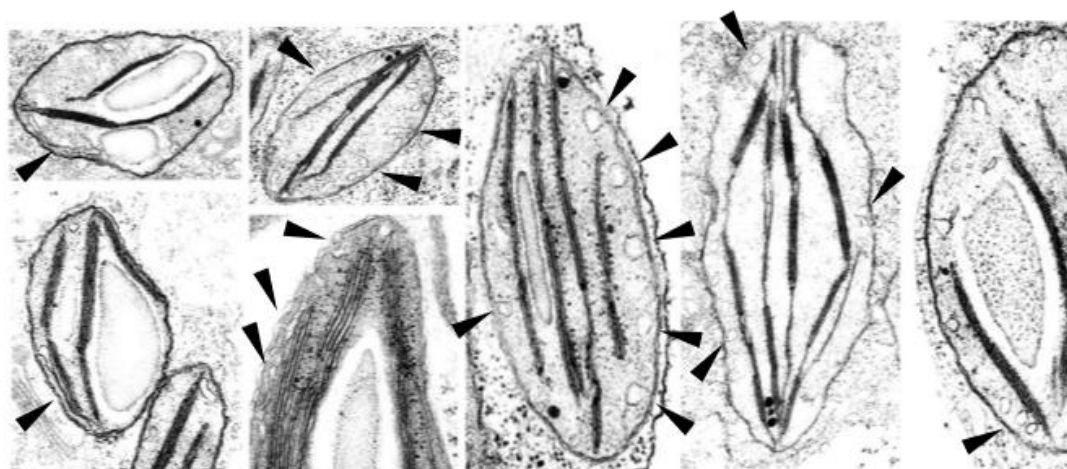


**Figure 5: Plastid vesicles occur in the stroma of young pea chloroplasts.** Black triangles pinpoint vesicles and invaginations as seen in young pea chloroplasts. The right side of the figure shows tubular invaginations

extending from the inner membrane to the thylakoids. The middle part shows plastid vesicles, which occur freely in the stroma and are no longer connected to the inner membrane. On the right side, one can see stromal vesicles docking to the thylakoid membrane. Figure partially taken from Mechela et al. (2019), modified.

Even though their presence can be increased in chloroplasts under certain circumstances as low temperature or special pre-treatment, it could be shown that vesicles are a persistent feature not only of chloroplasts, but also of other forms of plastids such as etioplasts, leucoplasts, chromoplasts and desiccoplasts. This is true for plastids of C3 and C4 plants, of different cell types and different organs. Observed vesicles were generally 50 nm in diameter and occurred with an approximate frequency of 1-8 vesicles per plastid section (Lindquist et al., 2016). A possible reason for the rare detection of vesicles in mature chloroplasts could be their velocity. It was shown that diffusion velocities of molecules differ between stroma, cytosol, and aqueous solution. Furthermore, two photon excitation (2PE) fluorescence correlation spectroscopy revealed that GFP units within stromal-filled tubules (stromules) actively moved with a velocity of about 0.12  $\mu\text{m}$  per second (Köhler et al., 2000). Even though stromules differ from stromal vesicles as they are not present inside the organelle but form tubular connections between plastids, stromules give a first hint on how fast movement through the stroma could be.

As biochemical and molecular biological evidence for a vesicular transport system inside chloroplasts increased, the search for homologous components of the cytosolic vesicle system started. For some of these components and additional associated factors, homologs targeted to the chloroplast could be identified by bioinformatic approaches. Most of the identified homologs corresponded to yeast COPII coated vesicle components (Andersson and Sandelius, 2004, Khan et al., 2013, Lindquist et al., 2014). An overview of the most relevant proteins is given below.

### **cpSAR1 and cpRabA5e**

So far, only two of the identified candidates namely chloroplast localised SAR1 (cpSAR1) and chloroplast localised RabA5e (cpRabA5e) were experimentally confirmed to be chloroplast proteins. cpSAR1 was verified to have GTPase activity and to be dually located in the inner envelope as well as in chloroplast vesicles (Garcia et al., 2010). Nevertheless, it is debated, if cpSar1 really is a homolog of the yeast ARF GTPase Sar1p which belongs to the extended Ras-like family or if it rather belongs to the OBG-like GTPases, a subfamily of bacterial P-loop GTPases. In prokaryotes, OBG-like proteins play an important role during sporulation and differentiation. Homologs of these GTPases are widely distributed among algae and plants indicating that the protein has retained an important function even though functional adaptation has to be considered. In this context, cpSar1 was renamed AtOBGL and suggested to be essential for embryo development in *Arabidopsis* (Chigri et al., 2009). This proposal contrasts with a possible participation plastid vesicle transport. cpRab5Ae was found to be localised in

the stroma and the thylakoids. Due to its homology to yeast Ypt31/32 it is also thought to have a role for regulating vesicle transport (Karim et al., 2014). Nevertheless, it must be emphasised that the final proof of a role in vesicle transport is still missing for both proteins.

### Vipp1

In addition to bioinformatic approaches, numerous mutant studies were conducted to unravel putative proteins involved in thylakoid biogenesis as well as plastid vesicle transport. One protein with a critical role in thylakoid biogenesis is the vesicle-inducing protein in plastids 1 (Vipp1). It was first described in pea as the inner membrane associated protein of 30 kDa (IM30) (Li et al., 1994). Vipp1 derived from the bacterial phage shock protein A (PspA) via gene duplication. During duplication of the *pspA* gene, a novel  $\alpha$ -helical extension at the C-terminal domain comprising 30 amino acids was added that seems essential for its function in thylakoid formation. As Vipp1 is exclusively found in cyanobacteria and chloroplasts, it probably developed in parallel to the emergence of the thylakoid membrane system. In contrast to algae and higher plants, cyanobacteria still possess both proteins, PspA and Vipp1, which strengthens the hypothesis that algal and plant Vipp1 evolved from a cyanobacterial PspA (Gao and Xu, 2009, Westphal et al., 2001b, Kroll et al., 2001, Vothknecht et al., 2012). Furthermore, it could be shown that PspA in cyanobacteria carrying a mutation in the *vipp1* gene is not sufficient to compensate the deficiency (Gao and Xu, 2009, Westphal et al., 2001b), while cyanobacterial as well as plant Vipp1 can functionally complement *E. coli* PspA (DeLisa et al., 2004, Zhang et al., 2012). Interestingly, the unicellular photosynthetic cyanobacterium *Gloeobacter violaceus* sp. PCC 7421 lacks both, Vipp1 and a thylakoid membrane system. The only present membrane unit is the cytoplasmic membrane where photosynthesis is thought to take place in specialised lipid domains (Rippka et al., 1974, Nakamura et al., 2003). The example of *Gloeobacter* is another strong indication that Vipp1 and thylakoid biogenesis are linked.

More recently, strong focus was laid on investigating the detailed physiological function of Vipp1 in generating and/or maintaining the thylakoid membrane system. It was found in cyanobacteria, that Vipp1 forms oligomeric rings that disassemble to located puncta. These puncta for their part associate with highly curved regions of the thylakoid membrane where they are supposed to act as scaffold-like aggregates. Taken together, it is very likely that Vipp1 fulfils a protective function for membranes with high curvature stress in order to control integrity and biogenesis of thylakoid membranes (Gutu et al., 2018, Junglas and Schneider, 2018).

Membrane remodelling in general requires nucleotide binding and/or hydrolysis. Indeed, it was shown that Vipp1 as well as its homolog PspA are capable of both GTP binding and hydrolysis. Even though Vipp1 doesn't contain a canonical G domain, that is typical for GTPases, heterologous expressed Vipp1 seems to bind and hydrolyse GTP via its N-terminal  $\alpha$ -helix *in vitro* which seems to promote

oligomerization. With that, Vipp1 could represent a novel type of GTPase acting in chloroplast membrane fusion and/or remodelling (Heidrich et al., 2017, Ohnishi et al., 2018).

### **FZL, THF1 and SCO2**

Besides Vipp 1, most promising are the fuzzy-onion (FZO) like protein (FZL) (Gao et al., 2006, Patil et al., 2018), the thylakoid formation protein 1 (THF1) (Wang et al., 2004) and snowy cotyledon 2 (SCO2) (Shimada et al., 2007, Zagari et al., 2017). All of them show interesting phenotypes that indicate a role in thylakoid biogenesis and vesicle transport.

FZL is a protein of the dynamin superfamily of membrane-remodelling GTPases that is assumed to facilitate membrane fusion processes. Within the chloroplast, FZL is found at the envelope as well as the thylakoid membrane. Loss-of-function mutants of FZL, like Vipp1, show an altered thylakoid structure and unusually shaped chloroplasts (Gao et al., 2006, Lindquist and Aronsson, 2018). Vipp1-depleted plants furthermore display fewer vesicles and a disturbed photosynthetic electron transport chain. In contrast, more vesicles accumulate in the stroma of *fzl*, *thf1* and *sco2*.

THF1 is supposed to be a multifunctional protein residing in the outer plastid envelope membrane where it seems to be involved in sugar signalling as well as in the stroma where it could be involved in shuttling LHCb proteins as a possible cargo in the vesicle transport system (Huang et al., 2013). Beside the vesicle accumulation in the stroma, *thf* mutant plants show a variegated leaf pattern with a lack of thylakoid membranes in the white sections (Wang et al., 2004).

SCO2 is a disulphide isomerase located in the thylakoid membrane. Like THF1, SCO2 has been shown to interact with LHCb proteins (Huang et al., 2013, Tanz et al., 2012). In *sco2* mutants, vesicle formation and movement are impaired leading to defects in chloroplast development at cotyledon stage, but this normalises later and leads to green leaves (Albrecht et al., 2008, Tanz et al., 2012).

### **cpSFL1**

The latest described candidate protein is the chloroplast-localised Sec14-ike protein (cpSFL1). Sec14-domain proteins are exclusively found in eukaryotes, where they regulate vesicle budding at the *trans*-Golgi network (Curwin et al., 2009, Mousley et al., 2007). In chloroplasts, cpSFL1 was found to be necessary for photoautotrophic growth and vesicle formation at the inner envelope membrane. Loss-of-function mutants of cpSFL1 are seedling lethal, show a defect in thylakoid structure, and lack chloroplast vesicles. Like its yeast counterpart, cpSFL1 is able to bind phosphatidylinositol phosphates (PIPs) and phosphatidic acid (PA). It is believed that cpSFL1 acts as a phosphatidylinositol transfer protein and with that facilitates vesicle formation by transporting PIP into PA-rich membrane bilayers (Hertle et al., 2020).

Interestingly, it could be shown that cpSFL1 is also essential for normal chloroplast development in the green alga *Chlamydomonas reinhardtii*. Mutants depicted a decreased accumulation of plastid isoprenoid-derived pigments like carotenoids and consequently a deficiency of carotenoid-rich chloroplasts structure like eyespot or plastoglobules. It is suggested that cpSFL1 is involved in the biosynthesis of phytoene, a carotenoid precursors, as well as in the transport of carotenoids (García-Cerdán et al., 2020). As green algae don't possess a vesicle transport system, *Chlamydomonas reinhardtii* gives interesting insights into the functional role of cpSFL1 in transport processes and membrane adhesion.

Despite numerous promising experiments to elucidate vesicle transport and thylakoid biogenesis, it must be underlined that none of the proteins presented plays a proven role in these processes. The exact function of the individual proteins for the chloroplast must be further investigated. Until then, all assumptions remain speculative.

### 1.2.3 Design of a working model for a plastid vesicle transport system

Altogether, it can be resumed that vesicles exist in chloroplasts at different developmental stages as well as in different forms. In general, it can be said that vesicles occur more often in young stages of development. This suggests that the transport of vesicles plays an important role particularly during the early biogenesis of thylakoids. Vesicles could not only be observed upon specific pre-treatments, but also occur in natural plastids. With that it is excluded that these vesicles are an artefact of electron microscopic preparation techniques. Yet, their general function and contribution to thylakoid biogenesis is largely unknown. Bioinformatic approaches suggesting similarity to the COPII vesicular trafficking system of the cytosol made it tempting to also assume plastid vesicles as cargo shuttles for thylakoid building blocks. This plastid vesicle system could be an ongoing and protein-mediated transport in order to build and maintain the thylakoid network. Based on the latest research, a working model for a plastid vesicle transport system providing an overview of putative processes involved in thylakoid biogenesis was created (Fig. 6).

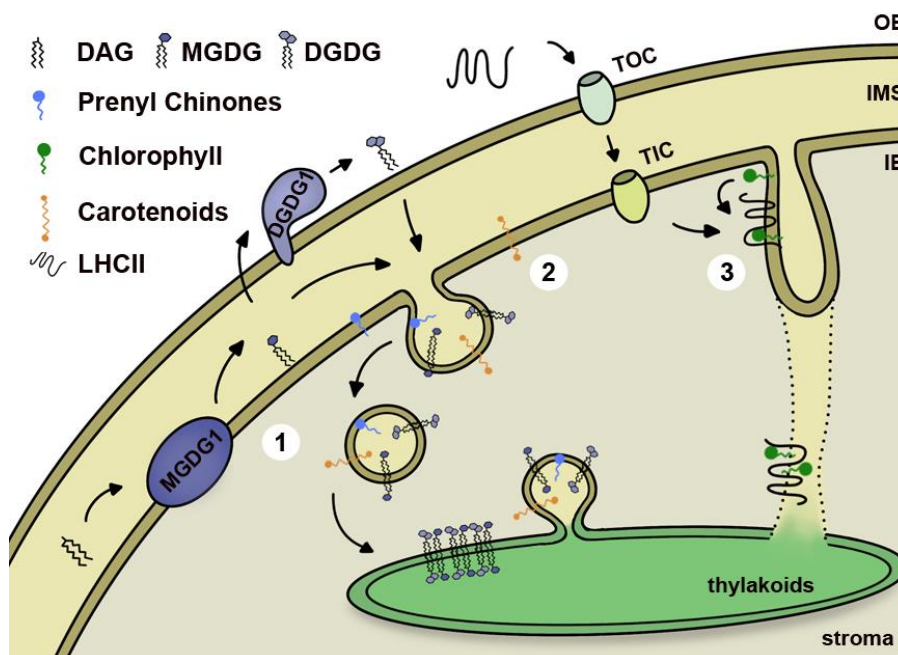


**Figure 6: Suggestion of processes contributing to thylakoid biogenesis in chloroplasts of land plants.** Lipids, prenyl lipids, pigments and proteins are needed to build a functional thylakoid membrane. These components must somehow travel through the aqueous stroma to reach the thylakoids. **1.** The galactolipids DGDG and MGDG are synthesised from their synthases DGD1 and MGD1 at the outer and inner envelope, respectively (Andersson and Dörmann, 2008, Cline and Keegstra, 1983, Joyard et al., 1998). **2.** Together with prenyl lipids (Soll et al., 1985) and carotenoids (Jeffrey et al., 1974) that are also made at the inner envelope, they could be a putative cargo of a suggested plastid vesicle transport system. Vesicles are thought to bud off from the inner envelope, travel across the stroma to finally fuse with the thylakoid membrane to deliver their cargo. **3.** Another connection between both membranes could be provided by invaginations forming lateral fusions. Plastid-targeted proteins like LHCII are imported via the TOC and TIC translocons residing in the envelope membranes. These proteins could furthermore be preassembled with chlorophylls (Eggink et al., 1999, Hooper and Eggink, 2001) in the incipient invaginating membrane before being delivered to their target membrane. Figure taken from Mechela et al. (2019).

Lipids, prenyl lipids, pigments and proteins are needed to build a functional thylakoid membrane. These components must somehow travel through the aqueous stroma to reach the thylakoids. The galactolipids DGDG and MGDG are synthesised from their synthases DGD1 and MGD1 at the outer and inner envelope, respectively (Cline and Keegstra, 1983, Joyard et al., 1998, Andersson and Dörmann, 2008). Together with prenyl lipids (Soll et al., 1985) and carotenoids (Jeffrey et al., 1974) that are also made at the inner envelope, they could be a putative cargo of a suggested plastid vesicle transport system. Vesicles are thought to bud off from the inner envelope, travel across the stroma to finally fuse with the thylakoid membrane to deliver their cargo. Another connection between both membranes could be provided by invaginations forming lateral fusions. Plastid targeted proteins like LHCII are imported via the TOC and TIC translocons residing in the envelope membranes. These proteins could furthermore be preassembled with chlorophylls (Eggink et al., 1999, Hooper and Eggink,

2001) in the incipient invaginating membrane before being delivered to their target membrane. Nevertheless, exact processes and involvements remain an open question.

### 1.3 Putative new players in plastid vesicle transport

Although proteins have been repeatedly found that may play an important role in plastid vesicle transport, many gaps still need to be filled. Therefore, our group also increasingly searched for such candidates, a selection of which is presented in the following section.

#### 1.3.1 Putative vesicle transport SNARE-associated protein (SNARE AP)

The putative vesicle transport soluble N-ethylmaleimide-sensitive-factor attachment receptor-associated protein (SNARE AP) was found as a putative chloroplast protein during a bioinformatic screen performed by Khan et al. (2013). SNARE AP exhibits sequence similarities to Tvp38 in yeast and DedA in bacteria. Proteins of the Tvp38/DedA family have been shown to function in membrane organization, stabilization, transport and/or fusion of internal membrane systems. In chloroplasts, only one single Tvp38-homolog can be found whereas cyanobacterial genomes encode multiple homologs (Keller and Schneider, 2013).

In a proposed model, SNARE AP is thought to support SNARE-assisted vesicle fusion at the thylakoid membrane via modulation of tethering, formation, and disassembly of the SNARE complex. Furthermore, it is also conceivable, that SNARE AP acts as a scaffold for the SNARE complex by having additional interacting and binding partners (Inoue et al., 2016, Khan et al., 2013).

SNARE AP is a 36.9 kDa protein with a predicted N-terminal chloroplast transit peptide (TP) of 10.4 kDa (Emanuelsson et al., 1999) and four transmembrane domains (TMDs) with the N-terminus facing the outside (<http://aramemnon.uni-koeln.de/>). *In silico* expression data using the AtGenExpress eFP ([bar.utoronto.ca/eplant](http://bar.utoronto.ca/eplant)) indicate high expression values for the cotyledons and the leaves of the vegetative rosette (Waese et al., 2017), which was also confirmed by RNA-seq profiling (Klepikova et al., 2016).

#### 1.3.2 Synaptotagmin- like protein 5.2 (SYTL5.2/AtNTMC2T5.2)

Proteins of the synaptotagmin (SYT) family have initially been identified in metazoans and are famous for their role in neurotransmitter release from synaptic vesicles (Chapman, 2008, Sudhof, 2013). All members of this protein family depict a conserved domain structure with an N-terminal TMD for membrane anchorage and one or more subsequent tandem C2 domains that are responsible for calcium- and phospholipid-binding. Upon binding of  $Ca^{2+}$ , the C2 domains undergo a conformational change that allows the partial insertion of SYT proteins into the lipid bilayer (Craxton, 2001, Schulz and Creutz, 2004, Sudhof, 2002). Moreover, C2 domains are also known to interact with SNAREs and other proteins involved in the tethering, docking and fusion process of vesicle traffic. The interplay of these

proteins induces membrane curvature that eventually allows the vesicle membrane and the acceptor membrane to fuse (Chicka et al., 2008, Zhou et al., 2017).

SYT proteins have also been identified to be present in plants. 13 SYT and SYT-like genes were classified in *Arabidopsis* so far (Craxton, 2004, Craxton, 2007). Due to their N-terminal TM region followed by a C2 domain the SYTs were termed as N-terminal-TM-C2 (NTMC2) domain genes in plants, which are grouped into six sub-groups based on the conserved gene structure, type1-6 (Craxton, 2001, Craxton, 2004, Craxton, 2007). Nevertheless, functional characterization of plant SYTs is still scarce.

One of these proteins, the SYT-like 5.2 (SYTL5.2/AtNTMC2T5.2) protein was identified in a phosphoproteomic analysis of pea chloroplast envelope membranes performed in our group. SYTL5.2 belongs to the NTMC2-type-5 proteins that are exclusively found in plants. These proteins contain a single C2 domain along with four TMDs instead of one and a N-terminal TP which makes them putative chloroplast proteins. SYTL5.2 is 77 kDa in size with a predicted TP of 2.96 kDa (Emanuelsson et al., 1999). No *in silico* expression data is currently available for this protein, but RNA-seq data indicate high expression in leaves and petals (Klepikova et al., 2016).

### 1.3.3 Embryo defective 1303 (EMB1303)

While searching for other potential SNARE proteins in chloroplasts, EMB1303 became an interesting candidate due to its drastic phenotype and chloroplast localisation. In addition, EMB1303 has one single C-terminal TMD which is a common feature of SNARE proteins.

EMB1303 has first been described by Huang et al. (2009) as a novel protein mainly expressed in young leaves, roots and flowers that is essential for chloroplast development and plant growth in *Arabidopsis*. Loss-of-function of EMB1303 lead to seedling lethal albino mutant plants that could only survive on sugar-supplied medium but remained infertile. Beside a reduced number of mesophyll cells and abnormal pavement cells, they also depicted much shorter primary roots in comparison to WT. Furthermore, embryogenesis in *emb1303* mutant plants was delayed in early stages of seed development while tissue organization was unaltered. Eventually, mutants were able to form mature embryos although their size was smaller, and their colour was paler compared to WT.

It could also be confirmed with the help of a GFP-fusion construct (*p35S::EMB1393-GFP*) that EMB1303 localises to the chloroplasts. Microscopic analyses furthermore indicated that EMB1303 could reside in the inner envelope.

TEM that was also performed by Huang et al. (2009) revealed abnormal developed plastids in mutant plants. Plastids of *emb1303* were smaller and lacked the typical lens-shaped structure. Moreover, the thylakoid membrane consisted of only few non-stacked membranes with no differentiation into grana and stroma thylakoids. As the morphology of other organelles like the ER or mitochondria was unaffected, it was suggested that EMB1303 specifically affects chloroplast biogenesis in leaves via mediating plastid differentiation and internal thylakoid membrane formation.

As *emb1303* mutants depict an albino phenotype, it is not surprising that the expression of key genes of the chlorophyll as well as the carotenoid biosynthesis pathways was found to be downregulated. In turn, other genes related to plastid transcription and translation were not significantly affected in the mutant. A lack of EMB1303 most strongly affected genes involved in photosynthesis and chloroplast development. This could also be confirmed at the protein level where the accumulation of photosynthetic protein complexes was severely impaired in *emb1303* (Huang et al., 2009).

Taken together, EMB1303 is an interesting candidate for a putative chloroplast SNARE protein involved in thylakoid membrane formation and chloroplast development. EMB1303 is 16 kDa in size with a predicted TP of 1.67 kDa (Emanuelsson et al., 1999). *In silico* expression data using the AtGenExpress eFP ([bar.utoronto.ca/eplant](http://bar.utoronto.ca/eplant)) indicate high expression values for seeds, cotyledons and leaves (Waese et al., 2017), which was also confirmed by RNA-seq profiling (Klepikova et al., 2016).

#### 1.3.4 Plastid nucleoid-associated protein of 45 kDa (ptNAP45)

Initially, ptNAP45 and its paralog ptNAP45-like were found in a proteomic screen of our group that was performed on chloroplasts of very young pea plants. During this experiment, so-called light-dense membrane (LDM) fractions were isolated. LDM fractions were supposed to contain vesicles associated to proteins that could be involved in early chloroplast biogenesis. Both proteins were completely uncharacterised at the beginning of this work. As a consequence of the experimental process preliminary data now suggest that at least ptNAP45 is associated with plastid nucleoids and seems to be essential for plastid translation and chloroplast biogenesis.

As chloroplasts still possess their own little genome, compact structures of plastid DNA (ptDNA), RNA, enzymes and DNA binding proteins regulate DNA architecture as well as transcription, replication, and recombination. These structures are named plastid nucleoids and are unique regarding their number, genome copy content and dynamic distribution within plastids (Powikrowska et al., 2014b). In contrast to bacteria, one single plastid owns multiple nucleoids with a varying number of genome copies (Sakai et al., 2004). Plastid nucleoids are also thought to play an important role in ribosome assembly as well as RNA splicing and editing (Majeran et al., 2012, Bohne, 2014).

In chloroplasts, gene expression is mainly regulated in a posttranscriptional manner. Numerous proteins are required for proper RNA maturation, processing as well as degradation. Protein synthesis is carried out by bacterial-type 70S ribosomes composed of a large 50S subunit and a small 30S subunit (Tiller and Bock, 2014). The large subunit harbours three different ribosomal RNAs (rRNAs), namely 23S rRNA, 5S rRNA and 4.5S rRNA, while in the small subunit only one rRNA (16S rRNA) is found. Both subunits are in complex with several proteins, some of which are of eubacterial origin while others have been shown to be plastid-specific ribosomal proteins (Yamaguchi and Subramanian, 2000, Yamaguchi and Subramanian, 2003, Manuell et al., 2007).

Moreover, number and position of plastid nucleoids changes depending on the respective developmental stage of the plastid (Boffey et al., 1979, Kuroiwa et al., 1981, Greiner et al., 2019). While nucleoids in proplastids are mainly found in the centre, they move towards the inner envelope membrane during seed germination to perform extensive DNA amplification. During the process of light-induced transition from proplastid to mature chloroplasts, plastid nucleoids again change location and settle along the developing thylakoid membrane (Sakai et al., 2004). It was suggested that nucleoid morphology and distribution are tightly linked to thylakoid biogenesis during chloroplast development (Kobayashi et al., 2013).

It is highly likely that the dynamic structure of plastid nucleoids determines gene expression in concert with the nuclear genome. However, although some plastid nucleoid associated proteins (ptNAPs) have already been identified, the exact function of most of them remains unclear (Powikrowska et al., 2014b). One of the most intensively studied ptNAPs is the plastid envelope DNA binding protein (PEND). PEND functions in tethering nucleoids to the inner envelope in developing pea chloroplasts (Sato et al., 1993, Sato et al., 1998). Without its transit peptide that ensures its targeting to the chloroplast, PEND localises to the nucleus (Terasawa and Sato, 2009). Other abundant proteins of plastid nucleoids are DCP68 with a putative function in compacting ptDNA (Cannon et al., 1999, Chi-Ham et al., 2002), the WHIRLY proteins that are also suggested to play a role in condensation (Krause et al., 2005, Krupinska et al., 2014), and the SVR4 and SVR4-like proteins (Yu et al., 2011), also named MRL7 and MRL7-like (Qiao et al., 2011). It is assumed that the latter ensure the correct organization of the nucleoids (Powikrowska et al., 2014a). Even though ptNAPs seem to differ in their respective roles, most of the so far identified are unique to land plants (Powikrowska et al., 2014b).

ptNAP45 is a soluble protein of 48.7 kDa in size with a predicted TP of 6.8 kDa (Emanuelsson et al., 1999). No *in silico* expression data is currently available for this protein, but RNA-seq data indicate high expression in young leaves (Klepikova et al., 2016).

## 1.4 Aims of this study

The thylakoid membrane is one of the most fascinating biological systems as it harbours protein complexes and pigments that are essential for oxygenic photosynthesis and the subsequent production of starch and oxygen, both of which enabling life on Earth. Even though much is known about photosynthesis and its metabolic impacts, little is known on how exactly the complex intertwined thylakoid network forms. While there is strong evidence for a plastid vesicle transport system contributing to thylakoid biogenesis in higher plants, experimental proof for the mechanistic processes, putatively involved proteins and regulators is still missing.

For this reason, it has become more and more important to not only collect theoretical *in silico* data on putative players of the game, but in addition experimentally analyse candidate proteins regarding

their respective molecular functions. This step-by-step approach allows putative candidates to be integrated with higher confidence into existing plastid vesicle models or else to be assigned to other processes in the chloroplast.

This thesis aims to investigate four new putative vesicle candidate proteins residing in the chloroplast of higher plants and to elucidate their role and function for the organelle. These proteins are SNARE AP, SYTL5.2, EMB1303 and ptNAP45. For all of them, phenotypes, and chloroplast ultrastructure of knock-out mutants as well as greening, *in vitro* import, sub-localization studies as well as putative interaction partners should be analysed to gain a deeper understanding of the respective molecular functions and to be able to assess whether the chosen candidates could indeed play a role in plastid vesicle transport.

## 2. Material and Methods

### 2.1 Material

#### 2.1.1 Chemicals, beads and membranes

Chemicals used in the following experiments were purchased from Fluka (Buchs, Schweiz), Merck (Darmstadt, Germany), New England Biolabs (Frankfurt am Main, Germany), Serva (Heidelberg, Germany), Sigma-Aldrich (Taufkirchen, Germany), ThermoFisher Scientific (Braunschweig, Germany) and Roth (Karlsruhe, Germany). <sup>35</sup>S-methionine was received from PerkinElmer (Walluf, Germany). PVDF transfer membrane was purchased from Millipore (Billerica, MA, USA) and the blotting paper from Macherey-Nagel (Düren, Germany).

#### 2.1.2 Enzymes and Kits

Restriction endonucleases, T4 DNA Ligase, Q5 DNA Polymerase, SP6 RNA Polymerase and Phusion® High Fidelity DNA Polymerase were purchased from New England Biolabs (Frankfurt am Main, Germany), DFS-Taq DNA Polymerase from Bioron (Ludwigshafen, Germany) and M-MLV Reverse Transcriptase from Promega (Madison, WI, USA). BP and LR Clonase® II mix and Proteinase K for Gateway® cloning were purchased from Invitrogen (Karlsruhe, Germany). Cellulase Onozuka R10 and macerozyme R10 were received from Serva (Heidelberg, Germany). rRNasin® Ribonuclease Inhibitor were obtained from Promega (Madison, WI, USA) and cOmplete™ Mini EDTA-free Protease Inhibitor Cocktail from Roche (Penzberg, Germany). TNT® Coupled Reticulocyte Lysate Systems for *in vitro* transcription/translation were purchased from Promega (Madison, WI, USA). The NucleoSpin® Plasmid EasyPure Kit as well as the NucleoBond® Xtra Midi Kit from Macherey-Nagel (Düren, Germany) were used for plasmid isolation from *Escherichia coli*. Gel extraction or purification of PCR products was performed using the NucleoSpin® Gel and PCR Clean-up Kit from Macherey-Nagel (Düren, Germany). Isolation of RNA was done with the RNeasy® (Plant) Mini Kit from Qiagen (Hilden, Germany). Site-directed mutagenesis was performed with the Q5® Site-Directed Mutagenesis Kit from New England Biolabs (Frankfurt am Main, Germany).

#### 2.1.3 Molecular weight site marker and DNA standard

PstI digested lambda phage DNA (Thermo Fisher Scientific) was used as a marker for agarose gel electrophoresis. Either peqGOLD® protein marker I (VWR, Ismaning, Germany) or the prestained SpectraHR (NEB, Frankfurt am Main, Germany) were used for SDS-PAGE.

#### 2.1.4 Plant material

*Arabidopsis thaliana* ecotype Columbia (Col-0) was used as wild-type (WT). The *snare ap* and *syt15.2* T-DNA insertion lines (SAIL\_593\_G09, SAIL\_1144\_G11 and SALK\_003927) were obtained from the European Arabidopsis Stock Centre (<http://arabidopsis.info/>) while the *syt15.2* T-DNA insertion line (GK-456H02), the *ptnap45* T-DNA insertion line (GK-635E11.01) as well as the *emb1303* T-DNA insertion line (GK\_568E02) were obtained from the GABI-Kat collection (<https://www.gabi-kat.de/>). Seeds of homozygous knock-out mutants *pac* and *cptatc* were kindly provided by Nikolai Manavsky/Jörg Meurer and Christopher Carrie, respectively. *Arabidopsis* seeds were stored in the dark at room temperature. *Nicotiana benthamiana* was used for *Agrobacterium*-mediated transient transfection.

#### 2.1.5 Bacterial strains

Chemically competent *Escherichia coli* Top10 cells were used for cloning and general plasmid amplification, whereas *ccdB*-resistant DB3.1 cells were used for amplification of empty Gateway® cloning vectors. *Escherichia coli* BL21(DE3) pLysS and BL21-CodonPlus(DE3)-RIPL cells were used for heterologous protein overexpression. Stable transfection of *Arabidopsis* plants as well as transient transfection of tobacco leaves was performed using *Agrobacterium tumefaciens* AGL1 (Carbenicillin resistance) or GV3101 (Rifampicin/Gentamycin resistance). Chemically competent cells used in this study were prepared by Tamara Bergius and Carina Engstler.

#### 2.1.6 Accession numbers

Accession numbers of proteins used in this study are listed in Table 1. Detailed sequence data can be found under respective accession numbers in the NCBI data libraries (<https://www.ncbi.nlm.nih.gov/>).

**Table 1:** Accession numbers of proteins and their respective species.

Protein	Accession number	Species
cpAtp $\alpha$	AtCg00120	<i>Arabidopsis thaliana</i>
cpAtp $\beta$	AtCg00480	<i>Arabidopsis thaliana</i>
EMB1303	At1g56200	<i>Arabidopsis thaliana</i>
FBPase	AT3G54050	<i>Arabidopsis thaliana</i>
FNR	At5g66190	<i>Arabidopsis thaliana</i>
LHCB1	At1g29910	<i>Arabidopsis thaliana</i>
LHCB5	AT4G10340	<i>Arabidopsis thaliana</i>
PAC	At2g48120	<i>Arabidopsis thaliana</i>
PsaF	At1g3133	<i>Arabidopsis thaliana</i>
PsbA	AtCg00020	<i>Arabidopsis thaliana</i>

PsbO	At4g37230	<i>Arabidopsis thaliana</i>
ptNAP45	At4g37920	<i>Arabidopsis thaliana</i>
	XP_002947236.1	<i>Volvox carteri</i>
	PNW69832.1	<i>Chlamydomonas reinhardtii</i>
	XP_005645753.1	<i>Chlamydomonas reinhardtii</i>
	XP_024372527.1	<i>Physcomitrium patens</i>
	OAE27386.1	<i>Marchantia polymorpha</i>
	Sphfalx0018s0060.1	<i>Sphagnum fallax</i>
	PIA47990.1	<i>Aquilegia coerulea</i>
	PIA51907.1	<i>Aquilegia coerulea</i>
	PNT72139.1	<i>Brachypodium. distachyon</i>
	XP_003573561.2	<i>Brachypodium. distachyon</i>
	XP_002285817.1	<i>Vitis vinifera</i>
	XP_003635095.1	<i>Vitis vinifera</i>
	XP_002437093.1	<i>Sorghum bicolor</i>
	XP_021901451.1	<i>Carica papaya</i>
	EEF35142.1	<i>Ricinus communis</i>
	EEF48437.1	<i>Ricinus communis</i>
	SapurV1A.0766s0170	<i>Sarracenia purpurea</i>
	SapurV1A.0331s0180.1	<i>Sarracenia purpurea</i>
	Kalax.0018s0077.1	<i>Kadua laxiflora</i>
Kalax.0502s0018.1	<i>Kadua laxiflora</i>	
Spipo4G0017800	<i>Spirodela polyrhiza</i>	
Spipo0G0096800	<i>Spirodela polyrhiza</i>	
ptNAP45-like	At1g36320	<i>Arabidopsis thaliana</i>
RPL2	AtCg00830	<i>Arabidopsis thaliana</i>
RPL4	At1g07320	<i>Arabidopsis thaliana</i>
Sec62	At3g20920	<i>Arabidopsis thaliana</i>
SNARE AP	At1g22850	<i>Arabidopsis thaliana</i>
SYTL5.2/AtNTMC2T5.2	At3g19830	<i>Arabidopsis thaliana</i>
cpTatC	At2g01110	<i>Arabidopsis thaliana</i>
Tic110	At1g06950	<i>Arabidopsis thaliana</i>
VAR2 (AtFtsH2)	At2g30950	<i>Arabidopsis thaliana</i>
vATPase	At4g11150	<i>Arabidopsis thaliana</i>

### 2.1.7 Vectors and clones

Gateway® vectors pDONR, pDEST14, pBGW, pHGW pB7CWG2, pB7FWG2, pK7FWG2 and pK7WIWG2 have been described recently (Karimi et al., 2002, Karimi et al., 2007). The helper plasmid p19 was additionally added, if necessary, to enhance protein expression in transiently transfected tobacco plants. Constructs used for this study are listed in Table 2 indicating restriction sites used for cloning and the purpose of generated constructs. As indicated, constructs were partially generated under the control of the respective endogenous promoters predicted by ChloroP 1.1 Prediction Server (<http://www.cbs.dtu.dk/services/ChloroP/>).

**Table 2:** Clones with respective genes, vectors, sequence description, restriction sites and purpose.

Gene	Vector	Description	Restriction Site	Purpose
<i>AtEMB1303</i>	pDONR207	full length	Gateway®	complementation
		no TMD	Gateway®	complementation
	pB7FWG2	full length	Gateway®	complementation
		no TMD	Gateway®	complementation
	pSP65	full length, 5 artificial Met at C-term	EcoRI/Sall	<i>in vitro</i> import
	49	ABI3 promoter	Golden Gate®	complementation
49	endogenous promoter, At1g30475 CDS	Golden Gate®	complementation	
<i>AtSec62</i>	pB7YWG2	amino acids 1-160	Gateway®	localization
<i>FNR</i>	pSP65	full length	EcoRI/Sall	<i>in vitro</i> import
<i>PAC</i>	pB7CWG2	no stop	Gateway®	localization
<i>ptNAP45</i>	pDONR207	full length	Gateway®	complementation <i>in vitro</i> import
		no stop	Gateway®	localization
		without TP	Gateway®	localization
	pK7FWG2	no stop	Gateway®	localization
	pK7WIWG2	full length	Gateway®	RNAi
	pH2GW7	full length	Gateway®	complementation
	pB7FWG2	without TP no stop	Gateway®	localization
	pB7CWG2	without TP no stop	Gateway®	localization

	pDEST14	full length	Gateway®	<i>in vitro</i> import
<i>ptNAP45-like</i>	pDONR207	no stop	Gateway®	localization
	pK7FWG2	full length	Gateway®	localization
<i>SNARE AP</i>	pDONR207	endogenous promoter full length	Gateway®	complementation
	pHGW	endogenous promoter full length	Gateway®	complementation

### 2.1.8 Oligonucleotides

Used oligonucleotides are listed in Table 3 and were ordered in standard desalted quality from Metabion (Planegg, Germany). Oligonucleotides for Gateway® Cloning were designed according to the manufacturer's Gateway® Technology manual (<https://tools.thermofisher.com/content/sfs/manuals/gatewayman.pdf>).

**Table 3:** Oligonucleotides with their respective sequence and purpose.

Oligonucleotide	5'-3' sequence	Purpose
16S-f	GTAAGCGTCTGTAGGTG	Northern Blot
16S-r	GCCTAGTATCCATCGTTT	Northern Blot
23S-f	TTCAAACGAGGAAAGGCTTA	Northern Blot
23S-r	AGGAGAGCACTCATCTTG	Northern Blot
35S-prom-f	GTTCAATTCATTTGGAGAGGACTC	Sequencing
35S-prom-r	GACTGGTGATTTTTGCGGAC	Sequencing
4.5S-f	CGAGACGAGCCGTTTATCAT	Northern Blot
4.5S-r	TTCAAGTCTACCGGTCTGTT	Northern Blot
accD-f	TCGCAATTCATATCGGATG	Northern Blot
accD-r	CTTCTTGCATTCGTGCTCCT	Northern Blot
At1g30475-CDS-C-D-f	ATGAAGACTTTACGGGTCTCACACCATG CCGGTAATGAATCCATC	Golden Gate®, Complementation
At1g30475-CDS-C-D-r	ATGAAGACTTCAGAGGTCTCACCTTTT AATGGTTGTTTCATGTTCCGCC	Golden Gate®, Complementation
EMB1303-3'UTR-r	CCGAGTATCACGGTTAAACAATC	Genotyping
EMB1303-attB-f	GGGG ACA AGT TTG TAC AAA AAA GCA GGC TTC ATGGCTATGGCGCGTCTAT	Gateway® Cloning, Complementation
EMB1303-attB-r	GGG GAC CAC TTT GTA CAA GAA AGC TGG GTC TCGCCTTCTGCTCCCTCGG	Gateway® Cloning,

		Complementation
EMB1303-f	TCTTTCTCACTCTATTAGCTCGCC	Genotyping, Sequencing
EMB1303-FL-attB-r	GGG GAC CAC TTT GTA CAA GAA AGC TGG GTC TTATCGCCTTCTGCTCCC	Gateway® Cloning, Complementation
EMB1303-prom-A-B-f	ATGAAGACTTTACGGGTCTCAGCGGACACTCCTT GCCAAGGCTAA	Golden Gate®, Complementation
EMB1303-prom-A-B-r	ATGAAGACTTCAGAGGTCTCACAGAGGCTAAAG CAGCTTGACGGG	Golden Gate®, Complementation
EMB1303-pSP65-f	CGAT GAATTC ATGGCTATGGCGGCGTC	<i>in vitro</i> import
EMB1303-pSP65-r	CGAT GTCGAC TTATCGCCTTCTGCTCC	<i>in vitro</i> import
EMB1303-r	TTATCGCCTTCTGCTCCCTC	Genotyping, Sequencing
EMB1303-TMD-attB-r	GGG GAC CAC TTT GTA CAA GAA AGC TGG GTC TTACCCACCCGACCAGTTG	Gateway® Cloning, Complementation
Gabi-8474	ATAATAACGCTGCGGACATCTACATTTT	Genotyping
GFP-r	CTCGCCGGACACGCTGAACTTG	Sequencing
M13-f	GTAAAACGACGGCCAGT	Sequencing
M13-r	GGAAACAGCTATGACCATG	Sequencing
pDONR207-f	TCGCGTTAACGCTAGCATGGATCT	Sequencing
pDONR207-r	GTAACATCAGAGATTTTGAGACAC	Sequencing
petA-f	CATATCCGATTTTTGCCCA	Northern Blot
petA-r	CTTTTCTTTCATCTCGGG	Northern Blot
pre-16S 3'-f	AGGGAGAGCTAATGCTTCTT	Northern Blot
pre-16S 3'-r	AACGAAAGAAGGCTTCCACC	Northern Blot
pre-16S 5'-f	TCGCTGTGATCGAATAAGAA	Northern Blot
pre-16S 5'-r	GCTTCCTTCTTCGTAGACAA	Northern Blot
psbD-f	TGGATGACTGGTTACGGA	Northern Blot
psbD-r	CTATTAATGCGAAAGCGCC	Northern Blot
pSP65-f	CACATACGATTTAGGTGACAC	Sequencing
pSP65-r	CAGCTATGACCATGATTACGC	Sequencing
ptNAP45-3'UTR-r	AGTCGTAATTGCAATTATAGCTGA	Genotyping
ptNAP45-attB-f	GGGG ACA AGT TTG TAC AAA AAA GCA GGC TTC ATGGCGAATTTACTGGAAAC	Gateway® Cloning,

		Complementation, Localization
ptNAP45-attB-r	GGG GAC CAC TTT GTA CAA GAA AGC TGG GTC GTTCAAAAAATCTTCAATAGTCG	Gateway® Cloning, Complementation, Localization
ptNAP45-f	ATGGCGAATTTACTGGAAAC	Genotyping, qPCR, Sequencing
ptNAP45-FL-attB-r	GGGGACCACTTTGTACAAGAAAG CTGGGTCTCCACCTCCGGATCAG TTCAAAAAATC	Gateway® Cloning, Complementation
ptNAP45-r	TCAGTTCAAAAAATCTTCAATAGTCG	Genotyping, qPCR, Sequencing
ptNAP45-RNAi-f	GGGGACAAGTTTGTACAAAAAAG CAGGCTTAGTTTAAACATTTT	Gateway® Cloning, RNAi
ptNAP45-RNAi-r	GGGGACCACTTTGTACAAGAAAG CTGGGTCTTTGTAAGTGACAGTG	Gateway® Cloning, RNAi
ptNAP45-TP-attB-f	GGGG ACA AGT TTG TAC AAA AAA GCA GGC TTC TTCATCAATGGAGGAAGAAAG	Gateway® Cloning, Localization
ptNAP45-TP-attB-f	GGGG ACA AGT TTG TAC AAA AAA GCA GGC TTC TTCATCAATGGAGGAAGAAAG	Gateway® Cloning, Localization
SAIL Lb	TAGCATCTGAATTTTATAACCAATCTCGATACAC	Genotyping
SALK Lb	ATTTTGCCGATTTTCGGAAC	Genotyping
SNARE AP-3' UTR-r	TGATTCTGAGTTGTTAAGTCTC	Genotyping
SNARE AP-attB-f	GGGGACAAGTTTGTACAAAAAAGCAGGC TTCATGCGCAGCCTCACTCTA	Gateway® Cloning, Complementation
SNARE AP-attB-r	GGGGACCACTTTGTACAAGAAAGCTGGGTC CTTTGCATCTCTTCTCATC	Gateway® Cloning, Complementation
SNARE AP-f	ATGCGCAGCCTCACTCTAG	Genotyping, RT-PCR, Sequencing
SNARE AP-prom-attb-f	GGGGACAAGTTTGTACAAAAAAGCAGGCTCT AACATCACTCACAAGATTCC	Gateway® Cloning, Complementation
SNARE AP-r	CTGGAAGCATACCCAACCAG	Genotyping, RT-PCR, Sequencing
SYTL5.2-f	TATAGAGGTGGGATTGAGAATTGG	Genotyping,

		Sequencing
SYTL5.2-r	CTCTCCGATACCAATAGCCA	Genotyping, Sequencing
T7-prom-f	TAATACGACTCACTATAGG	Sequencing
T7-prom-f	GCTAGTTATTGCTCAGCGG	Sequencing

### 2.1.9 Antisera

Primary  $\alpha$ -ptNAP45 antiserum (1:250 dilution used in 40 mM Tris/HCl pH 7.5, 270 mM NaCl, 0.05% (v/v) Tween 20) was generated against the full-length protein in rabbits by Pineda (Berlin, Germany). Previous overexpression and purification were performed by Dr. Roberto Espinoza-Corral. Further affinity purification of  $\alpha$ -ptNAP45 serum was conducted according to the Agrisera manual (<https://www.agrisera.com/en/info/affinity-purification-of-antibodies-low-amount-of-antigen-available.html>). Primary anti-GFP antibody (1:1,000 dilution) was purchased from Roche (Penzberg, Germany), while secondary anti-rabbit (1:20,000 dilution) as well as anti-mouse (1:20,000 dilution) antibodies coupled to horseradish peroxidase were purchased from Sigma-Aldrich (Taufkirchen, Germany). Antisera against PsbA, PsaF, LHCB1, LHCB5, RPL2, RPL4 and AtFtsH11-1 were purchased from Agrisera (<https://www.agrisera.com/>). ATP $\alpha/\beta$  synthase and D1 antisera were provided by Stephan Greiner, vATP synthase was obtained from Hans-Henning Kunz, Tic110 was provided by Bettina Bölter, PsbO (OE33) antiserum was obtained from Jörg Meurer and FBPase was provided by Jürgen Soll.

### 2.1.10 Computational analysis and software

Transmembrane domains were defined based on predictions by TMHMM2.0 (<http://www.cbs.dtu.dk/services/TMHMM/>). Amino acid sequence alignments were generated using BioEdit (version 7.2.6.1). Promoter regions were narrowed down using PlantPAN2.0 (<http://plantpan2.itps.ncku.edu.tw/>) and ChloroP 1.1 Prediction Server (<http://www.cbs.dtu.dk/services/ChloroP/>). NEB tools (<https://international.neb.com/tools-and-resources/interactive-tools>) were used for classical cloning, designing site-directed mutagenesis oligonucleotides and for calculating annealing temperatures. Potential restriction sites within coding regions were identified using RestrictionMapper (<http://www.restrictionmapper.org/>).

Sequences from *Arabidopsis* and *Synechocystis* were obtained from TAIR (<https://www.arabidopsis.org>) and CyanoBase (<http://genome.microbedb.jp/cyanobase>), respectively. Homologs from other species were collected from NCBI/BLAST (<http://blast.ncbi.nlm.nih.gov/Blast.cgi>) and Phytozome (<https://phytozome.jgi.doe.gov/pz/portal.ht>

ml). Phylogenetic trees were generated by using the CLC Main Workbench software (CLC bio, Aarhus, Denmark). Alignments were generated by using the algorithm provided by CLC Main Workbench (developed by QIAGEN Aarhus).

Microscopy images were taken and analysed using Leica Application Suite (version 4.1.0), Leica Application Suite X (version 3.3.0) or Leica Application Suite Advanced Fluorescence (version 2.6.3.8173) for fluorescent images. ImageQuant LAS 4000 (version 3.1) was used to detect chemiluminescent signals. Analysis of fluorescent images and general image analyses were done using ImageJ (version 1.51j8)/Fiji (1.52i).

## 2.2 Plant methods

### 2.2.1 Growth conditions for *Arabidopsis thaliana*, *Nicotiana benthamiana* and *Pisum sativum*

Seeds were either directly sown on soil or on half-strength Murashige and Skoog ( $1/2$  MS) medium plates (1% (w/v) sucrose, 0.238% (w/v) MS salts including vitamins, 0.05% (w/v) MES pH 5.7, 1% (w/v) Phytoagar). To ensure sterile conditions when growing on plates, seeds were surface sterilised using 0.05% (v/v) Triton X-100 in 70% (v/v) ethanol for 10 min prior to three times washing in 100% (v/v) ethanol and subsequent drying on sterile filter paper. To synchronise germination, seeds were stratified at 4°C for one to three nights in the dark, before being transferred to climate chambers featuring long day conditions (16 h 100  $\mu\text{mol photons m}^{-2} \text{s}^{-1}$ , 22°C, 8 h dark). Kanamycin and Hygromycin selection were performed with plants growing on  $1/2$  MS medium plates containing the respective amount of antibiotic (see Table 4). For BASTA® selection, plants were grown either on  $1/2$  MS medium plates or on soil with seedlings being sprayed after two to three weeks of growth.

To test different environmental conditions, respective plants were exposed to continuous low light (24 h 20  $\mu\text{mol photons m}^{-2} \text{s}^{-1}$ , 20°C), high light (24 h 1,000  $\mu\text{mol photons m}^{-2} \text{s}^{-1}$ , 20°C), fluctuating high light (24h 5 min 1,000  $\mu\text{mol photons m}^{-2} \text{s}^{-1}$  followed by 5 min 100  $\mu\text{mol photons m}^{-2} \text{s}^{-1}$ , 22°C) or cold conditions (16 h 100  $\mu\text{mol photons m}^{-2} \text{s}^{-1}$ , 8 h dark, 4°C) in the LED chambers. *Nicotiana benthamiana* plants were grown on soil under long day conditions in the greenhouse for four to six weeks. Peas (*Pisum sativum*) var. “Arvica” were ordered from Bayerische Futtersaatbau (Ismaning, Germany) and grown in climate chambers with long day conditions.

### 2.2.2 Isolation of genomic DNA from *Arabidopsis thaliana*

Single leaves of two- to three-week-old plants were homogenised in 500  $\mu\text{l}$  extraction buffer (1 M Tris/HCl pH 7.5, 0.05 M NaCl, 0.05 M EDTA pH 8.0, 1% (w/v) PVP-40) with a tungsten carbide ball using the TissueLyser (Qiagen). Afterwards, 66  $\mu\text{L}$  of 10% (w/v) SDS and 166  $\mu\text{l}$  5 M KOAc solution (3 M potassium acetate, 11.5% (v/v) glacial acetic acid pH 5.8) were added and the tubes were mixed by inverting. Samples were then centrifuged for 15 min at 16,200 g and the supernatant was transferred

to new tubes. Then, 0.7 volumes of isopropanol were added to each tube, mixed by inverting and incubated at -20°C for at least 30 min or overnight. Samples were again centrifuged for 15 min at 16,200 g, pellets were washed in 500 µl 70% (v/v) ethanol and centrifuged for 5 min at 16,200 g. The pellet was dried for 10 min at 50°C, dissolved in 45 µl ddH<sub>2</sub>O and stored at -20°C.

### 2.2.3 RNA extraction from *Arabidopsis thaliana* leaves

RNA was isolated from leaves of four- to five-week-old *Arabidopsis* plants using the RNeasy® Plant Mini Kit (Qiagen) according to manufacturer's instructions. Additionally, DNase I digest was performed for 30 min at room temperature. The resulting pellet was resuspended in 30 µl RNase free H<sub>2</sub>O. RNA concentration was measured, and RNA quality was investigated by loading samples onto 1% (w/v) agarose gels. RNA was stored at -80°C.

### 2.2.4 RNA extraction from *Arabidopsis thaliana* seeds

RNA from *Arabidopsis* seeds was performed as previously described (Footitt et al., 2018). Hydrated seeds were homogenised in 450 µl hot extraction buffer (100 mM Tris/HCl pH 8.0, 25 mM EDTA, 2 M NaCl, 2% (w/v) CTAB, 2% (v/v) PEG 20,000, 2% (v/v) β-mercaptoethanol) using a pellet pestle attached to an electric drill. Another 450 µl hot extraction buffer were immediately added before samples were mixed and incubated at 65°C for 15 min. Samples were put on ice, 500 µl chloroform were added and tubes were vortexed briefly. After centrifugation at 13,000 g for 10 min at 4°C, the upper supernatant was transferred to fresh tubes. Centrifugation was repeated and the supernatant was again transferred to a new tube. Half a volume of 100% isopropanol and half a volume of 1.2M NaCl/0.8 M tri-Na citrate dehydrate were added, samples were mixed gently and stored at RT for 15 min. RNA was recovered by centrifugation at 13,000 g for 10 min at 4°C. The supernatant was discarded, and the pellet was washed twice with ice-cold 75% (v/v) EtOH via centrifugation for 10 min at 13,000 g and 4°C. The resulting pellet was air-dried for 10 min and subsequently dissolved in 120 µl nuclease-free water. Seed RNA was stored at -80°C.

### 2.2.5 *Agrobacterium*-mediated transient expression of fluorescent proteins in *Nicotiana benthamiana*

Infiltration of four- to six-week-old *Nicotiana benthamiana* leaves as well as subsequent protoplast isolation were performed as described previously (Koop et al., 1996, Schweiger and Schwenkert, 2014). Transformed *Agrobacterium tumefaciens* cells were grown in selective LB medium, pelleted at 3,200 g and 4°C for 15 min and resuspended in infiltration medium (10 mM MES pH 6.0, 100 µM acetosyringone (in 60% (v/v) ethanol), 10 mM MgCl<sub>2</sub>) with an OD<sub>600</sub> of 1.0. Cells were rotated at room temperature for two to four hours in the dark and mixed in a 1:1 ratio in case of co-infiltration, before infiltrating tobacco leaves. Plants were covered overnight, and protoplasts were isolated after

two to three days growth. All centrifugation steps for protoplast isolation were performed at room temperature with low acceleration and deceleration. Osmolarity of buffers was adjusted to 550 mosmolkg<sup>-1</sup> and protoplasts were slowly pipetted with cut tips. One tobacco leaf was cut into small pieces in 10 ml enzyme solution (1% (w/v) cellulase Onozuka R10, 0.3% (w/v), macerozyme R10, 0.1% (w/v) BSA in F-PIN solution containing 10 mM KNO<sub>3</sub>, 3 mM CaCl<sub>2</sub>, 1.5 mM MgSO<sub>4</sub>, 1.2 mM KH<sub>2</sub>PO<sub>4</sub>, 20 mM NH<sub>4</sub>-succinate (4 M KOH pH 5.8, 2 M succinic acid, 2 M NH<sub>4</sub>Cl), 2 mM MES pH 5.8, 4.5 μM KI, 0.1 mM EDTA iron(III) sodium salt, 0.05 mM H<sub>3</sub>BO<sub>3</sub>, 60 μM MnSO<sub>4</sub>, 7 μM ZnSO<sub>4</sub>, 1 μM Na<sub>2</sub>MoO<sub>4</sub>, 0.1 μM CuSO<sub>4</sub>, 0.1 μM CoCl<sub>2</sub>, 120 gL<sup>-1</sup> (approximately 350 mM) sucrose). Leaf pieces were vacuum infiltrated for 30 sec and shaken at 40 rpm for 90 min in the dark on an orbital shaker. Protoplasts were released at 80 rpm for 1 min, filtered through a nylon mesh/gauze and overlaid with 2 ml F-PCN (same as F-PIN solution but 80 gL<sup>-1</sup> (approximately 440 mM) glucose instead of sucrose). Intact protoplasts accumulated at the interface between enzyme solution and F-PCN after 10 min at 70 g and were transferred to new tubes. Protoplasts were washed with 10 ml W5 buffer (125 mM CaCl<sub>2</sub>, 5 mM KCl, 2 mM MES pH 5.7, 7 gL<sup>-1</sup> (approximately 120 mM) NaCl). Protoplasts were pelleted for 10 min at 50 g and gently resuspended in 0.5 ml W5 buffer.

### 2.2.6 *Agrobacterium*-mediated stable expression of fluorescent proteins in *Arabidopsis thaliana*

Stable transfection of *Arabidopsis* plants was conducted by floral dip (Clough and Bent, 1998). 400 ml selective LB medium were inoculated with transformed *Agrobacterium tumefaciens* preculture and grown for 24 h at 28°C. Cells were pelleted at 2,800 g and 4°C for 20 min and solved in equal volume of sucrose solution (5% (w/v) sucrose, 0.05% (v/v) Silwet L-77). Four- to five-week-old plants were dipped into bacterial suspensions, covered overnight and then grown under greenhouse conditions. Floral dipping was repeated once after five to seven days.

### 2.2.7 Greening and chlorophyll measurement

Sterile seeds were densely put on 1/2 MS plates containing 1% (w/v) sugar and vernalised at 4°C overnight. Plates were then exposed to light (100 μmol photons m<sup>-2</sup>s<sup>-1</sup>) for 2 h and kept in the dark for 6 days to induce etiolation. Afterwards, the plates were illuminated for 0 h, 1 h, 4 h or 6 h, respectively, before transferring 200 mg leaf material each into 2 ml dimethylformamide. Chlorophyll was measured and normalised to fresh weight as previously described (Porra et al., 1989, Arnon, 1949).

### 2.2.8 Confocal microscopy

Fluorescent signals in leaves or protoplasts were detected at room temperature by confocal laser scanning microscopy (Leica TCS SP5, objective: HCX PL APO, magnification: 63x, imaging medium: glycerol) using the Leica Application Suite Advanced Fluorescence for image acquisition (Schweiger and

Schwenkert, 2014). Pictures were taken in 512 x 512 or 1024 x 1024 format (width x height) and a scan speed of 100 Hz. The maximum distance between stacks for z-stackings of isolated protoplasts was set at 0.5  $\mu\text{m}$ .

### 2.2.9 Analysis of chloroplast ultrastructure

The ultrastructure of chloroplasts was analysed via conventional transmission electron microscopy (TEM) following chemical fixation of two-week old or three-week-old plants with 2.5% (v/v) glutaraldehyde in 75 mM cacodylate buffer (including 2 mM  $\text{MgCl}_2$ , pH7) as described previously (Espinoza-Corral et al., 2019). After postfixation with 1% (w/v) osmium tetroxide for 1h, en bloc staining with 1% (w/v) uranyl acetate in 20% (v/v) acetone for 30 min and dehydration in a graded acetone series, the plant material was embedded in Spurr's resin. Transmission electron microscopy of ultrathin sections was carried out with a Zeiss EM 912 transmission electron microscope (Zeiss, Oberkochen, Germany), operated at 80 kV in the zero-loss mode. Images were acquired with a Tröndle 2k x 2k CCD camera (TRS Tröndle Restlichtverstärkersysteme, Moorenweis, Germany).

## 2.3 Molecular biological methods

### 2.3.1 Growth conditions for *Escherichia coli* and *Agrobacterium tumefaciens*

Bacterial strains were grown in LB medium (1% (w/v) peptone ex casein (tryptic digest), 0.5% (w/v) yeast extract, 1% (w/v) NaCl) and 160 rpm (Multitron and Minitron, INFORS HT). Solid media were supplemented with 1% (w/v) agar-agar. *Escherichia coli* were grown at 37°C overnight, while *Agrobacterium tumefaciens* cells were grown at 28°C for two to three days. Bacterial glycerol stocks were prepared with 25% (v/v) glycerol and subsequent freezing of the sample in liquid nitrogen for long term storage at -80°C. Required antibiotics used for selection are listed in Table 4.

**Table 4:** Antibiotics used for selection with their respective concentrations.

Antibiotic	Solvent	Stock concentration [mg ml <sup>-1</sup> ]	Final concentration [ $\mu\text{g ml}^{-1}$ ]
Ampicillin	ddH <sub>2</sub> O	100	100
BASTA	ddH <sub>2</sub> O	10	5
Carbenicillin	ddH <sub>2</sub> O	100	100
Gentamycin	ddH <sub>2</sub> O	10	20
Hygromycin	ddH <sub>2</sub> O	15	15
Kanamycin	ddH <sub>2</sub> O	50	50
Rifampicin	MeOH/DMSO	25	100

Spectinomycin	ddH <sub>2</sub> O	100	100
Streptomycin	ddH <sub>2</sub> O	100	100

### 2.3.2 Cloning strategies

Constructs were generated by traditional cloning, Gateway® Cloning, Golden Gate® Cloning or by site-directed mutagenesis and transformed into competent *Escherichia coli* Top10 cells. Colony PCR using DFS Taq-DNA polymerase was performed by directly adding individual colonies to the PCR reaction mix to confirm the presence of respective inserts. Proper insertion was verified by sequencing.

#### 2.3.2.1 Traditional cloning by restriction enzyme digest and ligation

Vectors and DNA fragments were double digested for 1 h at 37°C using appropriate restriction endonucleases based on the manufacturer's instructions (New England Biolabs). Digested samples were loaded onto 1% (w/v) agarose gels and subsequently purified using the NucleoSpin® Gel and PCR Clean-up Kit (Macherey-Nagel) according to the manufacturer's instructions. Ligation with T4 DNA Ligase was conducted for 3 h at room temperature based on the manufacturer's instructions (New England Biolabs) using 50 ng vector DNA and a vector to insert ratio of at least 1:3.

#### 2.3.2.2 Gateway® Technology based cloning

Gateway® Cloning was performed as described previously (Karimi et al., 2007, Karimi et al., 2002) and according to the manufacturer's instructions (Invitrogen, Carlsbad, USA). DNA fragments possessing respective *attB*-flanking sequences were cloned into the entry vector pDONR207 prior to transfer into binary destination vectors (pDEST14, pHGW, pH2GW7, pB7YWG2, pB7CWG2, pB7FWG2, pK7FWG2, pK7WIWG2).

#### 2.3.2.3 Golden Gate® based cloning

Golden Gate® Cloning was performed as described previously (Binder et al., 2014). Primary DNA fragments of the genes of interest were generated in the LI reaction. During LII reactions, different cassettes coding for respective promoters or resistances were assembled with the genes of interest resulting in the final constructs.

### 2.3.3 Sequencing

Sequencing of used plasmids and generated constructs was performed by the Sequencing Service of the Genomics Service Unit of the Ludwig-Maximilians-Universität München (<http://www.gi.bio.lmu.de/sequencing/help/index.html>). Required amounts of samples (compare to <http://www.gi.bio.lmu.de/sequencing/help/protocol>, sequencing service: Cycle, Clean & Run with BigDye v3.1 sequencing chemistry) were submitted in 10 mM Tris/HCl pH 8.5 with respective oligonucleotides.

#### 2.3.4 Amplification of DNA fragments by Polymerase chain reaction

PCR was performed with either plasmid DNA, genomic DNA or cDNA as templates using DFS-Taq DNA polymerase according to manufacturer's instructions. For generation of DNA fragments needed for subsequent cloning Phusion® High Fidelity DNA Polymerase was used based on manufacturer's instructions (New England Biolabs). Annealing temperature and elongation time were adjusted depending on used oligonucleotides and fragment length. Samples were run on 1% (w/v) agarose gels containing ethidium bromide in TAE buffer (40 mM Tris/HCl pH 8.0 – 8.5, 2.6 mM EDTA, 0.1% (v/v) acetic acid). Respective DNA fragments were excised under UV light and purified using the NucleoSpin® Gel and PCR Clean-up Kit (Macherey-Nagel) according to the manufacturer's instructions. Purified DNA was either frozen at -20°C or directly used for subsequent cloning.

#### 2.3.5 cDNA synthesis, RT-PCR and qPCR analysis

cDNA was synthesised from 1 µg RNA using the M-MLV Reverse transcriptase (Promega) according to manufacturer's instructions and was stored at -20°C. Subsequent reverse transcription PCR (RT-PCR) was conducted with 1 µg cDNA each using respective oligonucleotides (compare to Table 3). SYBR Green I-based real-time PCR (qPCR) was performed with the FastStart Essential DNA Green Master reaction mix (Roche, Penzberg, Germany) according to the manufacturer's instructions (<https://lifescience.roche.com/>).

#### 2.3.6 Transformation of *Escherichia coli*

Chemically competent cells were kindly provided by Tamara Bergius and Carina Engstler and prepared according to Hanahan (1983). Transformation of competent *Escherichia coli* cells was done using the heat shock method as previously described in Sambrook et al. (1989). *Escherichia coli* cells were thawed and incubated with 100 ng of plasmid DNA for 30 min on ice. After heat shock at 42°C for 60 s, the cells were first transferred on ice before adding 250 µL of LB medium (1% (w/v) tryptone, 0.5% (w/v) yeast extract, 1% (w/v) NaCl). Subsequently, the cells were grown for 1 h at 37°C shaking with 750 rpm (ThermoMixer®, Eppendorf). After a short centrifugation step of 3 min at 4,300 g, the supernatant was removed, and the pellet was resuspended in 100 µL LB medium. Cells were grown over night at 37°C on LB medium plates (1% (w/v) tryptone, 0.5% (w/v) yeast extract, 1% (w/v) NaCl, 1.5% (w/v) agar) containing appropriate antibiotics.

#### 2.3.7 Transformation of *Agrobacterium tumefaciens*

Chemically competent *Agrobacterium tumefaciens* cells were thawed on ice before 1 – 2 µg plasmid DNA were added. Cells were incubated for 5 min on ice, then 5 min in liquid nitrogen followed by 5 min heat shock at 37°C. 800 µL LB medium were added and cells were grown for 4 h at 28°C and 750 rpm

(ThermoMixer®, eppendorf). Cells were pelleted at 1,500 g for 2 min, resuspended in 100 µl LB medium and plated onto LB medium plates containing appropriate antibiotics.

### 2.3.8 Purification of plasmid DNA from *Escherichia coli*

Plasmid DNA was isolated from 4 ml overnight *Escherichia coli* cultures using the NucleoSpin Plasmid EasyPure kit (Macherey-Nagel) according to the manufacturer's instructions. Glycerol stocks were prepared mixing 750 µL sterile glycerol with 250 µL of the overnight *Escherichia coli* culture. After freezing in liquid nitrogen, glycerol stocks were stored at -80°C. Plasmid concentrations were determined using a Nanophotometer (IMPLEN) and isolated plasmid DNA was stored at -20°C.

## 2.4 Biochemical methods

### 2.4.1 Overexpression of recombinant proteins in *Escherichia coli*

*Escherichia coli* precultures were grown overnight to subsequently inoculate 1 L selective LB medium. Overexpression was induced at an OD<sub>600</sub> of 0.4 – 0.6 by 1 mM (w/v) IPTG. Cultures were grown overnight at 16°C. Cells were then pelleted for 15 min at 3,300 g and 4°C and used for subsequent protein purification.

### 2.4.2 Mass spectrometry

Mass spectrometric analysis (proteomics) was done at MSBioLMU core faculty (Mass Spectrometry of Biomolecules, Department Biology I, Ludwig-Maximilians-Universität München, for information concerning sample preparation compare to [http://www.en.biologie.uni-muenchen.de/core\\_facilities/massspectrometry/index.html](http://www.en.biologie.uni-muenchen.de/core_facilities/massspectrometry/index.html)) to identify putative interaction partners after immunoprecipitation. For subsequent evaluation, the score obtained from mass spectrometric analysis was aggregated for all protein sequences derived from the same accession number.

### 2.4.3 Isolation of total proteins

21 days old plants either grown on soil or on 1/2 MS medium plates were grinded in liquid N<sub>2</sub> and subsequently resuspended in total protein extraction buffer (50 mM Tris/HCl pH 8, 2% (w/v) LDS, 0.1 mM PMSF). The suspension was vortexed and incubated on ice for 30 min. After centrifugation at 16,000 g for 15 min at 4°C, the supernatant containing total proteins was transferred to a new tube. EDTA and DTT were added to a final concentration of 50 mM and 10 mM, respectively.

### 2.4.4 Isolation of soluble and membrane proteins from leaves

Leaves of 21 days old *Arabidopsis* plants were ground in liquid nitrogen, transferred to a beaker and mixed in equal volume of homogenization medium (10 mM EDTA, 2 mM EGTA, 50 mM Tris/HCl pH 8.0, 10 mM DTT, 1x protease inhibitor cocktail (Roche)). The homogenate was shortly stirred and then

incubated for 10 min on ice and in the dark for protein extraction before it was filtered through one layer of gauze. After a centrifugation step of 10 min with 27,000 g and at 4°C, the supernatant containing soluble proteins was transferred to new tubes and the pellet containing membrane proteins was resuspended in small amounts of homogenization buffer. Protein content was determined using the Bradford assay and samples were stored at -80°C.

#### 2.4.5 Determination of protein content by Bradford

Protein content was measured using the Bradford assay. Based on a calibration curve with bovine serum albumin (BSA), protein concentration was measured. Protein samples were diluted 1:10 with water or buffer before being added to 1 x Bradford reagent (0.1% (w/v) Coomassie brilliant blue G-250, 5% (v/v) ethanol, 10% (v/v) H<sub>3</sub>PO<sub>4</sub>). Absorption of each sample was measured at 595 nm in the photometer. All samples were measured as biological triplets.

#### 2.4.6 Chloroplast isolation from *Arabidopsis thaliana*

Chloroplasts were isolated according to Aronsson and Jarvis (2002) with the following modifications: 21-day-old plants grown on sugar plates were homogenised in 25 ml of isolation buffer (0.3 M sorbitol, 5 mM MgCl<sub>2</sub>, 5 mM EDTA, 20 mM HEPES/KOH pH 8.0, 10 mM NaHCO<sub>3</sub>, 50 mM ascorbic acid). After four rounds of homogenization and filtration, the combined homogenate was pelleted at 1,800 g in an HB-6 swing-out rotor (Sigma rotor 113901) for 4 min at 4°C and resuspended in isolation buffer. Resuspended chloroplasts were separated on a two-step Percoll gradient (30/82% (w/v) Percoll) at 1,800 g for 6 min at 4°C. The lower band comprising intact chloroplasts was washed in 50 mM HEPES/KOH, pH 8.0, 0.3 M sorbitol, 0.5 mM MgCl<sub>2</sub>. After a final wash, the chloroplasts were pelleted at 1,800 g for 4 min and resuspended in a small amount of wash buffer.

#### 2.4.7 Isolation of plastid sub-compartments from *Arabidopsis thaliana* chloroplasts

Chloroplasts from 2- or 3-week-old *Arabidopsis* plants were homogenised 250 ml in homogenization buffer (0.4 M sorbitol, 20 mM tricine, 10 mM EDTA, 5mM NaHCO<sub>3</sub>, 0.1% (w/v) BSA, pH 8.4) and filtered through two layers of gauze. The homogenate was pelleted at 1,465 g for 5 min, resuspended in 1 x resuspension buffer (0.4 M sorbitol, 20 mM HEPES, 2.5 mM EDTA, 5 mM MgCl<sub>2</sub>, 10 mM NaHCO<sub>3</sub>, 0.15% (w/v) BSA, pH 7.6) and separated on a Percoll gradient (100% Percoll mixed 1:1 with 2 x resuspension buffer (0.8 M sorbitol, 40 mM HEPES, 5mM EDTA, 10 mM MgCl<sub>2</sub>, 20 mM NaHCO<sub>3</sub>, 0.3% (w/v) BSA, pH 7.6)), centrifuged at 38,700 g for 55 min in a swing-out rotor (HB-6) at 13,300 g for 10 min. The lower band comprising intact chloroplasts was washed in resuspension buffer. The pelleted intact chloroplasts were resuspended in chloroplast burst buffer (10 mM HEPES, 5mM MgCl<sub>2</sub>, pH 7.6) and lysed in a dounce homogeniser with 50 strokes. Burst chloroplasts were loaded onto a three-step sucrose gradient (0.46M/1M/1.2M sucrose) and centrifuged at 58,000 g for 2 hours. The

resulting sub-compartments stroma, outer and inner envelope, envelope mix as well as thylakoids were transferred to new tubes. Envelope and mixed fraction were again centrifuged at 135,200 g for 1 h. All pellets were washed in chloroplast burst buffer.

#### 2.4.8 Thylakoid membrane association

In order to distinguish between a strong hydrophobic integral membrane association and weak electrostatic membrane complex association with the thylakoid membrane, thylakoids of *Arabidopsis* chloroplasts were isolated as described in 2.4.6 and subsequently treated with different salt conditions as described previously (Torabi et al., 2014). Immunoblotting revealed under which conditions proteins could be released into the supernatant or stayed attached to the thylakoid pellet, respectively.

#### 2.4.9 Chloroplast isolation from *Pisum sativum*

Chloroplasts from pea were isolated from leaves of pea seedlings and purified through Percoll density gradients as previously described (Waegemann and Soll, 1995). Leaves of 9-14 days old peas were mixed in isolation buffer (330 mM sorbitol, 20 mM MOPS, 13 mM Tris/HCl pH 7.6, 3 mM MgCl<sub>2</sub>, 0.1% (w/v) BSA) filtered and centrifuged for 1 min at 1,900 g, 4°C. Intact chloroplasts were isolated out of the pellet via a discontinuous Percoll gradient of 12 ml 40% Percoll solution (330 mM sorbitol, 50 mM HEPES/KOH pH 7.6, 40% (v/v) Percoll) and 8 ml 80% Percoll solution (330 mM sorbitol, 50 mM HEPES/KOH pH 7.6, 80% (v/v) Percoll) for 5 min at 8,000 g, 4°C and washed twice with washing buffer (330 mM sorbitol, 25 mM HEPES/KOH pH 7.6, 3 mM MgCl<sub>2</sub>). For determination of the chlorophyll content, samples were mixed with 80% (v/v) acetone in a 1:1,000 ratio. Extinction at 645 nm, 663 nm and 750 nm was measured and chlorophyll content was calculated using the following formula (Arnon, 1949):

$$\text{mg chlorophyll / ml} = 8.02 \times (E_{663} - E_{750}) + 20.2 \times (E_{645} - E_{750})$$

#### 2.4.10 *In vitro* transcription and translation

*In vitro* transcription and translation were performed simultaneously according to the TNT® Coupled Reticulocyte Lysate System (Promega, Fitchburg, USA) according to manufacturer's instructions. In some cases, 0.5 mM MgOAc was added to increase protein expression. The reaction mix was incubated for 90 min at 30°C.

#### 2.4.11 *In vitro* import into chloroplasts of *Pisum sativum*

A standard import assay into chloroplasts equivalent to 20 µg chlorophyll was performed in 100 µl import buffer (2 mM ATP, 10 mM methionine, 10 mM cysteine, 20 mM potassium gluconate, 10 mM NaHCO<sub>3</sub>, 3 mM MgSO<sub>4</sub>, 330 mM sorbitol, 50 mM HEPES/KOH pH 7.6, 0.2% (w/v) BSA) containing 10% of *in vitro* translated radiolabelled protein. Import was initiated by addition of

chloroplasts to the import mixture and was incubated at 25°C for 15 min. Chloroplasts were centrifuged at 4,500 g for 5 min, washed twice in wash buffer (330 mM sorbitol, 50 mM HEPES /KOH pH 7.6, 3 mM MgCl<sub>2</sub>) and either resuspended in loading buffer or treated with thermolysin to remove precursor proteins. Samples were analysed by SDS-PAGE and autoradiography.

#### 2.4.12 Detection of radiolabelled proteins

Radiolabelled proteins were visualised by overnight exposure of dried, Coomassie stained SDS-PAGE gels or dried BN PAGE gels on BAS-MS imaging plates (Fujifilm) and detected by a Typhoon Trio Variable Mode Imager (Amersham Biosciences).

#### 2.4.13 Isolation of plastid sub-compartments from *Pisum sativum* chloroplasts

Chloroplasts of pea were isolated as described in 2.4.9. Chloroplasts equivalent to 500 µg of chlorophyll were pelleted for 1 min at 1,900 g, taken up in tricine buffer (20 mM tricine pH 7.6, 5 mM MgCl<sub>2</sub>) and incubated on ice for at least 20 min. In the meantime, sucrose gradients (35% /w/v sucrose/15% (w/v) sucrose, each solved in tricine buffer) were prepared. 1 ml of the lysed chloroplast suspension was loaded on each gradient and the samples were centrifuged at 134,000 g (TH660 rotor) for 2 h. Stroma accumulated on top of the gradient, while envelope membranes could be taken from the 15%/35% interface. Stroma was precipitated by adding four volumes of ice cold 100% acetone and subsequent centrifugation for 15 min at 36,500 g. The supernatant was discarded, the pellet was air-dried and resuspended in 5 x SDS sample buffer. Envelopes were washed in tricine buffer and pelleted for 10 min at 86,500 g (TH660 rotor). The thylakoid pellets were also resuspended in tricine buffer. Envelope and thylakoid fractions were also mixed with 5 x SDS sample buffer. Samples were analysed by SDS-PAGE and immunodetection or autoradiography, respectively.

#### 2.4.14 Size exclusion chromatography (SEC) of native pea stroma

Chloroplasts from pea were isolated as described in section 2.4.9. Chloroplasts were pelleted at 1,900 g for 1 min at 4°C to fully remove the remaining wash buffer. Chloroplasts were taken up in lysis buffer (10 mM HEPES/KOH pH 7.6, 5 mM MgCl<sub>2</sub>) and burst by passing the chloroplast suspension 30 times through a needle. Membranes were pelleted by centrifugation at 3,000 g for 3 min followed by 46,000 g for 10 min at 4°C. Five milligram of either untreated or RNase ONE-treated (Promega, Fitchburg, WI, USA; 1 h on ice) stroma extracts were fractionated by SEC using a Superose 6 10/300 Increase GL column (GE Healthcare, Little Chalfont, UK) and an ÄKTA FPLC system (Amersham Biosciences, Little Chalfont, Buckinghamshire, UK) as described previously (Olinares et al., 2010). Fractions (1 ml) were separated on a 12% SDS-PAGE. Size of complexes were determined using the Gel Filtration HMW Calibration Kit (GE Healthcare, Little Chalfont, UK).

### 2.4.15 SDS-Polyacrylamide gel electrophoresis and immunoblotting

Proteins were separated by sodium dodecyl sulphate (SDS) polyacrylamide gel electrophoresis (PAGE) and either transferred onto PVDF membranes (Millipore) for subsequent immunodetection or stained with Coomassie.

#### 2.4.15.1 SDS-Polyacrylamide gel electrophoreses

SDS-PAGE was performed according to Laemmli (1970) using a 5% stacking gel (125 mM Tris/HCl pH 6.8, 0.1% (w/v) SDS, 5% (w/v) acrylamide, 0.1% (w/v) APS, 1% (v/v) TEMED) and a 10 – 15% separating gel (390 mM Tris/HCl pH 8.8, 0.1% (w/v) SDS, 10 – 15% (w/v) acrylamide, 0.1% (w/v) APS, 1% (v/v) TEMED). Protein samples were mixed with SDS sample buffer (62.5 mM Tris/HCl pH 6.8, 2% (w/v) SDS, 10% (v/v) glycerol, 5% (v/v)  $\beta$ -mercaptoethanol, 0.004% (w/v) bromophenol blue), heated at 95°C for 5 min or 80°C for 10 min for membrane proteins and loaded onto the gel. Gels were run at 35 mA per gel in SDS running buffer (25 mM Tris, 192 mM glycine, 0.1 % SDS).

#### 2.4.15.2 2<sup>nd</sup> dimension SDS-Polyacrylamide gel electrophoreses

Blue native (BN) PAGE was performed as described in 2.4.16. BN PAGE lanes were incubated in SDS solution (67 mM SDS, 67 mM Na<sub>2</sub>CO<sub>3</sub>). Subsequently, one 1<sup>st</sup> dimensional BN PAGE lane was applied on a 2<sup>nd</sup> dimensional SDS-PAGE with a 5% stacking gel (125 mM Tris/HCl pH 6.8, 0.1% (w/v) SDS, 5% (w/v) acrylamide, 0.1% (w/v) APS, 1% (v/v) TEMED) and a 12 – 15% separating gel (390 mM Tris/HCl pH 8.8, 0.1% (w/v) SDS, 12 – 15% (w/v) acrylamide, 4 M urea, 0.1% (w/v) APS, 1% (v/v) TEMED). Gels were run over night at RT with a current of 5 mA per gel in SDS running buffer (25 mM Tris, 192 mM glycine, 0.1% (w/v) SDS).

#### 2.4.15.3 Coomassie staining

SDS-PAGE gels were stained with Coomassie staining solution (45% (v/v) methanol, 9% (v/v) acetic acid, 0.2% (w/v) Coomassie brilliant blue R-250), destained (45% (v/v) methanol, 9% (v/v) acetic acid) and dried for storage or further analysis.

#### 2.4.15.4 Semi-dry western blot

Proteins were transferred from SDS-PAGE gels onto PVDF membranes by semi-dry electro blotting. All components were assembled on the anode as follows: one blotting paper soaked in anode buffer I (0.3 M Tris/HCl pH 10.4, 20% (v/v) methanol), two blotting paper soaked in anode buffer II (25 mM Tris/HCl pH 10.4, 20% (v/v) methanol), PVDF membrane (activated in 100% (v/v) methanol and washed in anode buffer II), SDS-PAGE gel soaked in cathode buffer (25 mM Tris/HCl pH 9.4, 40 mM 6-aminohexanoic acid, 20% (v/v) methanol) and three blotting paper soaked in cathode buffer. Transfer was performed for 1 h and 0.8 mAcm<sup>-2</sup>. Subsequently, proteins were visualised with Ponceau

staining solution (5% (v/v) acetic acid, 0.3% (w/v) Ponceau S) or Coomassie staining (25% (v/v) MeOH, 10% (v/v) acetic acid, 0.02% (w/v) Coomassie brilliant blue G-250).

#### 2.4.15.5 Immunodetection

PVDF membranes were blocked in 5% (w/v) milk in TBS-T (20 mM Tris/HCl pH 7.5, 135 mM NaCl, 0.05% (v/v) Tween 20) for 1 h. Membranes were washed in TBS-T three times for 10 min. Incubation with the respective primary antibodies was either conducted for 2 h at room temperature or at 4°C overnight. Membranes were again washed as described before and subsequently incubated with the secondary antibody either for 1 h at RT or at 4°C overnight. ECL (enhanced chemiluminescence) developing solutions (developing solution I: 100 mM Tris/HCl pH 8.5, 1% (w/v) luminol, 0.44% (w/v) coumaric acid; developing solution II: 100 mM Tris/HCl pH 8.5, 0.018% (v/v) H<sub>2</sub>O<sub>2</sub>) were mixed in equal volumes and added onto the membrane. The chemiluminescent signal was detected using ImageQuant LAS 500/4000 (GE Healthcare).

#### 2.4.16 Blue native (BN) polyacrylamide gel electrophoresis

BN-PAGE was performed as described previously (Schägger and von Jagow, 1991, Kikuchi et al., 2011, Nickel et al., 2016). For BN PAGE, chloroplasts, or thylakoids equivalent to 30 µg chlorophyll per lane or stroma equivalent to 100 µg protein content were used. Stromal extracts were used in their native form, while chloroplasts and thylakoid membranes first had to be solubilised. For solubilization samples were centrifuged at 4°C for 3 min at 9,000 g. The supernatant was discarded, and the pellet was resuspended in 80 µL ACA buffer (750 mM ε-aminocaproic acid, 50 mM Bis-Tris pH 7.0, 0.5 mM EDTA) and 9 µL 10% (w/v) n-dodecyl β-D-maltoside (β-DM) and incubated on ice for 10 min for solubilization. After a centrifugation step at 4°C and 50,000 g for 10 min, the supernatant was mixed with 5 µL loading buffer (750 mM ε-aminocaproic acid, 5% (w/v) Coomassie brilliant blue G-250). For conduction of BN PAGE, a gradient separating gel covering the range from 5% to 15% and a 5% stacking gel were poured. The gel was run at 30 V over night at 4°C in anode buffer (50 mM Bis-Tris pH 7.0) and blue cathode buffer (50 mM Tricine, 12 mM Bis-Tris pH 7.0, 0.2% (w/v) Coomassie brilliant blue G-250). After the gel reached half of the run, the blue cathode buffer was replaced by a cathode buffer without Coomassie brilliant blue (50 mM Tricine, 15 mM Bis-Tris pH 7.0) and the run was finished at 300 V at 4°C.

#### 2.4.17 Northern blot

Total cellular RNA was extracted as described in 2.2.3. 5 µg RNA of each sample were separated on 1% denaturing formaldehyde agarose gels. The agarose gel was rinsed twice in buffer 20 x SSC (3M NaCl, 300 mM sodium citrate pH 7) and placed onto wet Whatman paper connected to a beaker with 20 x SSC buffer. After separation, nucleic acids were transferred by capillarity overnight at room temperature onto positively charged nylon membranes (Roti®-Nylon plus, pore size 0.45 µm, Carl Roth

GmbH, Mannheim, Germany) followed by UV light cross-linking (UV Crosslinker, UVC 500, Hoefer Inc., San Francisco, USA). The northern blot was hybridised with probes either obtained by PCR using Digoxigenin-11-UDP (Roche, Basel, Switzerland) or ready-to-use probes that were kindly provided by Jörg Nickelsen. The membrane was transferred into a tube containing prewarmed (30 min, 68°C) hybridization buffer (0.25 M Na<sub>2</sub>HPO<sub>4</sub> pH 7.2, 1 mM EDTA, 20% (w/v) SDS, 0.5% (w/v) Blocking reagent [10 g Blocking (Roche) in 0.1 M maleic acid pH 8, 0.15 M NaCl]) and incubated for 1 h at 68°C. Denaturation of DIG-labelled probes was achieved by adding 25 ng of the respective probe to 100 µl water followed by incubation for 10 min at 99°C. Probes were then immediately placed on ice for 5 min before adding them to the membrane in hybridization buffer. Hybridization was performed overnight at 68°C. Membranes were subsequently washed three times for 20 min each with pre-heated hybridization wash buffer (20 mM Na<sub>2</sub>HPO<sub>4</sub>, 1 mM EDTA, 1% (w/v) SDS) at 65°C followed by washing in buffer I (0.1 M maleic acid pH 8.0, 3 M NaCl, 0.3% (v/v) Tween 20) at room temperature. Then, membranes were transferred to blocking buffer II (19 ml wash buffer I plus 1 ml 20 x blocking) and incubated for 1 h at room temperature. For immunodetection, conjugate buffer III was prepared by diluting α-DIG-AP 1: 20,000 with blocking buffer II (0.5 µl antibody / 10 ml). The membrane was incubated for 1 h in conjugate buffer containing α-DIG-AP and then washed four times for 10 min with buffer I. Then the membrane was incubated for 5 min in substrate buffer IV (0.1 M Tris-HCl pH 9.5, 0.1 M NaCl, 50 mM MgCl<sub>2</sub>) before signals were detected by ImageQuant LAS 500/4000 (GE Healthcare) after exposure using an alkaline-phosphatase conjugated anti-DIG antibody (Roche) and CDP\* (Roche) as reaction substrate.

### 3. Results

#### 3.1 SNARE AP

SNARE AP (At1g22850) was found in a bioinformatic screen in order to identify novel putative homologs of cytosolic vesicle trafficking components in plastids (Khan et al., 2013).

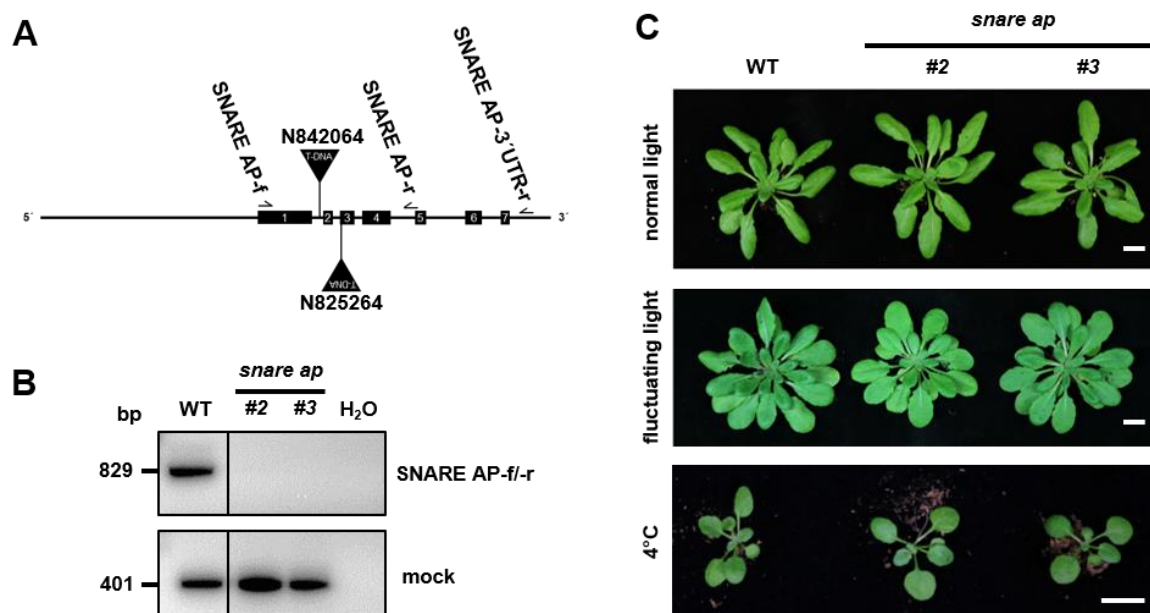


**Figure 7: Characterization of two *snare ap* T-DNA insertion lines.** **A** Gene structure of SNARE AP (At1g22850) and location of the respective T-DNA insertions in intron 1 for SAIL\_1144\_G11 (N842064) and exon 3 for SAIL\_593\_G09 (N825264). Exons are indicated by black boxes, T-DNA insertions are marked by black triangles. **B** RT-PCR for SNARE AP and the control ptNAP45-like using WT and both *snare ap* mutants. Oligonucleotide binding sites for SNARE AP-f, SNARE AP-r and SNARE AP-3'UTR-r are marked in **A**. **C** Phenotypes of WT and both *snare ap* mutant lines in different conditions. Plants grown under normal light as well as 4°C are four weeks old, plants grown under fluctuating light are eight weeks old. Scale bars represent 1cm.

Two T-DNA insertion lines, SAIL\_1144\_G11 (N842064, *snare ap* #2) and SAIL\_593\_G09 (N825264, *snare ap* #3), were used to investigate the consequences of a loss of SNARE AP. In a first step, homozygous mutants were identified through genotyping and the positions of the respective T-DNA insertions in intron 1 for *snare ap* #2 and in exon 3 for *snare ap* #3 were confirmed by sequencing (Fig. 7A). In addition, RT-PCR was performed to prove that both homozygous mutant lines were true knock-outs (Fig. 7B). Phenotype analyses under different light and climate conditions were performed to get a first impression of a possible function of SNARE AP. However, no specific phenotype could be detected under any of the conditions tested. Under normal light conditions, both mutant lines grew exactly the same as WT plants. When exposed to stressful fluctuating light, *snare ap* #2 seemed to be

slightly paler than WT, but this could not be confirmed by *snare ap #3*. Also, in cold conditions at 4°C, no difference between WT and mutant plants occurred in the course of the experiment (Fig. 7C).

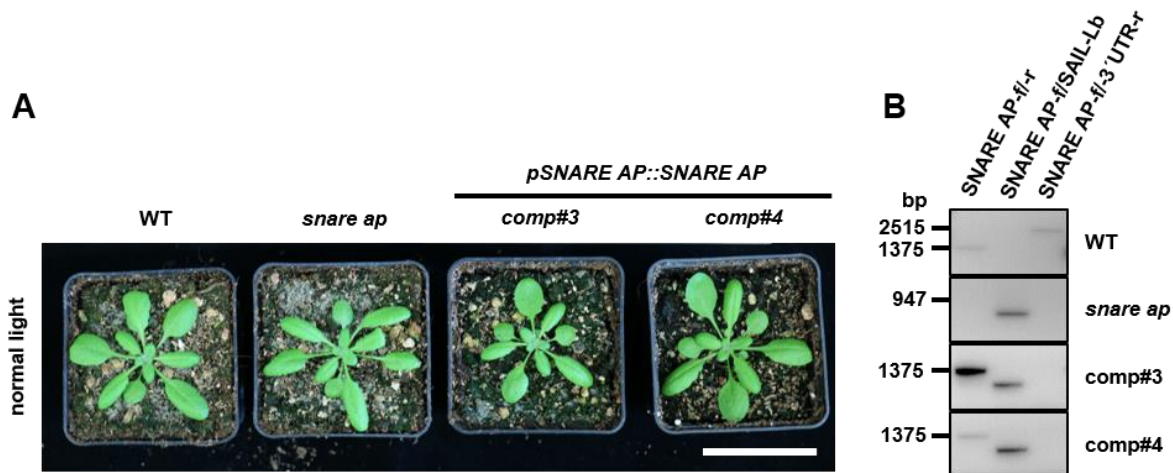


**Figure 8: Complementation of a *snare ap* T-DNA insertion line.** **A** Phenotype of three-week old WT, *snare ap* and complemented lines *pSNARE AP::SNARE AP comp#3* and *comp#4*. Scale bar represents 5 cm. **B** Genotyping PCR for WT, *snare ap* plants as well as complementation lines *comp#3* and *comp#4*. Binding sites of the used oligonucleotides are indicated in Fig. 7A.

Even though no obvious phenotype could be observed for *snare ap*, mutant plants were complemented. For this purpose, SNARE AP under the control of its endogenous promoter was transformed into *snare ap #3* mutant plants. The two resulting independent complemented lines *pSNARE AP::SNARE AP comp#3 (comp#3)* and *pSNARE AP::SNARE AP comp#4 (comp#4)* showed no difference to WT plants. (Fig. 8A). The presence of respective transcripts was confirmed by genotyping for *comp#3* and *comp#4* (Fig. 8B).

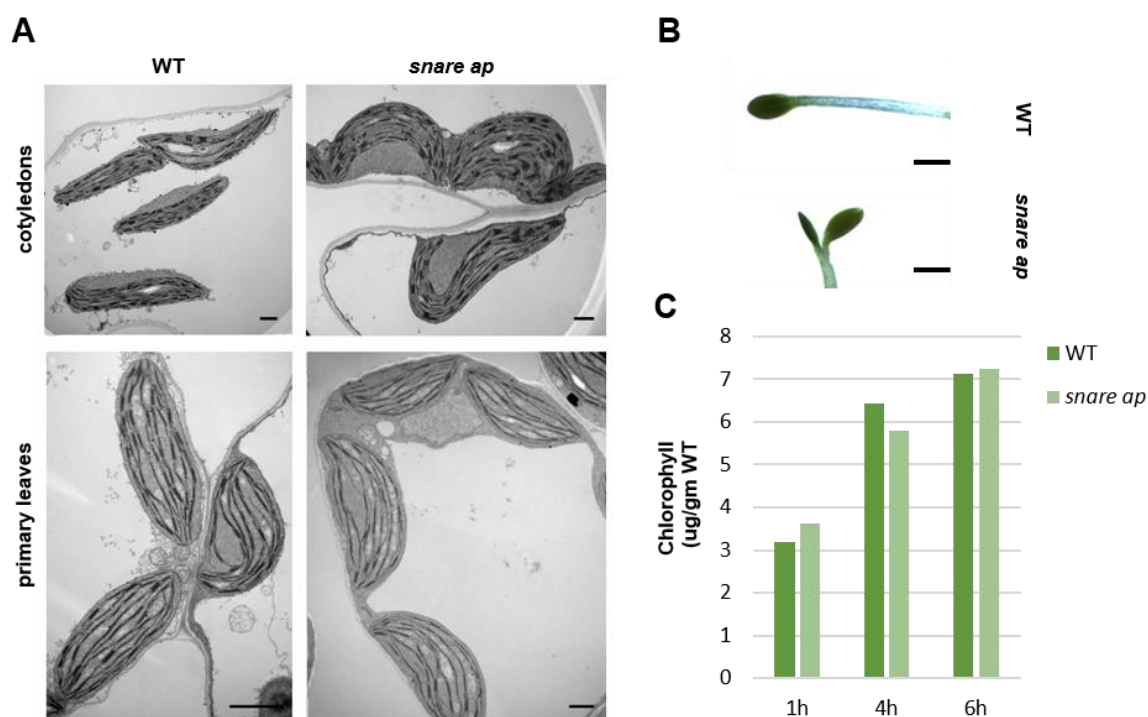


**Figure 9: Chloroplast ultrastructure and greening of WT and *snare ap* mutant plants.** **A** Cotyledons and primary leaves of two-week old WT and *snare ap* plants were given to TEM analyses. Pictures were taken by Prof. Dr. Andreas Klingl. Scale bars represent 1,000 nm. **B** WT and *snare ap* plants were grown for six days in the dark before getting exposed to light for 1 h, 4 h and 6 h, respectively. Binocular picture of early WT and *snare ap* cotyledons after 4 h of illumination. Scale bars represent 500  $\mu$ m. **C** Chlorophyll content of etiolated WT and *snare ap* seedlings after 1 h, 4 h and 6 h of illumination.

To gain a deeper understanding of a putative role of SNARE AP in the chloroplast, TEM was performed. The ultrastructure of cotyledons and primary leaves was analysed for WT and mutant plants, respectively. Neither cotyledon chloroplasts nor leaf chloroplasts of *snare ap* showed any difference to the ones of WT plants. Chloroplasts were in all cases normally shaped with the typical thylakoid pattern consisting of grana stacks and stroma lamellae (Fig. 9A).

Moreover, greening of *snare ap* mutant plants was investigated. After germination, plants were grown in the dark for several days before greening was initiated by light. As in the experiments before, no difference could be observed compared to WT. In both cases, plants showed the same green leaves (Fig. 9B) and chlorophyll content increased over the period of prolonged light exposure (Fig. 9C).

### 3.2 SYTL5.2/AtNTMC2T5.2

SYTL5.2 (At3g19830) has first been identified in a membrane proteomic analysis of our group. To gain insights into its putative function for the chloroplast, two T-DNA insertion lines named GK-456H02 (N443767, *sytl5.2* GK) and SALK\_003927 (N503927, *sytl5.2* SALK) were ordered.

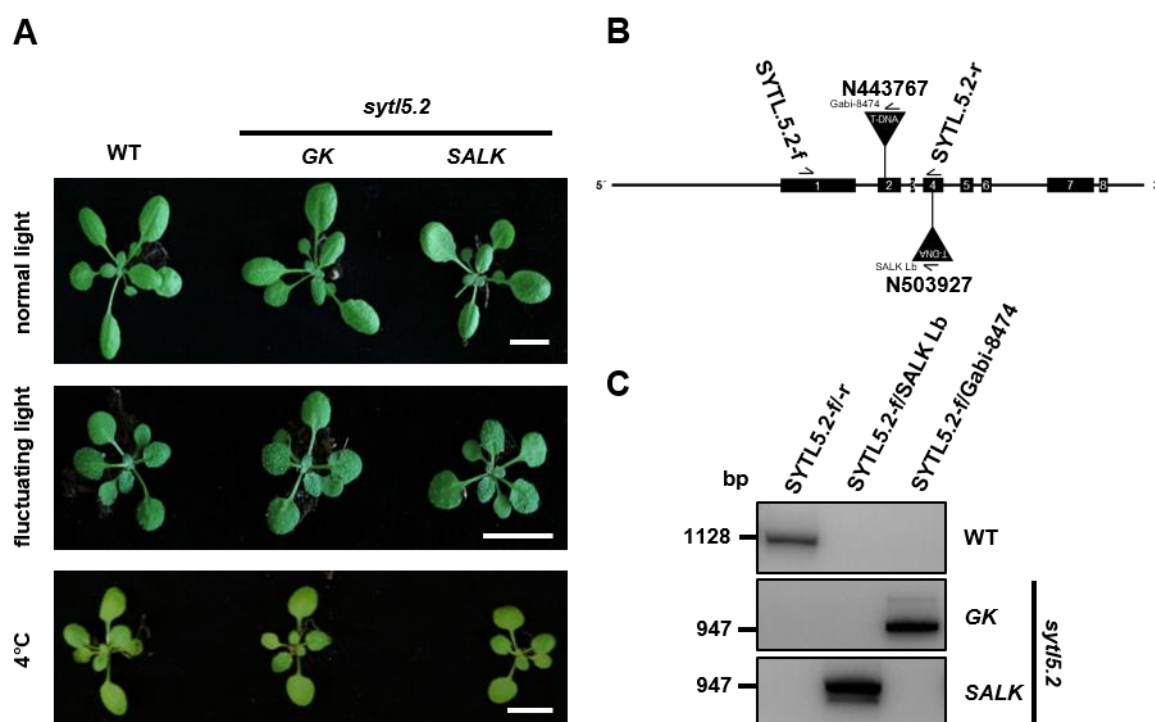


**Figure 10: Characterization of two *sytl5.2* T-DNA insertion lines.** **A** Phenotypes of WT and *sytl5.2* mutant lines in different conditions. Plants grown under normal light as well as under fluctuating light are three weeks old, plants grown in 4°C are four weeks old. Scale bars represent 1cm. **B** Gene structure of SYTL5.2 (At3g19830) and location of the respective T-DNA insertions in exon 2 for GK-456H02 (N443767, *sytl5.2* GK) and exon 4 for SALK\_003927 (N503927, *sytl5.2* SALK). Exons are indicated by black boxes, T-DNA insertions are marked by black triangles. **C** Genotyping PCR for WT, *sytl5.2* GK and *sytl5.2* SALK plants. Binding sites of the used oligonucleotides are indicated in **B**.

For phenotype analyses, WT plants and both mutant lines were grown under normal conditions as well as light and cold stress. A specific phenotype for *sytl5.2* GK or *sytl5.2* SALK could be observed in none of the mentioned setups as all mutants looked exactly like WT plants (Fig. 10A). To confirm the predicted positions of the respective T-DNA insertions in exon 2 for *sytl5.2* GK and in exon 4 for *sytl5.2* SALK, genotyping PCR was run on DNA of homozygous mutants (Fig 10B/C).

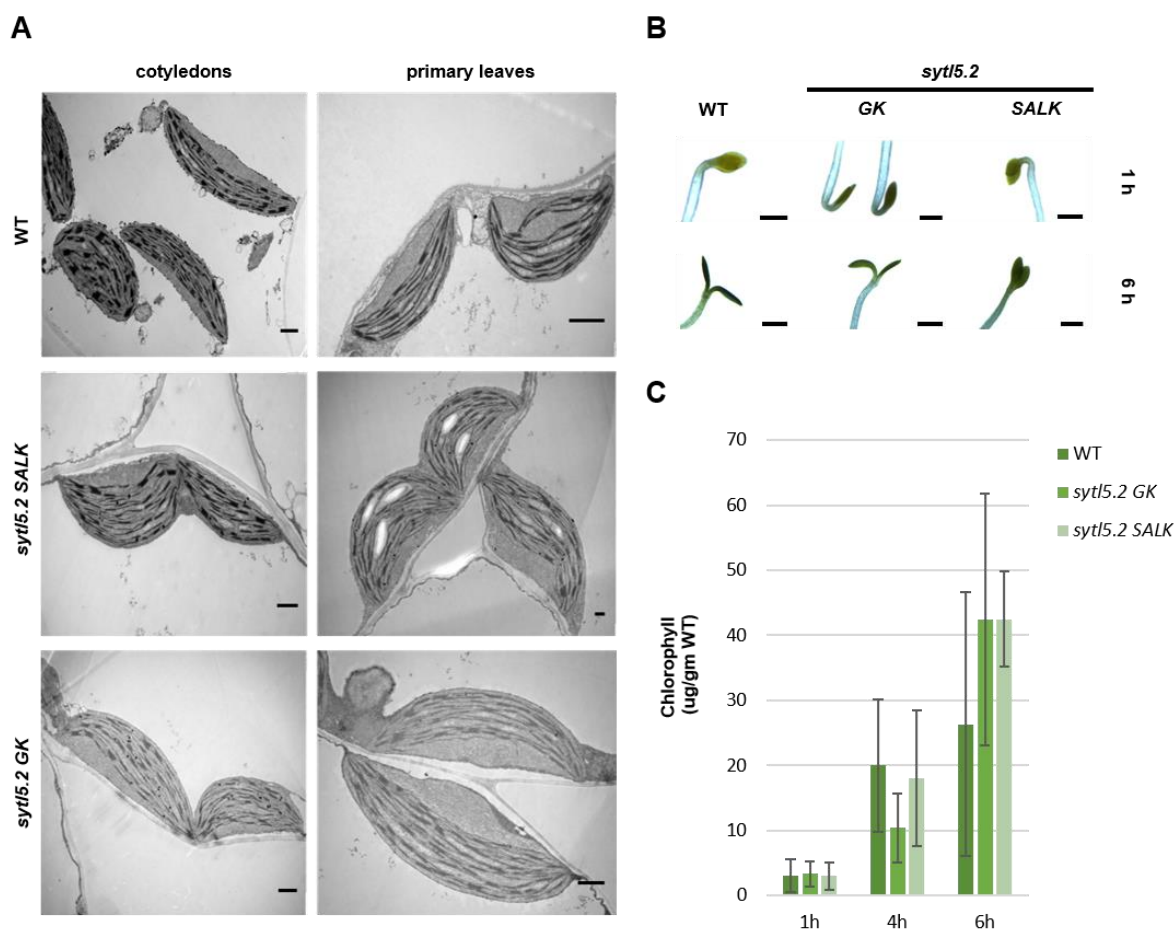


**Figure 11: Chloroplast ultrastructure and greening of WT and *syt15.2* mutant plants.** **A** Cotyledons and primary leaves of two-week old WT, *syt15.2 SALK* and *syt15.2 GK* plants were given to TEM analyses. Pictures were taken by Prof. Dr. Andreas Klingl. Scale bars represent 1,000 nm. **B** WT, *syt15.2 SALK* and *syt15.2 GK* plants were grown for six days in the dark before getting exposed to light for 1 h, 4 h and 6 h, respectively. Binocular pictures of early WT, *syt15.2 SALK* and *syt15.2 GK* cotyledons after 1 h and 6 h of illumination. Scale bars represent 500  $\mu$ m. **C** Chlorophyll content of etiolated WT, *syt15.2 SALK* and *syt15.2 GK* seedlings after 1 h, 4 h and 6 h of illumination. Biological triplicates were measured for each time point and plant line, respectively.

Although no phenotype could be observed, the ultrastructure of chloroplasts in *syt15.2* loss-of-function mutants was still of interest. However, as with SNARE AP, TEM revealed no differences between WT and mutants, neither in cotyledons nor primary leaves. Chloroplast shape and thylakoid structure were fully intact in *syt15.2 SALK* as well as *syt15.2 GK* (Fig. 11A). Also, during greening, no deviation from the WT could be observed. Leaves depicted the same green shades for all plants both at the beginning of greening after one hour of light exposure and at the end after six hours of light exposure (Fig. 11B). The chlorophyll content was also not significantly different between WT and mutants, although some of the variations in the triplet measurements were very high. In all cases, it increased with extended light duration (Fig. 11C).

### 3.3 EMB1303

For a database analysis to identify other possible SNARE-like proteins in the chloroplast, all nuclear-encoded plastid genes were screened for one single C-terminal transmembrane domain. Of the 180 possible proteins, the most promising were selected based on their size, sequence, and structural prediction. One of the most interesting proteins was EMB1303 (At1g56200). The chloroplast protein EMB1303 has previously been described as seedling lethal albino mutant required for chloroplast development in *Arabidopsis thaliana* (Huang et al., 2009). To gain a deeper understanding of its molecular function and its role as a putative SNARE protein in chloroplasts, the T-DNA insertion line GK-586E02 (N454482, *emb1303*) was used to investigate the consequences of a loss of EMB1303.

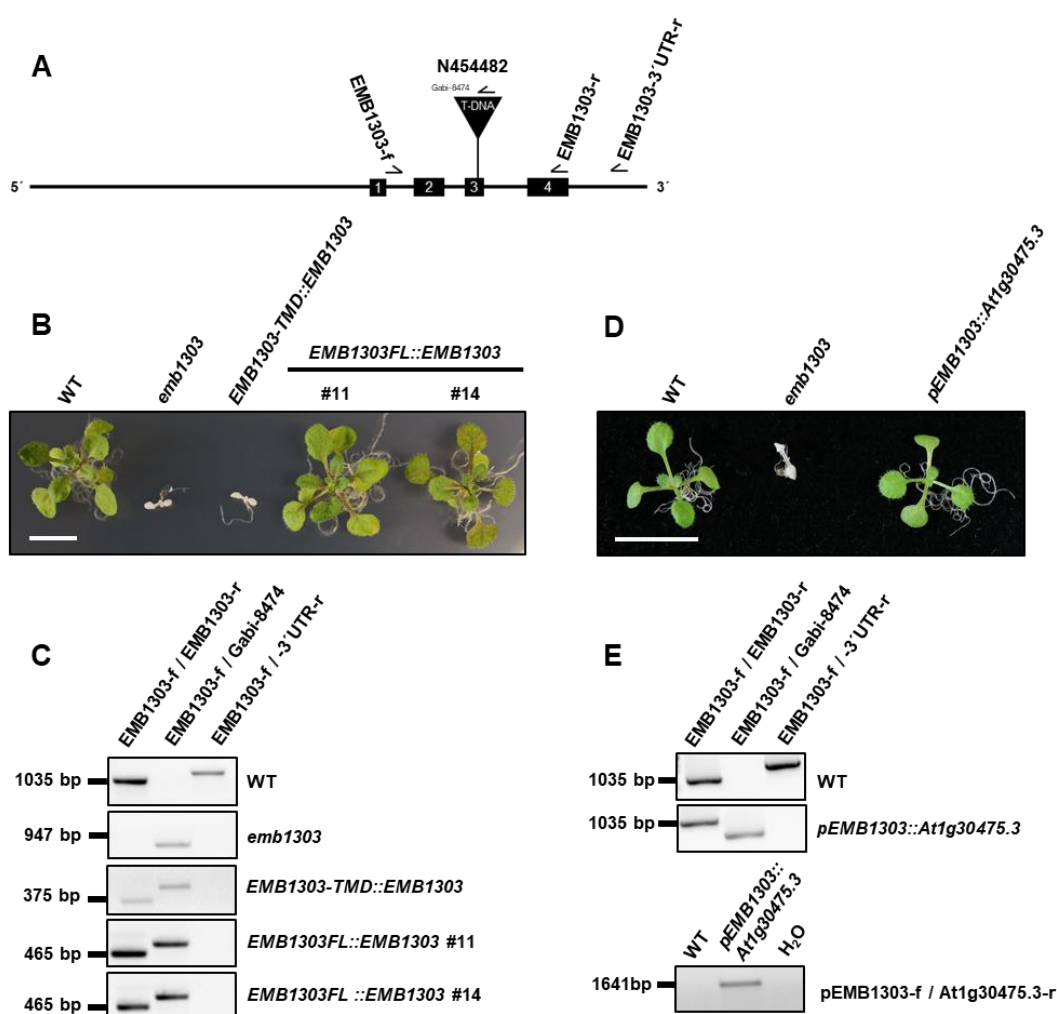


**Figure 12: Characterization and complementation of an *emb1303* T-DNA insertion line.** **A** Gene structure of EMB1303 (At1g56200) and location of the respective T-DNA insertions in exon 3 for GK-568E02 (N454482). Exons are indicated by black boxes, T-DNA insertions are marked by black triangles. **B** Phenotype of four-week-old WT and *emb1303* as well as the complementation lines *EMB1303-TMD::EMB1303* (-TMD), *EMB1303FL::EMB1303* #11 (#11) and *EMB1303FL::EMB1303* #14 (#14) grown on 1% sugar plates. Scale bar represents 1cm. **C** Genotyping PCR for WT, *emb1303* and the complementation lines -TMD, #11 and #14. Oligonucleotide binding sites are indicated in A.

**D** Phenotype of three-week-old WT and *emb1303* as well as the complementation line *pEMB1303::At1g30475.3* grown on 1% sugar plates. Scale bar represents 1cm. **E** Genotyping PCR for WT, *emb1303* and the complementation line *pEMB1303::At1g30475.3*. Oligonucleotide binding sites are indicated in **A**.

The predicted position of the T-DNA insertion in exon 3 and the used oligonucleotides for subsequent genotyping are schematically represented in Fig. 12A. Phenotypic analyses confirmed the seedling lethality of *emb1303* on soil (data not shown) as well as the albino mutant phenotype on 1% sugar plates (Fig. 12B). The absence of *EMB1303* in homozygous *emb1303* plants was confirmed by genotyping PCR (Fig. 12C). For complementation analysis, the full-length *EMB1303* transcript (*EMB1303FL*) as well as a transmembrane-deleted truncated *EMB1303* transcript (*EMB1303-TMD*) lacking the last 30 aa were transformed into plants heterozygous for *EMB1303*. The presence of respective transcripts was confirmed by PCR (Fig. 12C). It appeared that the *emb1303* phenotype could not be rescued by the truncated *EMB1303* lacking its TMD as complemented plants still depicted an albino phenotype. The full-length version of the protein, on the other hand, led to two independent lines *EMB1303FL::EMB1303 #11 (#11)* and *EMB1303FL::EMB1303 #14 (#14)* that both fully rescued the phenotype of *emb1303* plants (Fig. 12B).

Huang et al. have already described an *EMB1303* homolog (*At1g30475*) in *Arabidopsis thaliana* that shares 57% identity and 71% similarity at the aa level (Huang et al., 2009). RNA-seq data indicated a high expression of *At1g30475* in dry and early germinating seeds while *EMB1303* is mainly expressed in early germinating seeds and leaves (Klepikova et al., 2016). To investigate if the homolog would be able to complement a loss-of-function *EMB1303* phenotype, heterozygous plants for *EMB1303* were transformed with *At1g30475* encoded under the control of the endogenous promoter of *EMB1303*. Upon expression of the independent line *pEMB1303::At1g30475.3*, the observed *emb1303* phenotype could be rescued indicating that *At1g30475* is able to take over the lost function of *EMB1303* in mutant plants (Fig. 12D). Presence of the respective transcripts was confirmed for *pEMB1303::At1g30475.3* via PCR (Fig. 12E).

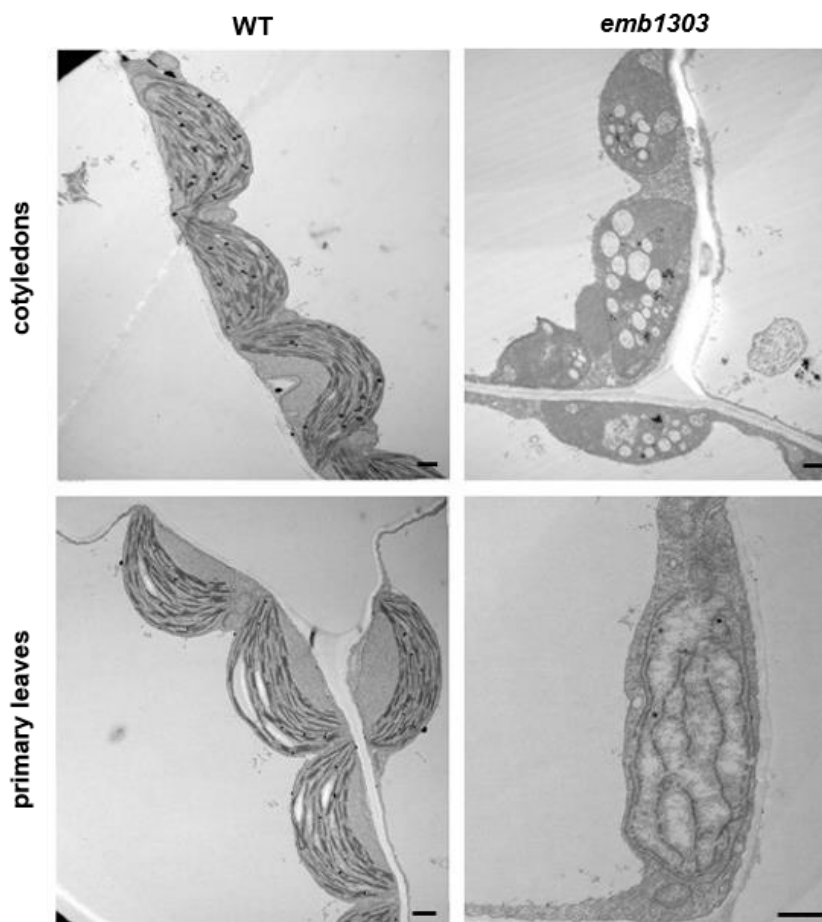


**Figure 13: Chloroplast ultrastructure of WT and *emb1303* mutant plants.** Cotyledons and primary leaves of two-week old WT and *emb1303* plants were given to TEM analyses. Pictures were taken by Prof. Dr. Andreas Klingl. Scale bars represent 500 nm.

The albino phenotype of *emb1303* mutant plants already indicates severe effects on all levels of chloroplast development. To gain a deeper understanding on structural defects of *emb1303*, TEM was conducted for cotyledons and primary leaves. Overall, chloroplasts of *emb1303* lack the typical lens-shaped structure of WT chloroplasts. In cotyledons, chloroplasts totally lacked an internal thylakoid membrane network. Instead, large vesicle-like structures appeared within the chloroplasts. Primary leaf chloroplasts showed at least some rudimentary thylakoid membrane residues, but also lacked the typical pattern of WT thylakoids with grana stacks and stroma lamellae (Fig. 13).

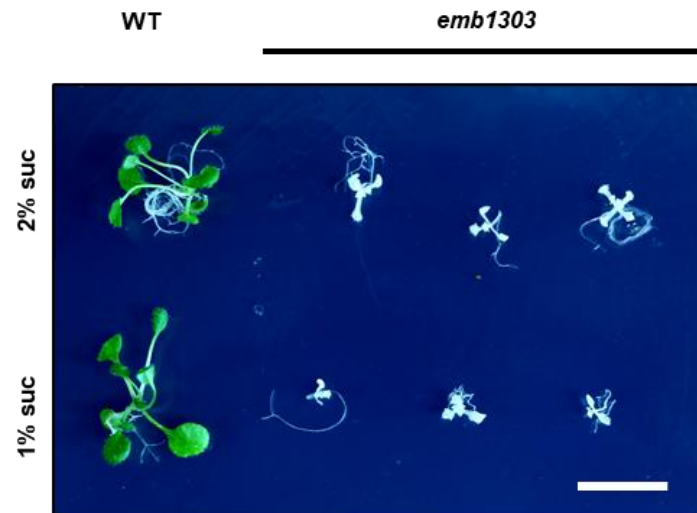


**Figure 14: Greening of WT and *emb1303* under continuous low light.** Phenotypes of WT and *emb1303* mutant lines grown on  $\frac{1}{2}$  MS medium supplemented with either 1% or 2% of sucrose. Plants were grown under continuous low light for four weeks. Scale bars represent 1 cm.

To further investigate if albino mutant plants could undergo greening, *emb1303* plants were grown on plates containing either 1% or 2% sugar and exposed to continuous low light. However, *emb1303* was not able to convert and accumulate chlorophyll under these conditions (Fig. 14).

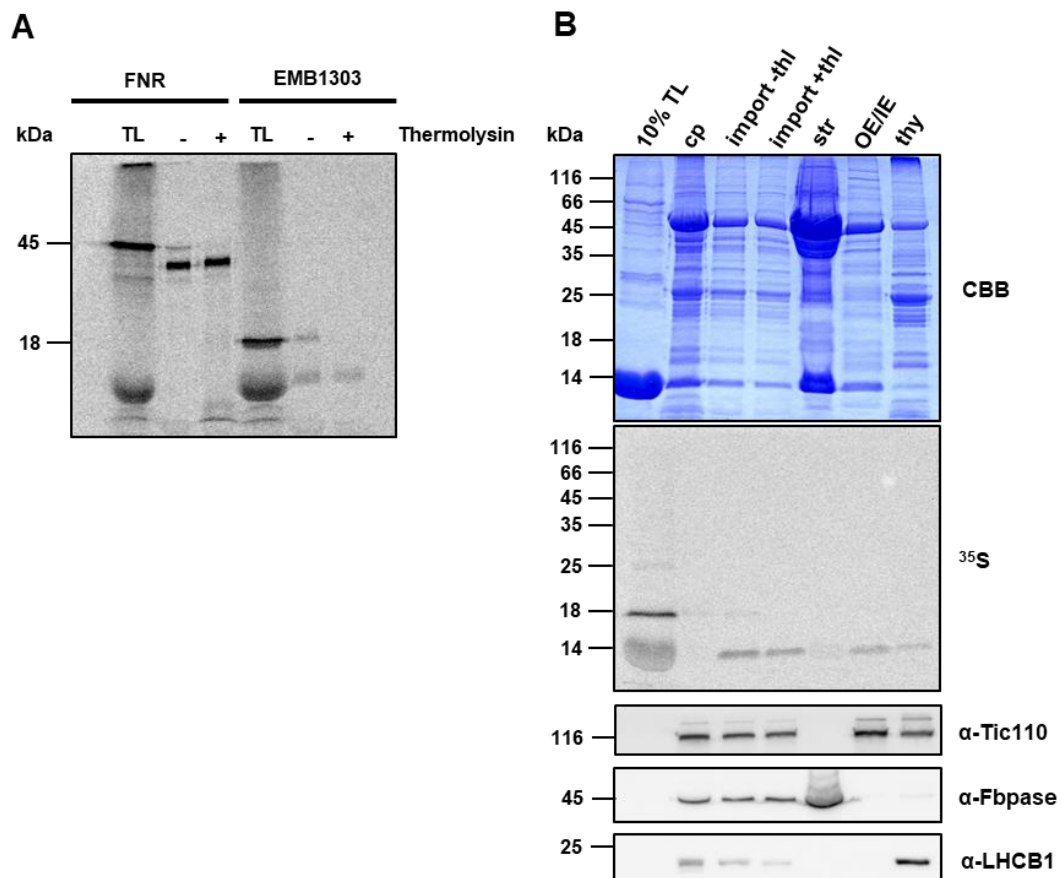


**Figure 15: *In vitro* import into chloroplasts and sub-localization of EMB1303.** A Intact pea chloroplasts (cp) were used for *in vitro* import using *in vitro* translated precursor proteins (TL) radiolabelled with  $^{35}\text{S}$

methionine. Subsequent thermolysin (thl) digest was performed to digest non-imported precursors. Presence and absence of thl is indicated with + and -, respectively. FNR served as the positive control. **B** *In vitro* import was performed as described in **A**. Ten samples were pooled after import and chloroplasts were lysed to separate their respective sub-compartments by discontinuous sucrose gradient fractionation. Fractions were separated via SDS PAGE and stained with Coomassie (CBB). EMB1303 was visualised by autoradiography ( $^{35}\text{S}$ ). Purity of the different fractions was controlled by immunoblots using the following antibodies against compartment-specific marker proteins: Tic110 (inner envelope, IE), Fbpase (stroma, str) and LHCB1 (thylakoids, thy).

Huang et al. have determined the subcellular localization of EMB1303 with a GFP-tagged construct of EMB1303. EMB1303 clearly localised to the chloroplasts where it depicted fluorescent rings around them suggesting a putative localization of EMB1303 to the inner envelope (Huang et al., 2009). To prove the sub-localization of EMB1303 with a different method, *in vitro* import experiments with subsequent sub-fractionation of the respective chloroplast compartments were conducted. Chloroplasts from pea were isolated and the EMB1303 precursor was synthesised *in vitro* containing five artificial methionines at its end as the endogenous protein sequence contained none for labelling. In addition, the stromal chloroplast protein ferredoxin-NADP<sup>+</sup>-oxidoreductase (FNR) was used as a positive control. To identify the TP-deficient, mature form of each protein, chloroplasts were further treated with thermolysin after import to digest all non-imported precursors. FNR and EMB1303 both showed a size shift upon import corresponding to the cleavage of their respective TPs. In the case of EMB1303, the mature protein had an estimated size of 14 kDa indicating a TP size of about 4 kDa (Fig. 15A). Furthermore, chloroplasts were lysed after import and fractionated in their respective compartments to investigate the sub-localization of EMB1303. Autoradiography revealed the strongest signal for EMB1303 in the outer/inner envelope (OE/IE) fraction and a lower signal in the thylakoid fraction while none of the protein could be detected in the stroma. Additional immunoblots with control antibodies were indicative of the purity of the respective sub-fractions. Since the thylakoid fraction was contaminated to some degree with envelopes, but the stroma and the OE/IE fraction were free of contamination, EMB1303 is indeed most likely located to the inner chloroplast membrane (Fig. 15B).

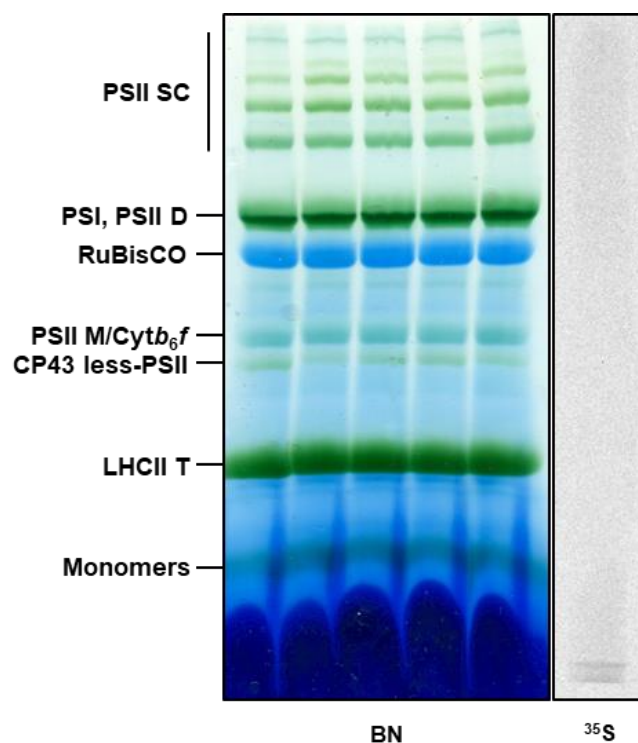


**Figure 16: Complex involvement of EMB1303 in the chloroplast inner envelope.** Radiolabelled EMB1303 was *in vitro* imported into pea chloroplasts. Subsequent BN PAGE was performed to natively separate chloroplast complexes (all lanes). EMB1303 was visualised by autoradiography (<sup>35</sup>S).

Finally, it should be investigated if EMB1303 appeared in complex with other chloroplast proteins. Intact pea chloroplasts were used after import for BN PAGE. The radioactive signal for EMB1303 showed a weak band at the very bottom of the gel referring to no obvious complex formation with other integral or attached proteins of the inner envelope (Fig. 16).

### 3.4 ptNAP45

ptNAP45 (At4g37920) and ptNAP45-like (At1g36320) were found in a proteomic screen of light-dense membrane (LDM) fractions performed by our group. LDM fractions of young pea plants were supposed to contain potential vesicle-associated proteins involved in early chloroplast biogenesis.

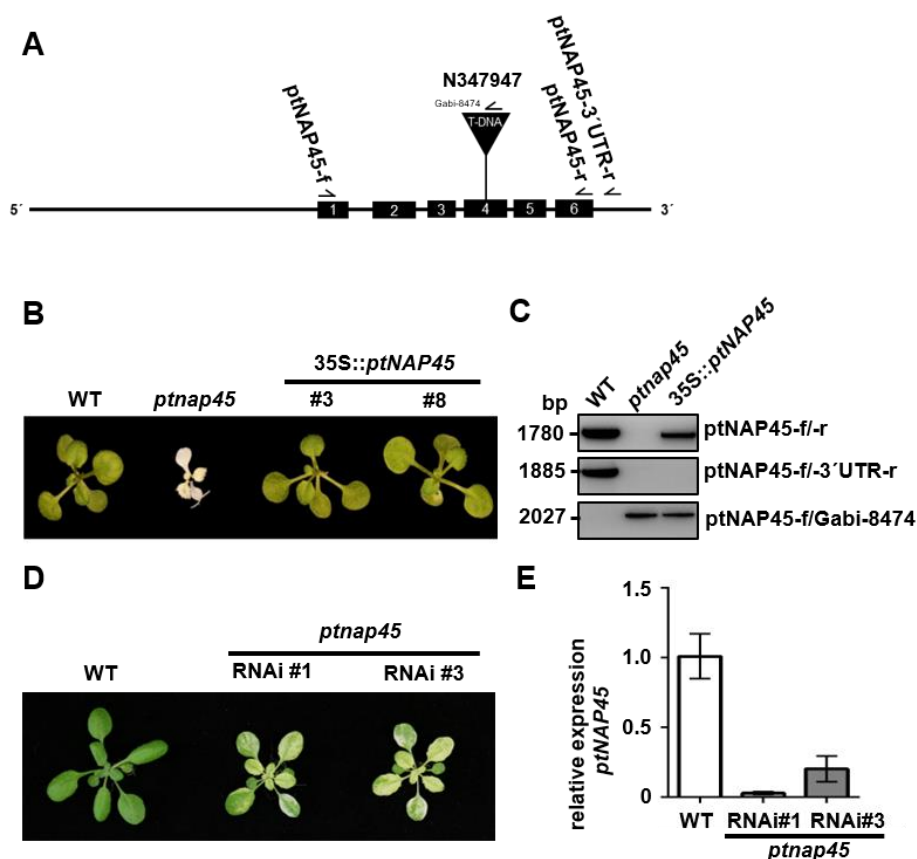


**Figure 17: ptNAP45 loss-of-function phenotype in *Arabidopsis thaliana*.** **A** Gene structure of ptNAP45 (At4g37920) and location of the respective T-DNA insertions in exon 4 for GK-635E11 (N347947). Exons are indicated by black boxes, T-DNA insertions are marked by black triangles. **B** Phenotypes of 3-week-old plants of the *ptnap45* T-DNA insertion line and the complementation lines *35S::ptNAP45* #3 and *35S::ptNAP45* #8 compared to WT grown on MS medium. **C** Genotyping PCR using the oligonucleotides ptNAP45-f, ptNAP45-r, ptNAP45-3'UTR-r and Gabi-8474. Oligonucleotide binding sites are indicated in **A**. **D** Phenotypes of 4-week-old *ptnap45* RNAi knockdown lines #1 and #3 in comparison to WT grown on soil. **E** mRNA levels of ptNAP45 determined by qPCR for *ptnap45* RNAi lines #1 and #3.

To analyse the function of ptNAP45 (At4g37920) a *ptnap45* T-DNA insertion line with an insertion in exon 4 of *ptNAP45* was used (Fig. 17A). Homozygous mutant plants were seedling lethal and displayed an albino leaf phenotype. These plants reached the stage of developing first true leaves when grown on MS plates containing 1% of sugar, but they could not increase in size nor produce seeds (Fig. 17B). When grown on soil, the albino mutants died after having reached the cotyledon stage. The T-DNA insertion was screened and confirmed by PCR using the oligonucleotides ptNAP45-f, ptNAP45-r and Gabi-8474 (Fig. 17C).

To ensure that the phenotype was caused by disruption of the *ptNAP45* locus, complementation analysis was performed. A construct coding for the full-length *ptNAP45* under the control of a 35S promoter was stably transformed into heterozygous *ptnap45* plants via floral dip by Dr. Roberto Espinoza-Corral. Following selection of plants over two generations, two individual lines of *ptnap45* plants were isolated carrying the construct coding for overexpression of *ptNAP45*, 35S::*ptNAP45* #3 and 35S::*ptNAP45* #8 (Fig. 17B). In both lines, the *ptnap45* growth phenotype was completely rescued by overexpression of *ptNAP45*. Presence of the *ptNAP45* transcripts within the mutant background was confirmed by PCR (Fig. 17C) using the oligonucleotides *ptNAP45*-f, *ptNAP45*-r, *ptNAP45*-3'UTR-r and Gabi-8474.

In addition, plants expressing RNA interference (RNAi) for the *ptNAP45* gene were generated in wild-type (WT) background by Dr. Roberto Espinoza-Corral. The obtained RNAi lines RNAi #1 and RNAi #3 for *ptNAP45* displayed a variegated leaf phenotype with leaves being sprinkled with white mutant-like and green WT-like areas (Fig. 17D). Even though RNAi plants were delayed in growth, they reached adulthood and were able to produce a small number of seeds. The correlation between a decrease in *ptNAP45* RNA levels and the resulting variegated leaf phenotype was verified by qPCR for which RNA was extracted from leaves of 3-week-old plants (Fig. 17E, performed by Beata Szulc). RNA levels were reduced to below 0.2-fold of WT levels.

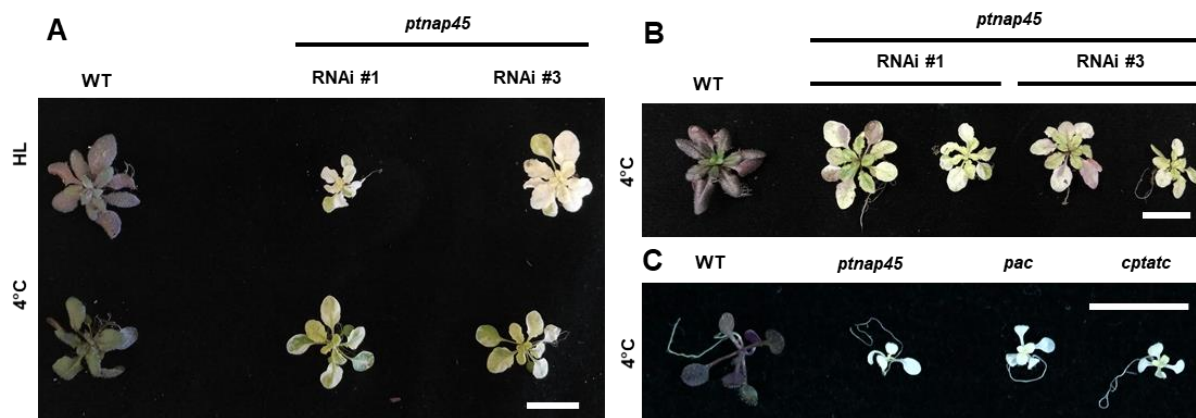


**Figure 18: Anthocyanin phenotype of *ptnap45* lines under stress conditions.** A WT and *ptnap45* RNAi lines were grown on soil and exposed to high light (HL) or cold conditions (4°C) for four weeks. B WT and *ptnap45* RNAi lines were grown on soil under cold conditions (4°C) for six weeks. C WT as well as *ptnap45*, *pac* and *cptatc* were grown on  $\frac{1}{2}$  MS medium supplemented with 1% sucrose under cold conditions (4°C) for five weeks. Scale bars represent 1 cm.

When grown under stress conditions such as high light or 4°C, *ptnap45* RNAi plants failed to produce anthocyanins (Fig. 18A). Especially in the cold, WT plants almost turned completely purple due to anthocyanin synthesis while RNAi plants mostly remained variegated with green and white leaf sections. Only in some cases, parts of the leaves developed a slight purple shade, probably due to lower RNAi expression in the respective parts (Fig. 18B). As a consequence, it was interesting to compare

*ptnap45* to other albino mutants like *pac* and *cptatc*. PAC was shown to bind 23S rRNA and to promote biogenesis of the chloroplast ribosome 50S subunit (Meurer et al., 2017). cpTatC was identified as an integral thylakoid protein with a direct role in thylakoid  $\Delta$ pH-dependent protein transport (Mori et al., 2001). WT plants and all three albino mutants were sown on MS medium supplemented with 1% sugar. After an initial growth phase under normal light conditions for two weeks, plants were shifted to 4°C. After three weeks in the cold, WT leaves had completely turned purple while no anthocyanins had been synthesised in any of the three mutants suggesting that the impaired anthocyanin biosynthesis is not specific for *ptnap45* but a general feature of albino mutants (Fig. 18C).

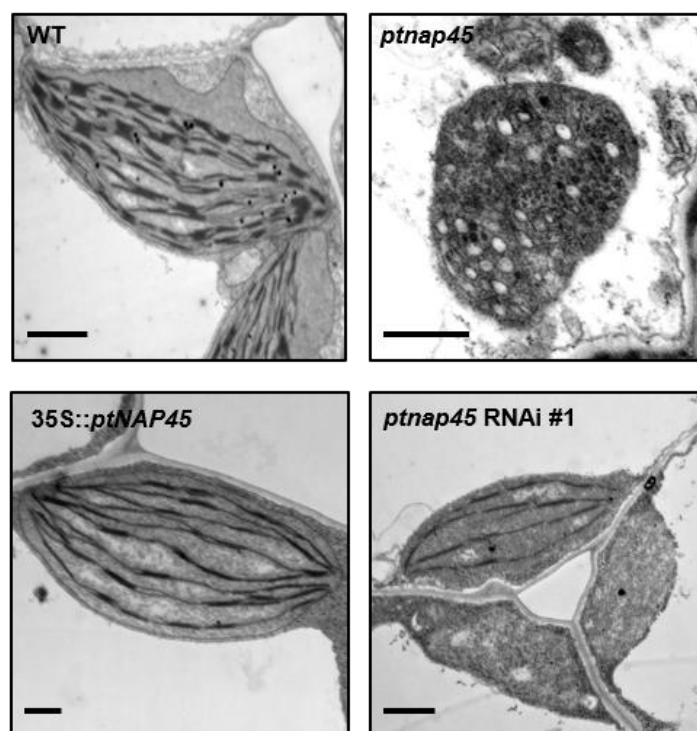


**Figure 19: Chloroplast ultrastructure of WT and *ptnap45*.** Plants were grown on sugar plates in long-day conditions for 3 weeks before leaves were excised for electron microscopy. Pictures were taken by Prof. Dr. Andreas Klingl. Scale bars represent 500 nm.

Due to its albino mutant phenotype *ptNAP45* seems to be essential for chloroplast biogenesis. To further investigate chloroplast morphology and thylakoid structure, ultrastructural transmission electron microscopy was performed with 3-week-old rosette leaves of WT, *ptnap45* mutants, complemented plants as well as RNAi lines (Fig. 19). When compared to WT, mutant chloroplasts not only lacked the typical lens-shaped structure but additionally showed no thylakoid membranes at all. Instead, large vesicles accumulated inside the mutant chloroplasts. This aberrant chloroplast morphology and the absence of thylakoid membranes could be completely rescued in complemented plants. In RNAi plants, cells with plastids containing no internal structures neighbouring cells with chloroplasts containing some thylakoids could be observed, as expected for the variegated phenotype (Fig. 19).

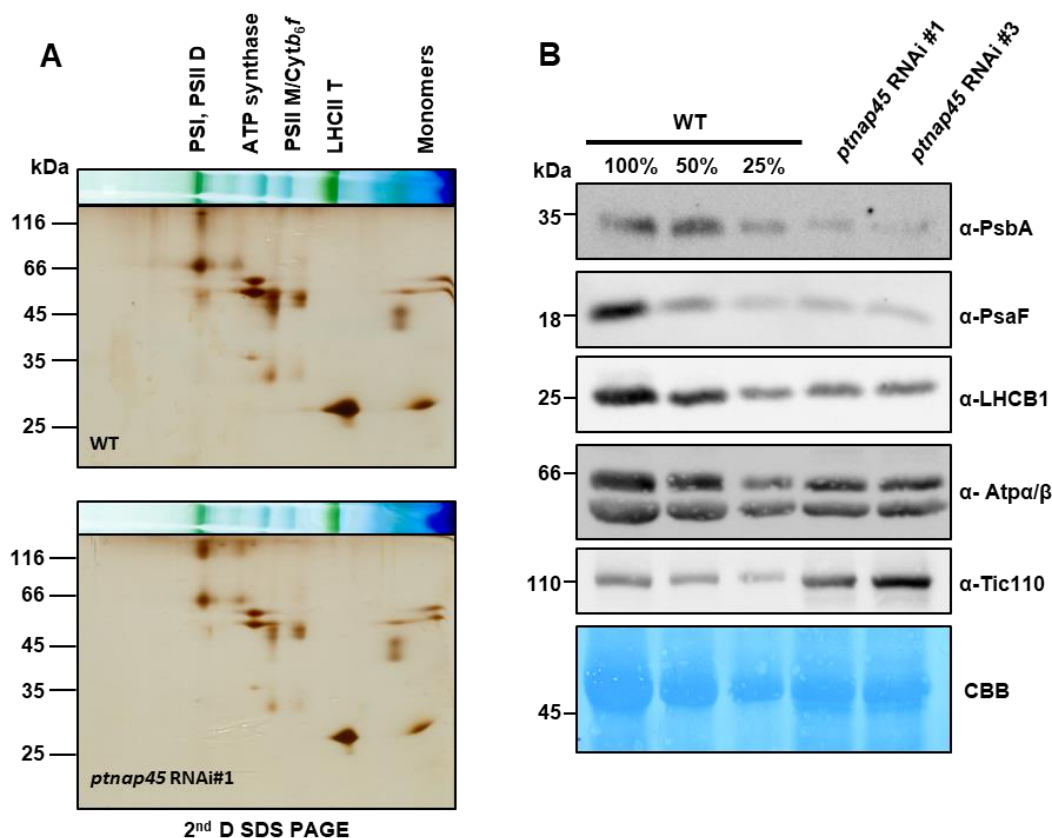


**Figure 20: Thylakoid composition in *ptnap45* RNAi lines.** **A** Thylakoid membranes were isolated from WT and *ptnap45* RNAi #1 and solubilised for BN PAGE with subsequent 2<sup>nd</sup> dimensional SDS PAGE. **B** Total protein was isolated from WT and *ptnap45* RNAi #1 and #3 for subsequent immunodetection of thylakoid membrane proteins PsbA, PsaF, LHCB1 and cpATP synthase subunits  $\alpha/\beta$ . The inner envelope protein Tic110 served as a control. Equal amounts of 30  $\mu$ g protein were loaded. To allow quantification of protein levels in RNAi lines, a dilution series of WT protein levels were loaded.

Since chloroplasts from the knockout mutant did not contain any membrane-like structures, thylakoid membranes were isolated from the RNAi line and Blue Native (BN) PAGE with subsequent second dimensional analysis was performed to analyse the accumulation of thylakoid membrane complexes. Silver staining suggested that in principle all thylakoid membrane complexes were able to assemble, albeit to a lower extent in the RNAi mutant (Fig. 20A, performed by Beata Szulc). To corroborate this finding, SDS-PAGE was performed using the isolated thylakoids and immunoblotting with antisera against proteins of PSI, PSII and the ATP synthase. Immunoblotting revealed that the PSII core protein PsbA, the LHCII complex chlorophyll a-b binding protein LHCB1 and the PSI reaction centre subunit PsaF as well as the  $\alpha/\beta$  subunits of the ATP synthase (Atp $\alpha/\beta$ ) were reduced by around 75% in RNAi lines compared to WT plants. Levels of the inner envelope protein Tic110 were not reduced, thereby serving as a loading control (Fig. 20B).

*In silico* analysis using ChloroP predicted a chloroplast TP in ptNAP45 (Emanuelsson et al., 1999). To verify chloroplast localization of ptNAP45, *in vitro* import was performed by Dr. Roberto Espinoza-Corral. Import-competent pea chloroplasts were isolated and precursor ptNAP45 was transcribed and

translated *in vitro* using  $^{35}\text{S}$  methionine for radioactive labelling. FNR was used as a positive control. Import was conducted and follow-up thermolysin treatment proteolyzed non-imported precursors. For ptNAP45, import showed a size shift from its precursor with a size of about 49 kDa towards a mature thermolysin protected fragment of 45 kDa (Fig. S1, Espinoza Corral (2019)).

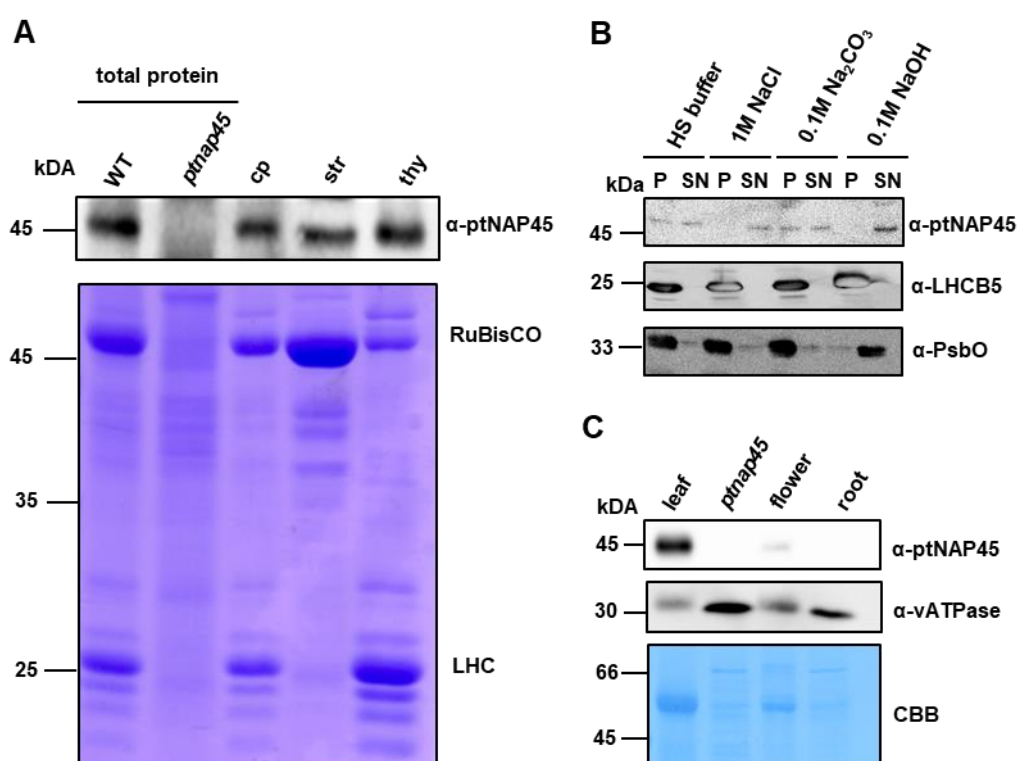


**Figure 21: Chloroplast localization and developmental expression of ptNAP45.** **A** Immunodetection of ptNAP45 in total protein of WT and *ptnap45* as well as in chloroplasts (cp), stroma (str) and thylakoids (thy) using a ptNAP45 antibody (upper panel) and Coomassie stain (lower panel). **B** Thylakoid membrane association of ptNAP45. Thylakoid membranes were isolated from WT plants and exposed to different buffer conditions as indicated. Subsequent SDS PAGE with pellet (P) and supernatant (SN) was analysed by immunodetection of ptNAP45. Detection of LHCb5 and PsbO served as controls. **C** Immunodetection of ptNAP45 in total protein of WT leaf, mutant, WT flower and WT root (upper panel) and Coomassie stain (lower panel). Detection of the vacuolar ATP synthase (vATPase) served as a control (middle panel).

To analyse the ptNAP45 localization on protein level, a specific antibody against full-length ptNAP45 was generated and immunoblotting was performed with total protein isolated from WT and ptNAP45 mutant. Coomassie staining confirmed the severe chloroplast defects in the mutant, since prominent plastid proteins, such as RuBisCO and LHC could not be detected (Fig. 21A). The ptNAP45 antibody detected a specific band at 45 kDa in WT that was absent in the mutant (Fig. 21A). In addition, ptNAP45 could be detected in isolated chloroplasts, confirming its localization. Probing against stroma and thylakoid fractions also gave us a first impression on its sub-localization within the chloroplast. Interestingly, ptNAP45 could be detected not only in the stroma but also in the thylakoid fraction (Fig. 21A). This finding was surprising, since ptNAP45 does not contain any predicted transmembrane

domains. To investigate whether the interaction with the thylakoid fraction is transient, thylakoid membranes were treated with different reagents to disturb hydrophobic or electrostatic membrane interactions. ptNAP45 already partly detached from the thylakoid membrane during a 30 min incubation with HS buffer. A complete detachment could be achieved with 1 M NaCl as well as 0.1 M NaOH while 0.1 M Na<sub>2</sub>CO<sub>3</sub> showed no further impact compared to the control buffer condition (Fig. 21B). Integral thylakoid membrane proteins like the light harvesting proteins of PSII (LHCB5) could not be released from the thylakoid membrane and were only detected in the pellet fraction. PsbO, a peripheral luminal protein associated with PSII, could be released completely from the membrane under high pH conditions (0.1M NaOH) as has been shown before (Torabi et al., 2014) (Fig. 21B). It can therefore be concluded that ptNAP45 is a soluble protein, which can be transiently associated with the thylakoid membrane.

Since it was observed that ptNAP45 mutants are affected in the development of green leaves the expression pattern of ptNAP45 was analysed in several plant organs on protein level. Isolation of total protein from different plant tissues and subsequent immunodetection revealed ptNAP45 to be almost exclusively expressed within green leaves. The protein could not be found in roots and only minor amounts were found in flowers, possibly originating from green sepals. This indicates that ptNAP45 is predominantly expressed in green tissue and especially important for chloroplast function (Fig. 21C).

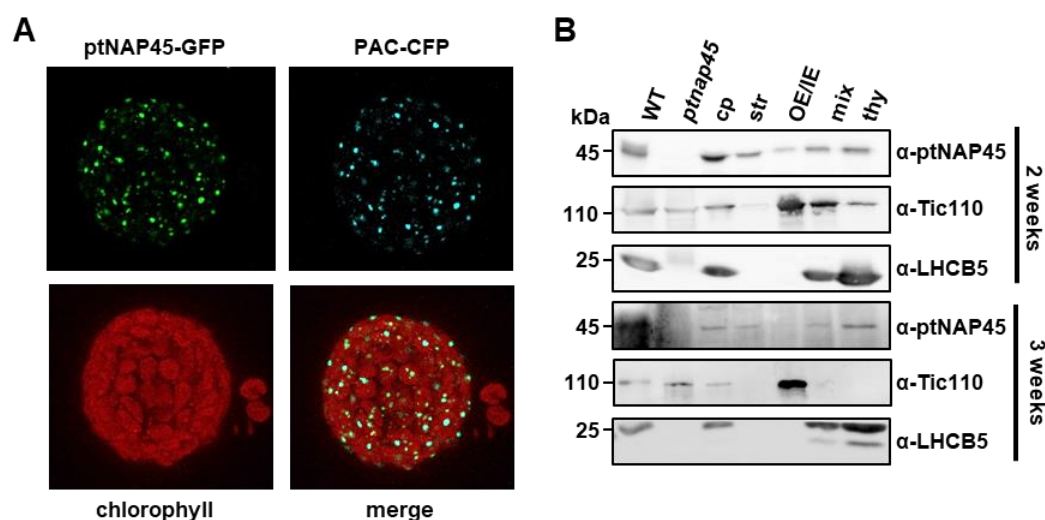


**Figure 22: Nucleoid localization of ptNAP45.** **A** Tobacco leaves were transformed with *Agrobacterium* carrying constructs for ptNAP45-GFP and the nucleoid marker PAC-CFP, respectively. Fluorescent signals were detected by confocal microscopy in intact protoplasts. **B** *Arabidopsis* chloroplasts were isolated from either two-week-old or three-week-old plants and lysed to obtain sub-compartments followed by immunodetection of ptNAP45 in total protein of WT and mutant, WT chloroplasts (cp), stroma (str), outer and inner envelopes (OE/IE), a mixed membrane fraction containing OE/IE and thylakoids (mix) and thylakoids (thy). Tic110 and LHCB5 antisera served as controls for the purity of the OE/IE and the thy fraction, respectively.

To further investigate the subcellular localization of ptNAP45 within the chloroplast, a ptNAP45-green fluorescent protein (GFP) fusion protein was transiently expressed under the control of the 35S promoter in leaves of tobacco. Leaves were infiltrated with *Agrobacterium* containing the fusion construct and protoplasts were isolated two days after the transfection. GFP fluorescence as well as chlorophyll autofluorescence were detected in isolated protoplasts using a confocal laser-scanning microscope. ptNAP45 appeared to be located inside the chloroplast where it strikingly formed distinct spots reminiscent of plastid nucleoids. Indeed, when co-expressed with a plastid nucleoid marker protein, PAC (Meurer et al., 2017), signals of both proteins merged perfectly indicating that ptNAP45 could be associated with plastid nucleoids (Fig. 22A).

Plastid nucleoids have previously been connected to thylakoid biogenesis as well as chloroplast biogenesis. As plastid nucleoids are known to switch their localization from the inner envelope in developing protoplasts towards the thylakoid membrane in mature chloroplasts (Powikrowska et al., 2014b), it was of interest to see if ptNAP45 behaves in a similar way. For this, sub-compartments from *Arabidopsis* plastids of different age were isolated and immunoblotted against ptNAP45. In 2-week-old plants and in 3-week-old plants it could be seen again that ptNAP45 equally localises to the stroma as well as to the thylakoids. In chloroplasts from younger leaves, ptNAP45 could additionally be detected in the outer/inner envelope fraction indicating that some of the protein is associated with the inner envelope. In contrast, this could no longer be observed in chloroplasts from more mature leaves, where ptNAP45 seems to be exclusively found in the stroma as well as attached to the thylakoid membrane. Purity of the individual fractions was checked with Tic110 as an inner envelope marker and LHCB5 as a marker for thylakoids (Fig. 22B).

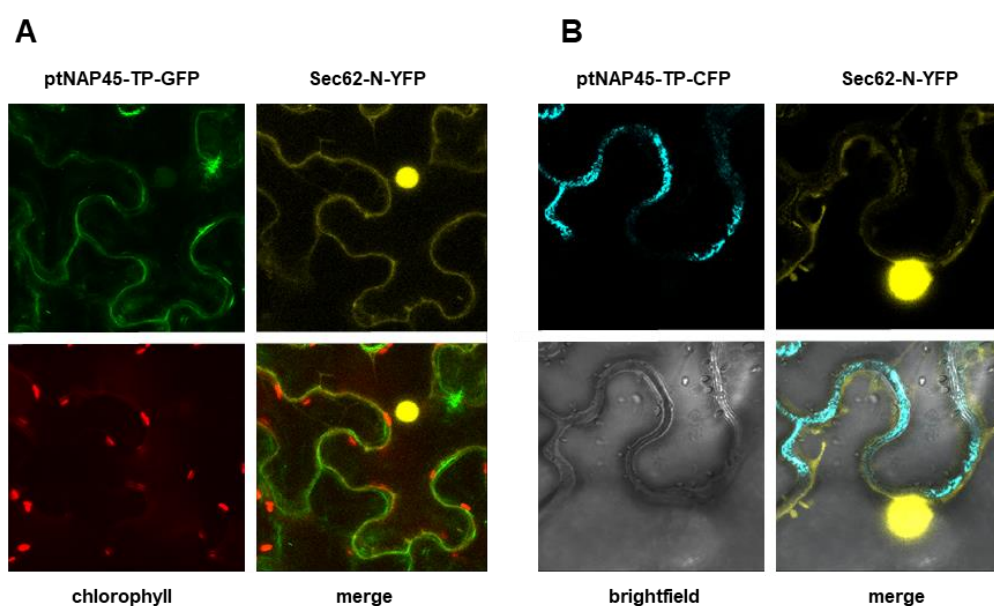


**Figure 23: Localisation of ptNAP45 without its transit peptide.** **A** Tobacco leaves were transformed with *Agrobacterium* carrying constructs for ptNAP45-TP-GFP and the cytosol and nucleus marker Sec62-N-YFP. **B** Tobacco leaves were transformed with *Agrobacterium* carrying constructs for

ptNAP45-TP-CFP and the cytosol and nucleus marker Sec62-N-YFP. In both cases, fluorescent signals were detected by confocal microscopy in leaf sections.

PEND, an intensively studied ptNAP, has been found to localise to the nucleus upon removal of its TP. It was therefore suggested that PEND might act as a transcription factor mediating chloroplast signalling to the nucleus (Terasawa and Sato, 2009). Additionally, another well-known ptNAP named WHIRLY1 has also been found to act as a transcription factor among other functions (Desveaux et al., 2000, Krupinska et al., 2014). Therefore, the consequences of removing the TP of ptNAP45 should be investigated. ptNAP45-TP-GFP and ptNAP45-TP-CFP fusion proteins, each under the control of the 35S promoter, were transformed into *Agrobacteria* and transiently co-expressed with Sec62-N-YFP (provided by Dr. Melanie Mitterreiter) serving as a control. Even though the full length Sec62 is a protein of the ER, its N-terminus without the transmembrane domains localises to the cytosol as well as the nucleus. Tobacco leaves were analysed using a confocal laser-scanning microscope. Both ptNAP45 fusion proteins could no longer be detected in chloroplasts. Instead, they clearly localised to the cytosol where the fluorescent signal merged with the control but could not be detected in the nucleus (Fig. 23). This makes it very unlikely that ptNAP45 functions as a transcription factor or in the direct signalling between chloroplast and nucleus.

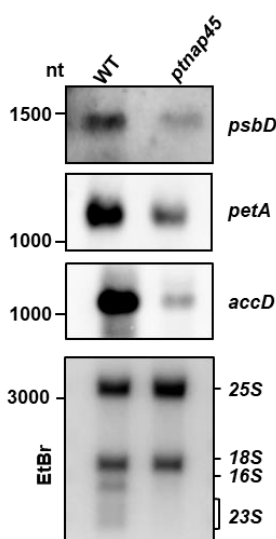


**Figure 24: Transcriptional defects in *ptnap45*.** RNA gel blots showing transcript levels of *psbD*, *petA* and *accD* in *ptnap45* and WT (upper panels) and an EtBr-stained agarose gel showing rRNA levels (lower panel) with 5 µg of each RNA loaded.

To investigate whether the reduction, i.e. lack of thylakoid membranes and the respective proteins in *ptnap45* RNAi and *ptnap45* was caused by a lack of plastid transcription, the transcript levels of some plastid encoded genes were analysed by RNA gel blot analysis. Albeit strongly reduced, it was found that transcripts for *psbD*, *petA* and *accD* were still present in mutant plants. Notably, *psbD* and *petA* transcripts are produced by the plastid-encoded RNA polymerase (PEP) in contrast to the *accD* transcript, which is produced by the nuclear-encoded RNA polymerase (NEP), pointing towards a general decrease in the accumulation of plastid transcripts (Fig 24).

Since it was observed that accumulation of plastid transcripts was downregulated, but not overall abolished, it was hypothesised that plastid protein translation was affected. To monitor plastid translation, intact seedlings of WT and mutant were incubated with cycloheximide, which inhibits cytosolic translation, and subsequently infiltrated with radiolabelled  $^{35}\text{S}$  methionine. After incubation under high light for 40 min, soluble as well as membrane proteins were extracted and loaded onto an SDS gel. Interestingly, the *ptnap45* mutant showed no accumulation of radiolabelled proteins compared to WT seedlings, in which especially freshly translated RubisCO as well as the PSII component D1 could be detected (Fig. S2A).

This raised the question whether ribosome accumulation was affected in the *ptnap45* mutants. To investigate accumulation of ribosomes, total proteins from WT and mutant plants were isolated and immunoblotting was performed using antibodies against two proteins of the 50S subunit of plastid ribosomes, namely RPL2 and RPL4. Interestingly, immunoblotting revealed the absence of these proteins in *ptnap45* suggesting that ptNAP45 might play a role in ribosome biogenesis (Fig. S2B).

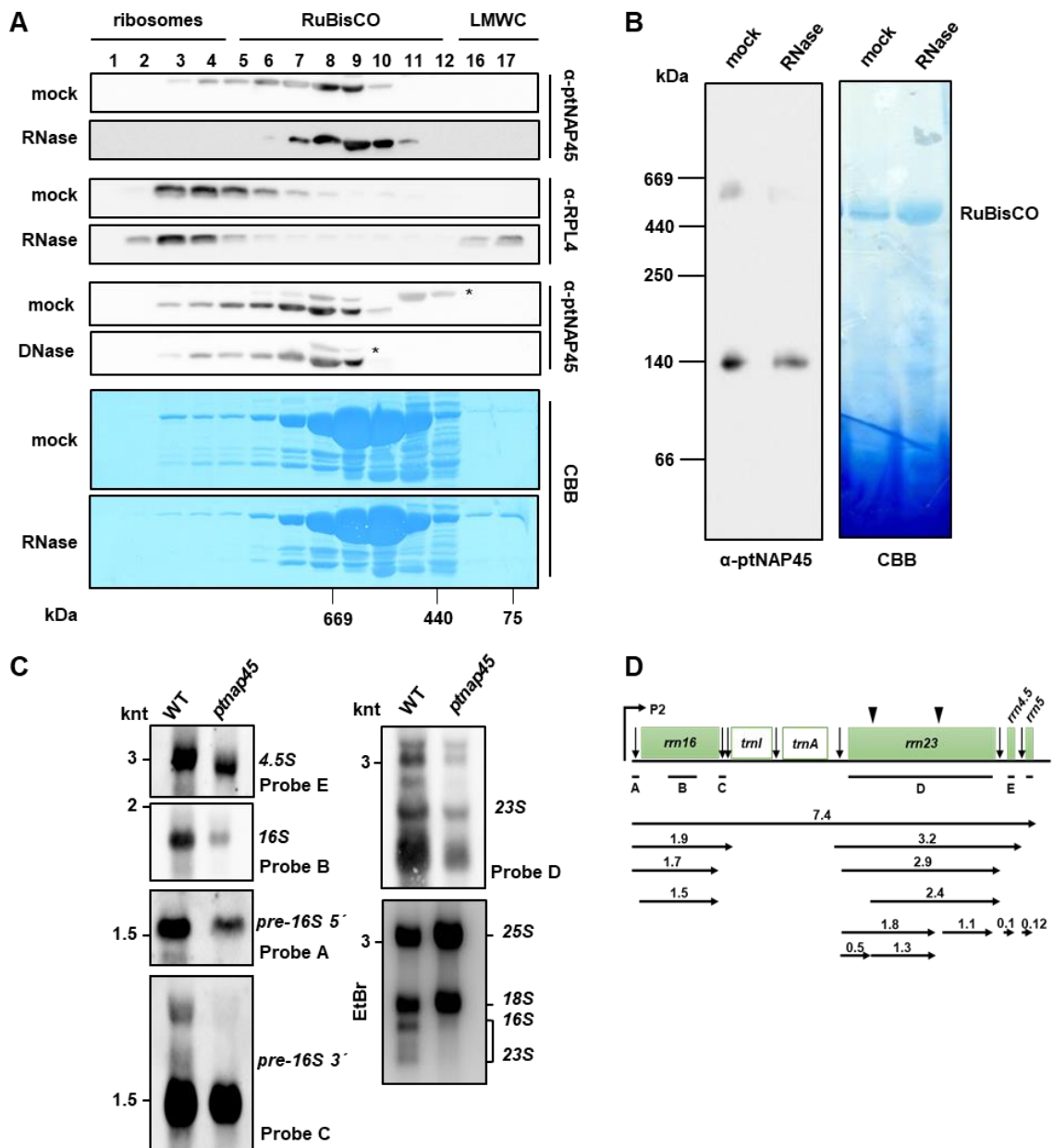


**Figure 25: ptNAP45 is part of an RNA containing complex.** **A** Native stroma extracts from pea chloroplasts were fractionated by SEC on a Superose 6 column before and after RNase or DNase treatment. Peak fractions were separated via SDS PAGE followed by immunodetection and Coomassie staining. Ribosomes, RubisCO and low molecular weight complexes (LMWC) are indicated as previously published (Olinares et al., 2010). The marker corresponds to Thyroglobulin (669 kDa), Ferritin (440 kDa) and Conalbumin (75 kDa). Unspecific signals of the ptNAP45 antibody are marked by asterisks. **B** 100 µg of RNase-treated and untreated native stroma extracts from pea were separated via BN PAGE with subsequent wet blotting and immunodetection. **C** RNA gel blots showing transcript levels of 23S, 16S and 4.5S rRNA in *ptnap45* and WT and an EtBr-stained agarose gel showing rRNA levels. **D** Scheme of the chloroplast *rrn* operon in *Arabidopsis* under control of the P2 promoter with green boxes representing exons and white boxes representing introns. Processing sites in the primary transcript of the *rrn* operon are indicated by vertical arrows. Lines A to E show the localization of the probes used in C. Positions of internal cleavage sites (hidden breaks) in the 23S rRNA are shown as triangles. Location and sizes (in knt) of the primary transcript and the various processing products are represented by horizontal arrows below the operon.

As a consequence, it was speculated that ptNAP45 might associate with ribosomes or pre-mature ribosomal particles. Therefore, native stroma extract was fractionated by size exclusion chromatography (SEC) and subsequently analysed by immunoblotting. The stroma was separated under conditions allowing the detection of complexes ranging from megadalton including plastid nucleoids to different assembly states of ribosomal complexes (Olinares et al., 2010, Meurer et al., 2017). Interestingly, ptNAP45 was found in high molecular weight complexes > 600 kDa as expected for ribosome or pre-mature ribosomal complex associated proteins. Since these complexes contain ribosomal RNA, the stroma was treated with RNase prior to separation via SEC. Strikingly, the ptNAP45 containing complex(es) proved to be RNase sensitive and shifted towards a lower molecular weight, indicating that ptNAP45 is part of an RNA containing complex. Next, an antibody directed against RPL4 was used to detect the 50S ribosome. As expected, RPL4 was also found in large megadalton complexes, partially co-migrating with ptNAP45. Upon RNase treatment a portion of RPL4 shifted towards low molecular weight fractions, whereas part of the protein was still detected in megadalton complexes. As mature ribosomal subunits are tightly packed, rRNA is less accessible for RNases in contrast to rRNA in partially assembled ribosomal subunits or free rRNA (Williams and Barkan, 2003). Since ptNAP45 seemed comparatively more accessible to RNase treatment, ptNAP45 seems to be associated to pre-assembled states of the 50S ribosomal subunit, rather than being part of mature ribosomes. As ptNAP45 was found to be associated with plastid nucleoids containing ptDNA, the effects of DNase treatment were additionally investigated. However, this treatment showed no effect on ptNAP45 complex formation, suggesting that ptNAP45 is not found in any complex with ptDNA. (Fig. 25A).

In addition, native stroma was separated by BN PAGE to analyse the ptNAP45 complex. Similar to the SEC results, ptNAP45 was found in a large complex of approx. 600 kDa. In addition, ptNAP45 was observed in a smaller complex of approx. 140 kDa. Interestingly, the larger complex again proved to be RNase sensitive. Possibly, ptNAP45 already partially dissociates from the RNA containing complex during the overnight BN run. The harsher conditions may also promote the accumulation of the smaller 140 kDa complex, in contrast to the separation by SEC. Both complexes were sent to mass spectrometry for further analysis. By the time this thesis was submitted, the results of the proteomic analysis were not yet available. Nevertheless, this result confirms that ptNAP45 is part of a distinct RNA containing high molecular weight complex (Fig. 25B).

Since rRNA accumulation and maturation is essential for ribosome biogenesis, it was of interest to analyse whether this was affected in mutant plants. As observed from the RNA agarose gel in Figure 24A, the chloroplast 16S and 23S rRNA of the 30S and 50S ribosomal subunit, respectively, appeared to be absent in the mutant while the 25S and 18S rRNAs of cytosolic ribosomes seemed to be even slightly more abundant in comparison to WT levels. It was therefore analysed whether

ptNAP45 could have an immediate effect on rRNA accumulation by binding to RNA. As no shift could be observed in EMSA experiments, it can be argued that ptNAP45 is not directly involved in rRNA binding but rather affects rRNA-related maturation processes by interacting with other RNA-binding proteins (data not shown).

Nevertheless, to further assess potential rRNA processing defects RNA gel blot analyses with radiolabelled probes directed against the mature 23S, 16S and 4.5S rRNA were performed. It was found that the rRNAs were still present, though highly reduced (Fig. 25C). In addition, the processing pattern of the 23S rRNA was unchanged in the mutant. Since a defect in rRNA processing can result in accumulation of unprocessed 3' and 5' 16S rRNA ends, probes directed against these regions were also used (Fig. 25D). However, no unprocessed 16S rRNA accumulated, suggesting that RNA maturation itself is not affected in the ptNAP45 mutant (Fig. 25C). In summary, the obtained data suggest that ptNAP45 is involved in ribosome assembly, independent of rRNA maturation.

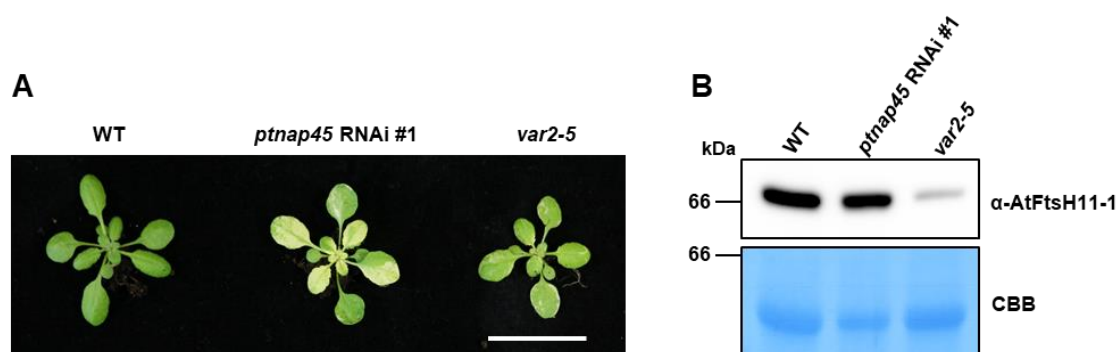


**Figure 26: Comparison of leaf variegation between *ptnap45* and *var2-5*.** **A** Phenotypes of 4-week-old *ptnap45* RNAi knockdown lines #1 and *var2-5* in comparison to WT grown on soil. Scale bar represents 3 cm. **B** Immunodetection of the ATP-dependent zinc metalloprotease AtFtsH11-1 in total protein of WT, *ptnap45* RNAi #1 and *var2-5* (upper panel) and Coomassie stain (lower panel).

The variegated leaf phenotype that is observed in *ptnap45* knock-down plants additionally hints toward a problem in chloroplast biogenesis as it has been described for other variegated lines like *var2-5* (Chen et al., 2000) (Fig. 26A). VAR2 is a chloroplast homolog of the *E. coli* ATP-dependent zinc metalloprotease FtsH that exhibits both chaperone and protease activity in bacteria (Suzuki et al., 1997). Chloroplast VAR2 has been shown to reside in the thylakoid membrane where it is involved in turnover of PSII core protein D1 as well as other processes related to the proper process of photosynthesis (Chen et al., 2000). It was found that, in contrast to *var2-5*, there is no loss of AtFtsH in *ptnap45* knockdown plants (Fig. 26B).

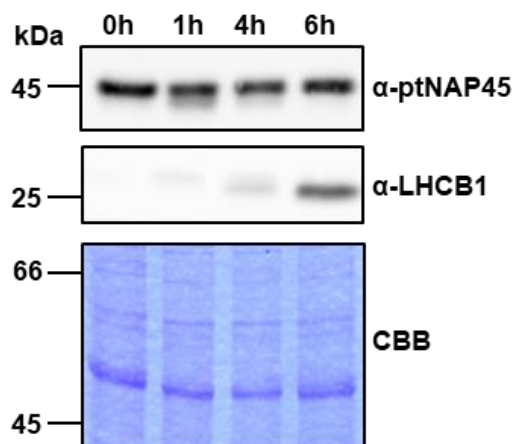


**Figure 27: ptNAP45 is present in etiolated seedlings.** Total protein of 7-day-old WT was isolated from either etiolated *Arabidopsis* seedlings (0 h) or after 1 h, 4 h or 6 h of light exposure for subsequent immunodetection (upper panels) and Coomassie staining (lower panel). LHCB1 antiserum served as a control.

Considering that functional ribosomes are required in all plastids, including etioplasts and proplastids, the question arose if ptNAP45 was present in these developmental stages. For this, greening experiments with etiolated WT plants and subsequent immunoblotting were performed. WT seedlings were grown on sugar plates for 2 hours exposed to light before they were shifted to the dark for 6 days. After this dark period, total protein was extracted after 0/1/4/6 hours of light exposure, respectively. Subsequent immunoblots against ptNAP45 revealed that the protein is already present in the dark and requires no light induction like the control protein LHCB1 (Fig. 27). This indicates that ptNAP45 is already needed in the very early stages of plant development, supporting the working hypothesis that ptNAP45 is required for ribosome assembly.

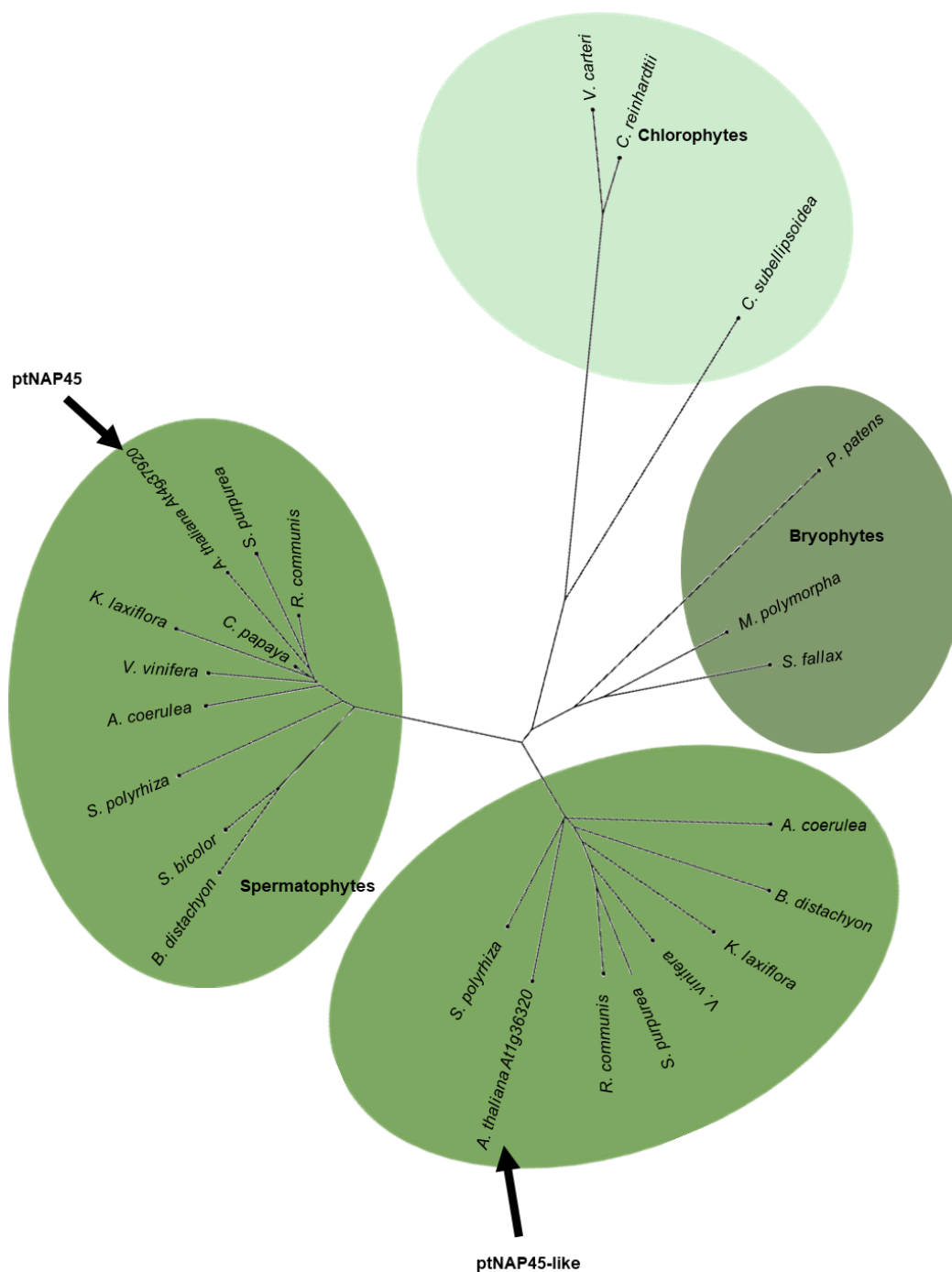


**Figure 28: Phylogenetic tree based on degrees of homology between protein sequences of ptNAP45 and ptNAP45-like from green algae to higher plants.** Representative members of each clade are shown. The phylogenetic tree was constructed by the distance-based method with the neighbor-joining algorithm using a bootstrap value of 100. R. Sequence data used in this study can be found in NCBI (<https://www.ncbi.nlm.nih.gov/>) or Phytozome (<https://phytozome.jgi.doe.gov/>) under following accession numbers: *V. carteri* XP\_002947236.1; *C. reinhardtii* PNW69832.1; *C. subellipsoidea* XP\_005645753.1; *P. patens* XP\_024372527.1; *M. polymorpha* OAE27386.1; *S. fallax* Sphfalx0018s0060.1, *A. coerulea* PIA47990.1, PIA51907.1; *B. distachyon* PNT72139.1, XP\_003573561.2; *V. vinifera* XP\_002285817.1, XP\_003635095.1; *S. bicolor* XP\_002437093.1; *C. papaya* XP\_021901451.1; *R. communis* EEF35142.1, EEF48437.1; *S. purpurea* SapurV1A.0766s0170, SapurV1A.0331s0180.1; *K. laxiflora* Kalax.0018s0077.1, Kalax.0502s0018.1; *S. polyrhiza* Spipo4G0017800, Spipo0G0096800.

Finally, the evolutionary conservation of ptNAP45 should be investigated. Several so far described ptNAPs have been reported to be found exclusively in higher plants (Powikrowska et al., 2014b). The same is true for plastid ribosome assembly factors and associated proteins, possibly since during the course of evolution many unique chloroplast specific factors have become necessary to drive the highly sophisticated process of ribosome assembly. Along this line, phylogenetic analyses of ptNAP45 revealed a clear conservation in higher plants, it is only found in spermatophytes, including various essential agricultural crops. ptNAP45 is not present in any lineage of algae, mosses, ferns or cyanobacteria. However, blast analysis showed that ptNAP45 has a paralogue, which was termed ptNAP45-like (At1g36320), showing 45% identity on protein level. In contrast to ptNAP45, its presence is not restricted to higher plants, but it is also found in mosses and green algae, suggesting that ptNAP45 evolved from ptNAP45-like at later stage during evolution (Fig. 28).

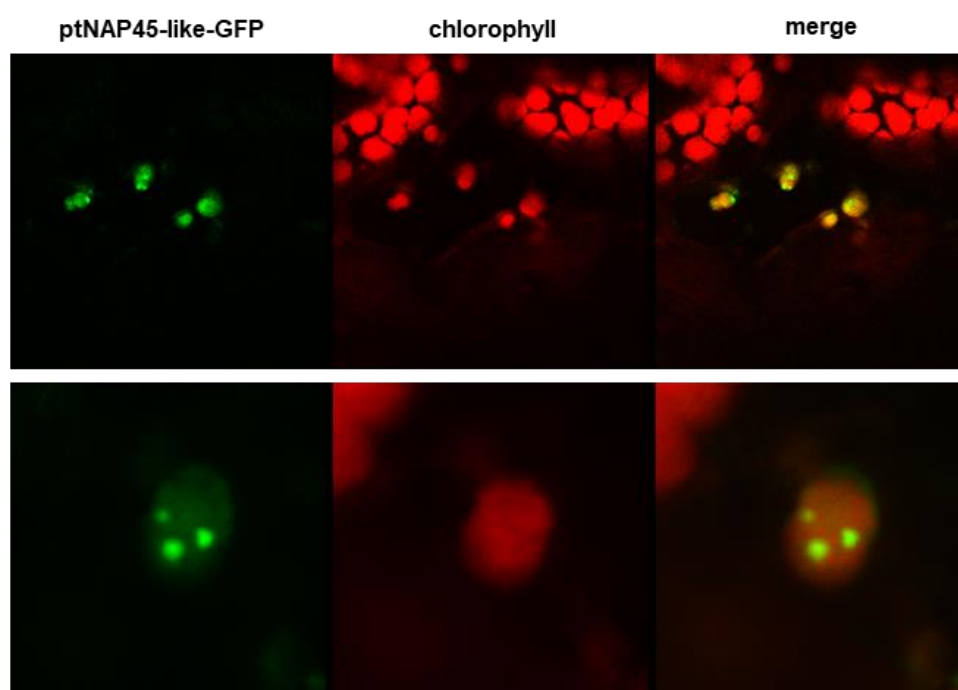


**Figure 29: Localisation of ptNAP45-like.** *Arabidopsis* leaves were stably transformed with *Agrobacterium* carrying ptNAP45-like-GFP via floral dip. Fluorescent signals were detected by confocal microscopy in intact leaves.

Even though a mitochondrial localisation for ptNAP45-like has been suggested previously (Espinoza Corral, 2019), ptNAP45-like is also predicted to harbour a chloroplast TP. To prove its chloroplast localization, a ptNAP45-like-GFP fusion protein under the control of the 35S promoter was stably expressed in leaves of *Arabidopsis* via flora dip. GFP fluorescence as well as chlorophyll autofluorescence of leaves were detected using a confocal laser-scanning microscope. ptNAP45-like-GFP could be detected inside chloroplasts where it formed distinct spots similar to ptNAP45 (Fig. 29). Unfortunately, it was not possible to complement the ptNAP45-like mutant line. New mutant lines and further studies are required to analyse its function.

## 4. Discussion

The thylakoid membrane is a fascinating and complex membrane network inside the chloroplast, but very little is known about mechanisms for thylakoid biogenesis. The thylakoid membrane is characterised by a unique composition of proteins, lipids, pigments as well as multiple cofactors and the interplay of lipids and proteins seems to be important for thylakoid formation. As many important building blocks derive from the inner envelope, they could either bridge the aqueous stroma via invaginations, soluble transfer proteins or a plastid vesicle transport. The latter has been in strong focus for the last years as it could be proven that vesicles are a persistent feature of plastids and that they accumulate in the stroma under special conditions (Lindquist et al., 2016). Previous bioinformatic approaches suggested a model for plastid vesicle transport in which cargo proteins are first imported into the chloroplast via the TOC-TIC complex before being packed into vesicles. For vesicle formation, a chloroplast Sar1 homolog would need to be activated by a guanine nucleotide exchange factor which subsequently would recruit further protein complexes functioning in cargo selection. When the membrane is highly curved, the vesicle buds from the donor membrane upon hydrolyzation. After passing the stroma, the vesicle fuses with the thylakoid membrane mediated by Rab GTPases, tethering factors, SNAREs and SNARE-associated proteins to deliver the cargo protein to the thylakoids (Khan et al., 2013).

As vesicle trafficking is a common feature of the secretory pathway in the cytosol, it was hypothesised that a putative plastid vesicle transport system as described above could be of eukaryotic origin. This idea is further supported by the lack of such a system in cyanobacteria as well as in algae. Since the first observations of vesicles, many proteins have been suggested as putative players. But still, details on molecular processes and regulators remain elusive. Here, four new putative proteins were characterised and screened for a possible role in plastid vesicle transport.

### 4.1 SNARE AP & SYTL5.2

Previous experiments performed by our group indicate that SNARE AP and SYTL5.2 are indeed both chloroplast proteins. While SNARE AP seems to be located to the chloroplast envelope membrane and/or the thylakoids, SYTL5.2 most likely resides in the envelope membrane. For both proteins, mutant phenotypes of different T-DNA insertion lines were described previously (Patil, 2018). Unfortunately, both analysed T-DNA insertion lines later turned out to carry additional knock-outs. For SNARE AP, an antisense RNA was detected that probably led to the observed pale green leaf phenotype with significantly reduced chlorophyll as this phenotype could not be detected in the here described T-DNA insertion lines. For SYTL5.2, a curly leaf phenotype has been described with mutant plants being retarded in growth and overall smaller than WT plants. This phenotype strongly resembled the one of

Asymmetric Leaves 1 (AS1) mutants (Byrne et al., 2002) and indeed it turned out that AS1 as well was knocked-out in the *sytl5.2* T-DNA insertion line. AS1 is a transcription factor that mediates leaf patterning and stem cell function in *Arabidopsis* by negatively regulating genes involved in differentiation (Byrne et al., 2002). In the *sytl5.2* mutant line used by Patil (2018), AS1 was responsible for the phenotype which explains why it could not be observed in other T-DNA knock-out lines for SYTL5.2 that were analysed in this thesis.

SNARE AP as well as SYTL5.2 are theoretically believed to be involved in the assistance of SNARE proteins during tethering, docking and fusion of vesicles with the thylakoid membrane. However, it turned out that both proteins are not essential for the plant because in both cases, new single loss-of-function mutants showed no phenotype under various conditions including light stress and cold. Furthermore, chloroplast ultrastructure was not changed in *snare ap* as well as *sytl5.2* mutant plants. Chloroplast morphology and thylakoid structure appeared totally normal in comparison to WT. Greening was also not affected in both mutant lines indicating that the transformation from etioplasts present in the dark via proplastids further to mature chloroplasts is unrestricted. Thylakoid biogenesis proceeds smoothly, including all processes involved in the transport and embedding of pigments, lipids, and proteins.

In the absence of a specific antibody for each of the proteins, further functional investigation was difficult. Based on the so far obtained results, it remains speculative to classify the role of SNARE AP as well as SYTL5.2 and to assess whether they have assisting functions in plastid vesicle transport. In the future, identification of the respective interaction partners like chloroplast SNARE proteins and subsequent creation of double mutants may provide deeper insights into the molecular roles of SNARE AP and SYTL5.2 and their possible involvement in vesicle trafficking in the chloroplast. Additionally, it will be essential to experimentally confirm the existence of chloroplast SNARE proteins at the inner envelope as well as at the thylakoid membrane. So far, only *in silico* predictions for one single tethering factor (AtCASP), one Qbc t-SNARE (AtSNAP33), one Qa t-SNARE (AtSYP21/AtPEP12) and one R v-SNARE (AtVAMP726) exist for the chloroplast (Khan et al., 2013).

## 4.2 EMB1303

EMB1303 has previously been described as an essential chloroplast protein indispensable for proper photoautotrophic growth and plant development expressed in almost all tissues and stages (Huang et al., 2009). Here, it could be confirmed that EMB1303 is indeed an essential protein in higher plants as loss-of-function results in seedling lethal albino mutant plants that are severely affected in chloroplast development and thylakoid biogenesis. This phenotype could only be rescued by expression of the full-length protein indicating that the C-terminal TMD is essential for the function of EMB1303. This fits the high degrees of conservation at the C-terminus among EMB1303 and homologous proteins

identified in rice, barrelclover and rape (Huang et al., 2009). Additionally, the attempt was made to complement the loss of EMB1303 with its homolog (At1g30475) in *Arabidopsis*. These two proteins share 57% identity and 71% similarity at the aa level (Huang et al., 2009). Interestingly, At1g30475 successfully complemented *emb1303* plants when expressed under the native EMB1303 promoter. This indicates that EMB1303 and its homolog in *Arabidopsis* fulfil the same functions for the plant, but probably in different tissues. As At1g30475 is mainly expressed in dry and early germinating seeds while EMB1303 is expressed in almost all tissues with a focus on leaves, it is quite conceivable that this function is initially performed by At1g30475 in seeds and later during development taken over by EMB1303.

Due to their albino phenotype, it was tempting to gain deeper insights in thylakoid biogenesis and chloroplast structure of *emb1303* plants. Ultrastructural imaging revealed an aberrant chloroplast morphology in mutants with round-shaped and overall smaller chloroplasts. In cotyledons of *emb1303*, chloroplasts contained no thylakoids at all, but accumulated large vesicular structures. However, some rudimental non-stacked thylakoid membranes appeared in the *emb1303* chloroplasts of primary leaves, possibly due to their previous heterotrophic growth on sugar-supplemented medium. Still, these thylakoid membrane fragments are free of pigments as the mutant leaves remained white even when they were grown on sugar. Greening did also not occur under low light conditions indicating that EMB1303 could play a role in ensuring pigment transfer to the thylakoid membrane. It could also be confirmed that EMB1303 is a chloroplast protein by import experiments. Moreover, the sub-localisation was successfully determined more precisely. EMB1303 most likely resides in the inner chloroplast envelope which fits to the previous GFP localisation performed by Huang et al. (2009). There, it doesn't seem to be part of any complex.

As several attempts to generate a specific antibody against EMB1303 failed, its functional prediction remains fairly speculative. Further research is needed to support the hypothesis that EMB1303 is a chloroplast SNARE protein residing in the inner envelope.

### 4.3 ptNAP45

Even though ptNAP45 has initially been identified in the context of plastid vesicle transport, it soon became clear that it rather plays a role in chloroplast ribosome biogenesis as it associated with plastid nucleoids. Plastid nucleoids have been shown to function in various chloroplast processes, beside ptDNA organization they are thought to play a role in ribosome biogenesis (Bohne, 2014). Chloroplast ribosome biogenesis is less well understood than that of their bacterial counterpart and so far, only few auxiliary proteins have been identified. ptNAP45 seems to be associated with ribosome assembly intermediates and is located in plastid nucleoids.

The albino phenotype of *ptnap45* mutants indicates that the protein is essential for chloroplast development and thylakoid biogenesis. Loss-of-function of ptNAP45 results in a severely disturbed chloroplast morphology with no internal membrane structures while knock-down of ptNAP45 leads to a variegated leaf phenotype. Other mutants like *var2-5* also depict variegated leaves due to a loss of the zinc metalloprotease AtFtsH residing in the thylakoid membrane. In contrast to *var2-5*, AtFtsH levels remained the same in *ptnap45* knock-down plants indicating that ptNAP45 differently influences chloroplast biogenesis and photosynthesis compared to VAR2.

Another observation was that *ptnap45* knock-down as well as knock-out lines fail to accumulate anthocyanins when exposed to cold stress. As this could also be observed in other albino mutant plants like *pac* and *cptatc*, the cold stress phenotype is not specific for *ptnap45* plants. Rather, this could be a more general phenotype due to a possible lack of photosynthetic products that may be required as signals for anthocyanin biosynthesis under cold conditions.

Interestingly, most ptNAPs are restricted to higher plants (Powikrowska et al., 2014b) and so is ptNAP45. However, its paralog ptNAP45-like was shown to be already present in mosses and green algae suggesting that ptNAP45-like came up earlier in evolution than ptNAP45. Previously, it was suggested that ptNAP45-like would be localised in mitochondria (Espinoza Corral, 2019). However, it could be shown that ptNAP45-like localises to the chloroplast like ptNAP45. Therefore, it is tempting to speculate that ptNAP45-like also contributes to ribosome assembly, possibly by fulfilling a more primal function. Alternatively, or additionally, its role could be expanded to other types of plastids since it could be shown that ptNAP45 seems not to be expressed in roots or flowers. However, *in silico* expression data using the AtGenExpress eFP ([bar.utoronto.ca/eplant](http://bar.utoronto.ca/eplant)) indicate that ptNAP45-like mRNA is most abundant in cotyledons and rosette leaves (Waese et al., 2017). Future studies will elucidate its function and its link to ptNAP45.

There are several other examples of higher plant specific ribosome assembly factors like DCL, RH39, RH22, RH50 or CGL20 which don't have orthologs in bacteria but first emerged in the green lineage as a consequence of structural divergence of plastid ribosomes and due to an increasing complexity of ribosome biogenesis due to the massive transfer of plastid genes to the nucleus (Bellaoui et al., 2003, Nishimura et al., 2010, Chi et al., 2012, Paieri et al., 2018, Reiter et al., 2020). Many ribosome biogenesis factors are known to be involved in rRNA maturation. One example is CRASS, a stromal protein that is found in association with the 30S subunit and the 16S rRNA. Even though CRASS is not essential for plant survival it lowers chloroplast translation activity, photosynthesis as well as growth under stress conditions indicating a role in the biogenesis and/or stability of the chloroplast ribosome (Pulido et al., 2018). Another interesting protein in this context is PAC that localises to plastid nucleoids. PAC was shown to bind 23S rRNA and to promote biogenesis of the chloroplast ribosome 50S subunit (Meurer et al., 2017). The 16S rRNA is bound by RAP, the only octatricopeptide repeat

(OPR) protein in *Arabidopsis thaliana*. RAP also localises to the plastid nucleoids where it is required for 16S rRNA maturation to ensure proper chloroplast translation and photosynthesis (Kleinknecht et al., 2014). Although ptNAP45 is annotated as an endoribonuclease E-like protein ([www.arabidopsis.org](http://www.arabidopsis.org)), which have been described to be involved in rRNA processing (Carpousis et al., 2009), no significant sequence homologies could be detected. Future studies will show whether ptNAP45-like possibly has the potential to bind or process rRNA.

Nevertheless, it could be shown that ptNAP45 is associated with plastid nucleoids. During chloroplast development ptNAP45 shows the same movement pattern as plastid nucleoids, that relocate from the inner envelope in young chloroplasts towards the thylakoid membrane in mature chloroplasts (Powikrowska et al., 2014b). Furthermore, changes of nucleoid structure have been studied in *whirly1* barley plants where plastids of white sections contained few large nucleoids whereas plastids in green sections became smaller, denser and more abundant (Krupinska et al., 2014). In future studies it will be interesting to also stain and analyse nucleoids of *ptnap45* RNAi and mutant lines.

ptNAP45 is only loosely attached to the thylakoid membrane and is not found in any complex with other prominent proteins of the thylakoid membrane. It is therefore assumed that ptNAP45 associates to the thylakoid membrane via plastid nucleoids. So far, only few proteins have been described to bind to plastid nucleoids and most of their functions remain elusive. However, it is striking that many of the other ptNAPs described so far are multifunctional e.g. by fulfilling a function in compacting DNA while the enzymatic activity as a sulphite reductase of the protein is maintained, as is the case with SiR (Krupinska et al., 2013) or by additionally functioning as a transcription factor like WHIRLY1 (Krupinska et al., 2014) or PEND (Sato et al., 1998). Upon removal of its TP, PEND localises to the cell nucleus supporting its role as a transcription factor (Terasawa and Sato, 2009). When the TP of ptNAP45 was removed, the protein simply accumulated in the cytosol arguing against an additional function as a transcription factor.

Beside the defects in chloroplast ribosome assembly, RNA levels of both PEP and NEP encoded transcripts appeared to be strongly reduced in the *ptnap45* mutant. The decreased RNA of both PEP and NEP transcripts is surprising as the architectural reorganization of nucleoids during light-dependent chloroplast differentiation has been described to be correlated with a switch in polymerase usage. PEP transcripts increase in mature chloroplasts while NEP transcripts decrease (Powikrowska et al., 2014b). The observed overall low transcript levels may therefore be a secondary effect resulting from the overall strong phenotype.

Taken together, it could be shown that ptNAP45 comigrates with pre-assembled states of the 50S ribosomal subunit indicating that ptNAP45 forms a complex with the chloroplast ribosomal 50S subunit. It is proposed that ptNAP45 plays a unique role for the accurate process of chloroplast biogenesis in higher plants by enabling plastid ribosome assembly as ptNAP45 is not only associated

with plastid nucleoids, the place of plastid ribosome assembly, but also builds complexes with rRNAs in the stroma. Therefore, ptNAP45 could function as an auxiliary factor during chloroplast ribosome assembly. As multifunctionality has been stated as a common feature of ptNAPs, it will be interesting to reveal putative additional molecular functions of ptNAP45. It is conceivable that ptNAP45 also acts as a chaperone ensuring proper organization of nucleoids or as a molecular anchor to attach the nucleoids to the thylakoid membrane. Previously, it could be shown for the ptNAPs SVR4 and SVR4-like that their primary aa sequence contains 20% negatively charged glutamic or aspartic acid residues which is a characteristic feature for chaperone proteins, that might assist in assembly and maintenance of DNA/RNA-protein complexes (Powikrowska et al., 2014a). In the primary aa sequence of ptNAP45, almost 17% negatively charged glutamic or aspartic acid residues can be found which strengthens the idea of an additional role of ptNAP45 as a chaperone. However, further investigation is needed to confirm this.

#### 4.4 Now, what's the deal with plastid vesicles?

Is there a plastid vesicle transport system? Indeed, it is very likely that there is, but still too little insight has been gained to eventually prove such system. Even if the proteins studied and described in this thesis cannot be assigned with certainty to such a vesicle transport system (in the case of SNARE AP, SYTL5.2, and EMB1303) or ended up playing another important role for the chloroplast (in the case of ptNAP45), our knowledge regarding the processes contributing to thylakoid biogenesis is steadily increasing.

Only recently, a Sec14-like protein was discovered in chloroplasts of *Arabidopsis thaliana* that seems to be necessary for photoautotrophic growth and vesicle formation at the inner envelope membrane of chloroplasts (Hertle et al., 2020). Sec14 proteins are exclusively found in eukaryotes where they play an essential role for vesicle formation, budding and trafficking at the *trans*-Golgi network (Bankaitis et al., 1990). The chloroplast-localised Sec14 domain protein (cpSFL1) is an essential protein as loss-of-function results in seedling lethal albino mutants with a defect in thylakoid structure and a lack of plastid vesicles. Moreover, it could be shown that cpSFL1 was not only able to complement its yeast counterpart *sec14* but also to fulfil the same function. Both proteins bind and transfer PIPs as well as PA between membrane bilayers suggesting that cpSFL1 potentially facilitates plastid vesicle formation (Hertle et al., 2020).

Still, many gaps concerning plastid vesicle transport need to be filled and further studies are needed in the future to experimentally identify more and more proteins involved in this complex process. It is also conceivable that the *de novo* formation of thylakoid membranes does not happen exclusively by plastid vesicle transport, but additionally by invaginations and/or direct contact sites with the inner envelope.

Another interesting area that needs to be covered is the question of eukaryotic and prokaryotic traits. In a sense, chloroplasts get their own way. Due to their endosymbiotic origin, processes are found everywhere in plastids that live from a coordinated interplay of eukaryotic and prokaryotic components. Therefore, it stands to reason that this could also be the case in plastid vesicle transport. It could be shown for example that a putative ATP-binding cassette transporter of bacterial origin resides in the chloroplast inner envelope that functions in transporting lipids putatively coming from the ER and needed for the thylakoids into the chloroplast (Roston et al., 2012). These processes could be linked to plastid vesicle transport and putatively involve numerous complexes of different origin. Finally, increasingly better microscopic resolution in combination with live cell imaging will provide us with fascinating insights into the processes within the chloroplast and perhaps eventually solve the mystery of thylakoid biogenesis.

## Supplement

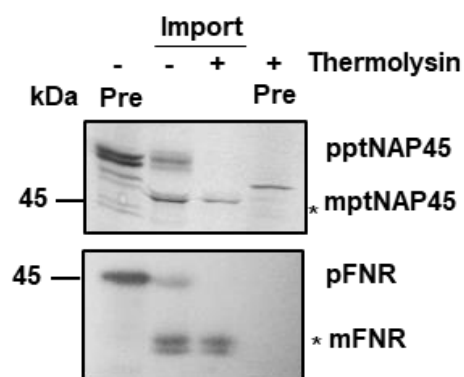


**Figure S1: *In vitro* import of ptNAP45 into chloroplasts.** ptNAP45 and the stromal control FNR were transcribed and translated *in vitro* and imported into isolated chloroplasts with subsequent thermolysin digest. Import was detected by autoradiography using a Typhoon imager. Figure partially taken from Espinoza Corral (2019).

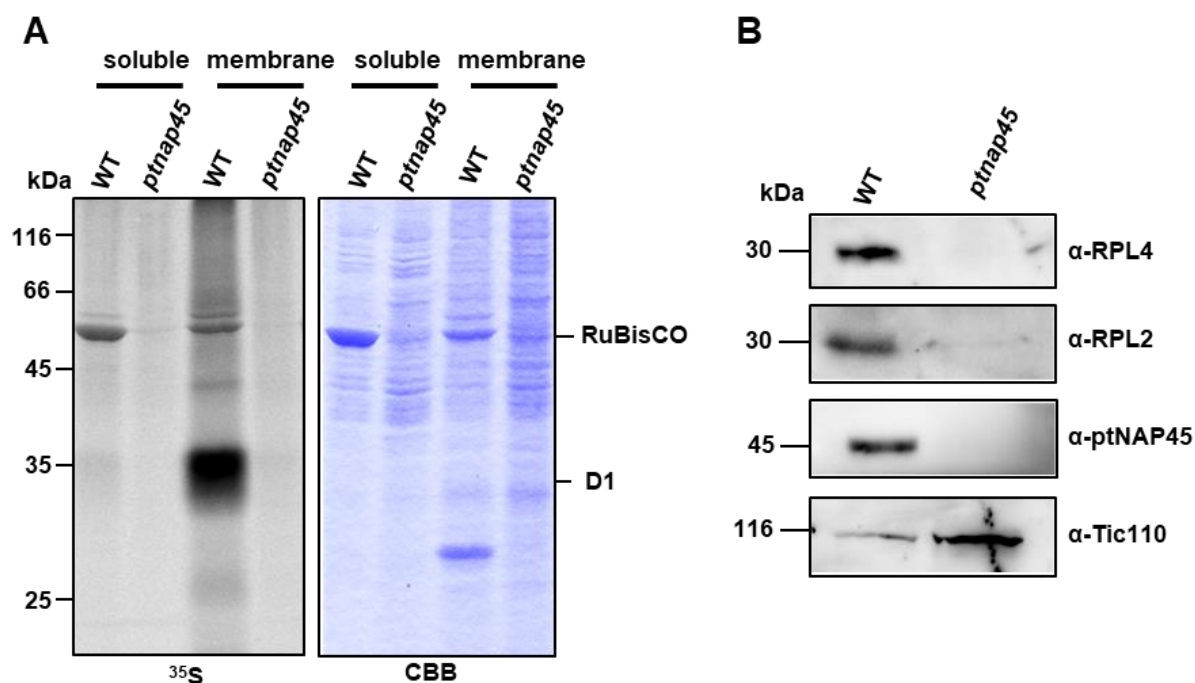


**Figure S2: Translational defects in *ptnap45*.** **A** *In vivo* radiolabelling with subsequent isolation of radioactively labelled soluble and membrane proteins (left panel) and Coomassie staining (right panel). **B** Immunodetection of the plastid ribosome subunits RPL4 and RPL2 in total protein fraction of *ptnap45* in comparison to WT. Antisera against ptNAP45 and Tic110 served as controls. Figure partially taken from Espinoza Corral (2019).

## References

- ADAM, Z., CHARUVI, D., TSABARI, O., KNOPF, R. R. & REICH, Z. 2011. Biogenesis of thylakoid networks in angiosperms: knowns and unknowns. *Plant Mol Biol*, 76, 221-34.
- ALBERTSSON, P.-Å. 1995. The structure and function of the chloroplast photosynthetic membrane—a model for the domain organization. *Photosynthesis Research*, 46, 141-149.
- ALBRECHT, V., INGENFELD, A. & APEL, K. 2008. Snowy cotyledon 2: the identification of a zinc finger domain protein essential for chloroplast development in cotyledons but not in true leaves. *Plant molecular biology*, 66, 599-608.
- ANDERSSON, B. & ANDERSON, J. M. 1980. Lateral heterogeneity in the distribution of chlorophyll-protein complexes of the thylakoid membranes of spinach chloroplasts. *Biochim Biophys Acta*, 593, 427-40.
- ANDERSSON, M. & DÖRMANN, P. 2008. Chloroplast membrane lipid biosynthesis and transport. *Plant Cell Monographs*, Springer, Berlin, Heidelberg.
- ANDERSSON, M. X. & SANDELIUS, A. S. 2004. A chloroplast-localized vesicular transport system: a bioinformatics approach. *BMC Genomics*, 5, 40.
- ARNON, D. 1949. Copper enzyme in isolated chloroplast and chlorophyll expressed in terms of mg per gram. *Plant Physiology*, 24, 15.
- ARONSSON, H. & JARVIS, P. 2002. A simple method for isolating import-competent Arabidopsis chloroplasts. *Febs Letters*, 529, 215-220.
- ARVIDSSON, P.-O. & SUNDBY, C. 1999. A model for the topology of the chloroplast thylakoid membrane. *Functional Plant Biology*, 26, 687-694.
- AUSTIN, J. R., 2ND & STAEHELIN, L. A. 2011. Three-dimensional architecture of grana and stroma thylakoids of higher plants as determined by electron tomography. *Plant Physiol*, 155, 1601-11.
- BANKAITIS, V. A., AITKEN, J. R., CLEVES, A. E. & DOWHAN, W. 1990. An essential role for a phospholipid transfer protein in yeast Golgi function. *Nature*, 347, 561-562.
- BELLAOUI, M., KEDDIE, J. S. & GRUISSEM, W. 2003. DCL is a plant-specific protein required for plastid ribosomal RNA processing and embryo development. *Plant Mol Biol*, 53, 531-43.
- BERRY, E. A., GUERGOVA-KURAS, M., HUANG, L.-S. & CROFTS, A. R. 2000. Structure and function of cytochrome bc complexes. *Annual review of biochemistry*, 69, 1005-1075.
- BINDER, A., LAMBERT, J., MORBITZER, R., POPP, C., OTT, T., LAHAYE, T. & PARNISKE, M. 2014. A modular plasmid assembly kit for multigene expression, gene silencing and silencing rescue in plants. *PLoS One*, 9, e88218.
- BOFFEY, S. A., ELLIS, J. R., SELLDÉN, G. & LEECH, R. M. 1979. Chloroplast division and DNA synthesis in light-grown wheat leaves. *Plant physiology*, 64, 502-505.

- BOHNE, A.-V. 2014. The nucleoid as a site of rRNA processing and ribosome assembly. *Frontiers in Plant Science*, 5, 257.
- BONIFACINO, J. S. & GLICK, B. S. 2004. The mechanisms of vesicle budding and fusion. *Cell*, 116, 153-66.
- BUICK, R. 2008. When did oxygenic photosynthesis evolve? *Philosophical Transactions of the Royal Society of London* 363, 2731-2743.
- BYRNE, M. E., SIMOROWSKI, J. & MARTIENSSEN, R. A. 2002. ASYMMETRIC LEAVES1 reveals knox gene redundancy in Arabidopsis. *Development*, 129, 1957-1965.
- CANNON, G. C., WARD, L. N., CASE, C. I. & HEINHORST, S. 1999. The 68 kDa DNA compacting nucleoid protein from soybean chloroplasts inhibits DNA synthesis in vitro. *Plant molecular biology*, 39, 835-845.
- CARPOUSIS, A. J., LUISI, B. F. & MCDOWALL, K. J. 2009. Endonucleolytic initiation of mRNA decay in Escherichia coli. *Progress in molecular biology and translational science*, 85, 91-135.
- CHAPMAN, E. R. 2008. How does synaptotagmin trigger neurotransmitter release? *Annu Rev Biochem*, 77, 615-41.
- CHARUVI, D., KISS, V., NEVO, R., SHIMONI, E., ADAM, Z. & REICH, Z. 2012. Gain and loss of photosynthetic membranes during plastid differentiation in the shoot apex of Arabidopsis. *Plant Cell*, 24, 1143-57.
- CHEN, M., CHOI, Y., VOYTAS, D. F. & RODERMEL, S. 2000. Mutations in the Arabidopsis VAR2 locus cause leaf variegation due to the loss of a chloroplast FtsH protease. *The Plant Journal*, 22, 303-313.
- CHI-HAM, C. L., KEATON, M. A., CANNON, G. C. & HEINHORST, S. 2002. The DNA-compacting protein DCP68 from soybean chloroplasts is ferredoxin: sulfite reductase and co-localizes with the organellar nucleoid. *Plant molecular biology*, 49, 621-630.
- CHI, W., HE, B., MAO, J., LI, Q., MA, J., JI, D., ZOU, M. & ZHANG, L. 2012. The function of RH22, a DEAD RNA helicase, in the biogenesis of the 50S ribosomal subunits of Arabidopsis chloroplasts. *Plant Physiol*, 158, 693-707.
- CHICKA, M. C., HUI, E., LIU, H. & CHAPMAN, E. R. 2008. Synaptotagmin arrests the SNARE complex before triggering fast, efficient membrane fusion in response to Ca<sup>2+</sup>. *Nat Struct Mol Biol*, 15, 827-35.
- CHIGRI, F., SIPPEL, C., KOLB, M. & VOTHKNECHT, U. C. 2009. Arabidopsis OBG-like GTPase (AtOBGL) is localized in chloroplasts and has an essential function in embryo development. *Mol Plant*, 2, 1373-83.
- CHITNIS, P. 2001. Photosystem I: function and physiology. *Annual review of plant biology*, 52, 593-626.
- CLINE, K. & KEEGSTRA, K. 1983. Galactosyltransferases involved in galactolipid biosynthesis are located in the outer membrane of pea chloroplast envelopes. *Plant Physiol*, 71, 366-72.

- CLOUGH, S. J. & BENT, A. F. 1998. Floral dip: a simplified method for *Agrobacterium*-mediated transformation of *Arabidopsis thaliana*. *The plant journal*, 16, 735-743.
- CRAN, D. & POSSINGHAM, J. 1974. Plastid thylakoid formation. *Annals of Botany*, 38, 843-847.
- CRAXTON, M. 2001. Genomic analysis of synaptotagmin genes. *Genomics*, 77, 43-9.
- CRAXTON, M. 2004. Synaptotagmin gene content of the sequenced genomes. *BMC Genomics*, 5, 43.
- CRAXTON, M. 2007. Evolutionary genomics of plant genes encoding N-terminal-TM-C2 domain proteins and the similar FAM62 genes and synaptotagmin genes of metazoans. *BMC Genomics*, 8, 259.
- CURWIN, A. J., FAIRN, G. D. & MCMASTER, C. R. 2009. Phospholipid transfer protein Sec14 is required for trafficking from endosomes and regulates distinct trans-Golgi export pathways. *Journal of Biological Chemistry*, 284, 7364-7375.
- DELISA, M. P., LEE, P., PALMER, T. & GEORGIU, G. 2004. Phage shock protein PspA of *Escherichia coli* relieves saturation of protein export via the Tat pathway. *J Bacteriol*, 186, 366-73.
- DESVEAUX, D., DESPRÉS, C., JOYEUX, A., SUBRAMANIAM, R. & BRISSON, N. 2000. PBF-2 is a novel single-stranded DNA binding factor implicated in PR-10a gene activation in potato. *The Plant Cell*, 12, 1477-1489.
- DIERSTEIN, R., SCHUMACHER, A. & DREWS, G. 1981. On insertion of pigment-associated polypeptides during membrane biogenesis in *Rhodospseudomonas capsulata*. *Archives of Microbiology*, 128, 376-383.
- DREWS, G. & GOLECKI, J. R. 1995. Structure, molecular organization, and biosynthesis of membranes of purple bacteria. *Anoxygenic photosynthetic bacteria*. Springer.
- DYALL, S. D., BROWN, M. T. & JOHNSON, P. J. 2004. Ancient invasions: from endosymbionts to organelles. *Science*, 304, 253-257.
- EGGINK, L. L., PARK, H. & HOOBER, J. K. 1999. The role of the envelope in assembly of light-harvesting complexes in the chloroplast: distribution of LHCP between chloroplast and vacuoles during chloroplast development in *Chlamydomonas reinhardtii*. *The Chloroplast: From Molecular Biology to Biotechnology*. Springer.
- EMANUELSSON, O., NIELSEN, H. & HEIJNE, G. V. 1999. ChloroP, a neural network-based method for predicting chloroplast transit peptides and their cleavage sites. *Protein Science*, 8, 978-984.
- ERIKSSON, G., KAHN, A., WALLE, B. & VON WETTSTEIN, D. 1961. Zur makromolekularen Physiologie der Chloroplasten. III. *Ber. dtsh. bot. Ges*, 74, 221-232.
- ESPINOZA-CORRAL, R., HEINZ, S., KLINGL, A., JAHNS, P., LEHMANN, M., MEURER, J., NICKELSEN, J., SOLL, J. & SCHWENKERT, S. 2019. Plastoglobular protein 18 is involved in chloroplast function and thylakoid formation. *Journal of experimental botany*, 70, 3981-3993.
- ESPINOZA CORRAL, R. A. 2019. *Characterization of new proteins involved in chloroplast biogenesis from Arabidopsis thaliana*. Imu.

- FOOTITT, S., AWAN, S. & FINCH-SAVAGE, W. E. 2018. An improved method for the rapid isolation of RNA from Arabidopsis and seeds of other species high in polyphenols and polysaccharides. *Seed Science Research*, 28, 360-364.
- FORESTI, O. & DENECKE, J. 2008. Intermediate organelles of the plant secretory pathway: identity and function. *Traffic*, 9, 1599-612.
- GAO, H., SAGE, T. L. & OSTERYOUNG, K. W. 2006. FZL, an FZO-like protein in plants, is a determinant of thylakoid and chloroplast morphology. *Proc Natl Acad Sci U S A*, 103, 6759-64.
- GAO, H. & XU, X. 2009. Depletion of Vipp1 in *Synechocystis* sp. PCC 6803 affects photosynthetic activity before the loss of thylakoid membranes. *FEMS Microbiol Lett*, 292, 63-70.
- GARCÍA-CERDÁN, J. G., SCHMID, E. M., TAKEUCHI, T., MCRAE, I., MCDONALD, K. L., YORDDUANGJUN, N., HASSAN, A. M., GROB, P., XU, C. S. & HESS, H. F. 2020. Chloroplast Sec14-like 1 (CPSFL1) is essential for normal chloroplast development and affects carotenoid accumulation in *Chlamydomonas*. *Proceedings of the National Academy of Sciences*, 117, 12452-12463.
- GARCIA, C., KHAN, N. Z., NANNMARK, U. & ARONSSON, H. 2010. The chloroplast protein CPSAR1, dually localized in the stroma and the inner envelope membrane, is involved in thylakoid biogenesis. *Plant J*, 63, 73-85.
- GREINER, S., GOLCZYK, H., MALINOVA, I., PELLIZZER, T., BOCK, R., BÖRNER, T. & HERRMANN, R. G. 2019. Chloroplast nucleoids are highly dynamic in ploidy, number, and structure during angiosperm leaf development. *bioRxiv*, 632240.
- GROTH, G. & STROTMANN, H. 1999. New results about structure, function and regulation of the chloroplast ATP synthase (CF<sub>1</sub>CF<sub>0</sub>). *Physiologia Plantarum*, 106, 142-148.
- GRZYB, J. M., SOLYMOSI, K., STRZALKA, K. & MYSLIWA-KURDZIEL, B. 2013. Visualization and characterization of prolamellar bodies with atomic force microscopy. *J Plant Physiol*, 170, 1217-27.
- GÜGEL, I. L. & SOLL, J. 2017. Chloroplast differentiation in the growing leaves of *Arabidopsis thaliana*. *Protoplasma*, 254, 1857-1866.
- GUNNING, B. 1965. The greening process in plastids. *Protoplasma*, 60, 111-130.
- GUTU, A., CHANG, F. & O'SHEA, E. K. 2018. Dynamical localization of a thylakoid membrane binding protein is required for acquisition of photosynthetic competency. *Mol Microbiol*, 108, 16-31.
- HANAHAN, D. 1983. Studies on transformation of *Escherichia coli* with plasmids. *Journal of molecular biology*, 166, 557-580.
- HANKAMER, B., BARBER, J. & BOEKEMA, E. J. 1997. Structure and membrane organization of photosystem II in green plants. *Annual review of plant biology*, 48, 641-671.
- HEIDRICH, J., THURLOTTE, A. & SCHNEIDER, D. 2017. Specific interaction of IM30/Vipp1 with cyanobacterial and chloroplast membranes results in membrane remodeling and eventually in membrane fusion. *Biochim Biophys Acta Biomembr*, 1859, 537-549.

- HERTLE, A. P., GARCÍA-CERDÁN, J. G., ARMBRUSTER, U., SHIH, R., LEE, J. J., WONG, W. & NIYOGI, K. K. 2020. A Sec14 domain protein is required for photoautotrophic growth and chloroplast vesicle formation in *Arabidopsis thaliana*. *Proceedings of the National Academy of Sciences*, 117, 9101-9111.
- HOOBER, J. K. & EGGINK, L. L. 2001. A potential role of chlorophylls b and c in assembly of light-harvesting complexes. *FEBS Lett*, 489, 1-3.
- HUANG, W., CHEN, Q., ZHU, Y., HU, F., ZHANG, L., MA, Z., HE, Z. & HUANG, J. 2013. *Arabidopsis* thylakoid formation 1 is a critical regulator for dynamics of PSII-LHCII complexes in leaf senescence and excess light. *Mol Plant*, 6, 1673-91.
- HUANG, X., ZHANG, X. & YANG, S. 2009. A novel chloroplast-localized protein EMB1303 is required for chloroplast development in *Arabidopsis*. *Cell Res*, 19, 1205-16.
- INOUE, H., TANI, K. & TAGAYA, M. 2016. SNARE-associated proteins and receptor trafficking. *Receptors & Clinical Investigation*, 3.
- JAHN, R. & SCHELLER, R. H. 2006. SNAREs—engines for membrane fusion. *Nature reviews Molecular cell biology*, 7, 631-643.
- JEFFREY, S. W., DOUCE, R. & BENSON, A. A. 1974. Carotenoid transformations in the chloroplast envelope. *Proc Natl Acad Sci U S A*, 71, 807-10.
- JOYARD, J., MARÉCHAL, E., MIÈGE, C., BLOCK, M. A., DORNE, A.-J. & DOUCE, R. 1998. Structure, distribution and biosynthesis of glycerolipids from higher plant chloroplasts. *Lipids in photosynthesis: Structure, function and genetics*. Springer.
- JUNGLAS, B. & SCHNEIDER, D. 2018. What is Vipp1 good for? *Mol Microbiol*, 108, 1-5.
- KARIM, S., ALEZZAWI, M., GARCIA-PETIT, C., SOLYMOSI, K., KHAN, N. Z., LINDQUIST, E., DAHL, P., HOHMANN, S. & ARONSSON, H. 2014. A novel chloroplast localized Rab GTPase protein CPRabA5e is involved in stress, development, thylakoid biogenesis and vesicle transport in *Arabidopsis*. *Plant Mol Biol*, 84, 675-92.
- KARIMI, M., DEPICKER, A. & HILSON, P. 2007. Recombinational cloning with plant gateway vectors. *Plant physiology*, 145, 1144-1154.
- KARIMI, M., INZÉ, D. & DEPICKER, A. 2002. GATEWAY™ vectors for *Agrobacterium*-mediated plant transformation. *Trends in plant science*, 7, 193-195.
- KEELING, P. J. 2010. The endosymbiotic origin, diversification and fate of plastids. *Philosophical Transactions of the Royal Society of London B: Biological Sciences*, 365, 729-748.
- KELLER, R. & SCHNEIDER, D. 2013. Homologs of the yeast Tvp38 vesicle-associated protein are conserved in chloroplasts and cyanobacteria. *Frontiers in plant science*, 4, 467.
- KELLY, A. A. & DORMANN, P. 2004. Green light for galactolipid trafficking. *Curr Opin Plant Biol*, 7, 262-9.

- KHAN, N. Z., LINDQUIST, E. & ARONSSON, H. 2013. New putative chloroplast vesicle transport components and cargo proteins revealed using a bioinformatics approach: an Arabidopsis model. *PLoS One*, 8, e59898.
- KIKUCHI, S., BÉDARD, J. & NAKAI, M. 2011. One- and two-dimensional blue native-PAGE and immunodetection of low-abundance chloroplast membrane protein complexes. *Chloroplast Research in Arabidopsis*. Springer.
- KLEIN, S., BRYAN, G. & BOGORAD, L. 1964. Early stages in the development of plastid fine structure in red and far-red light. *The Journal of cell biology*, 22, 433-442.
- KLEINKNECHT, L., WANG, F., STÜBE, R., PHILIPPAR, K., NICKELSEN, J. & BOHNE, A.-V. 2014. RAP, the sole octotricopeptide repeat protein in Arabidopsis, is required for chloroplast 16S rRNA maturation. *The Plant Cell*, 26, 777-787.
- KLEPIKOVA, A. V., KASIANOV, A. S., GERASIMOV, E. S., LOGACHEVA, M. D. & PENIN, A. A. 2016. A high resolution map of the Arabidopsis thaliana developmental transcriptome based on RNA-seq profiling. *The Plant Journal*, 88, 1058-1070.
- KOBAYASHI, K., KONDO, M., FUKUDA, H., NISHIMURA, M. & OHTA, H. 2007. Galactolipid synthesis in chloroplast inner envelope is essential for proper thylakoid biogenesis, photosynthesis, and embryogenesis. *Proc Natl Acad Sci U S A*, 104, 17216-21.
- KOBAYASHI, K., NARISE, T., SONOIKE, K., HASHIMOTO, H., SATO, N., KONDO, M., NISHIMURA, M., SATO, M., TOYOOKA, K. & SUGIMOTO, K. 2013. Role of galactolipid biosynthesis in coordinated development of photosynthetic complexes and thylakoid membranes during chloroplast biogenesis in Arabidopsis. *The Plant Journal*, 73, 250-261.
- KÖHLER, R. H., SCHWILLE, P., WEBB, W. W. & HANSON, M. R. 2000. Active protein transport through plastid tubules: velocity quantified by fluorescence correlation spectroscopy. *J Cell Sci*, 113 ( Pt 22), 3921-30.
- KOOP, H.-U., STEINMÜLLER, K., WAGNER, H., RÖBLER, C., EIBL, C. & SACHER, L. 1996. Integration of foreign sequences into the tobacco plastome via polyethylene glycol-mediated protoplast transformation. *Planta*, 199, 193-201.
- KOWALEWSKA, L., MAZUR, R., SUSKI, S., GARSTKA, M. & MOSTOWSKA, A. 2016. Three-Dimensional Visualization of the Tubular-Lamellar Transformation of the Internal Plastid Membrane Network during Runner Bean Chloroplast Biogenesis. *Plant Cell*, 28, 875-91.
- KRAUSE, K., KILBIENSKI, I., MULISCH, M., RÖDIGER, A., SCHÄFER, A. & KRUPINSKA, K. 2005. DNA-binding proteins of the Whirly family in Arabidopsis thaliana are targeted to the organelles. *FEBS letters*, 579, 3707-3712.
- KROLL, D., MEIERHOFF, K., BECHTOLD, N., KINOSHITA, M., WESTPHAL, S., VOTHKNECHT, U. C., SOLL, J. & WESTHOFF, P. 2001. VIPP1, a nuclear gene of Arabidopsis thaliana essential for thylakoid membrane formation. *Proc Natl Acad Sci U S A*, 98, 4238-42.
- KRUPINSKA, K., MELONEK, J. & KRAUSE, K. 2013. New insights into plastid nucleoid structure and functionality. *Planta*, 237, 653-664.

- KRUPINSKA, K., OETKE, S., DESEL, C., MULISCH, M., SCHÄFER, A., HOLLMANN, J., KUMLEHN, J. & HENSEL, G. 2014. WHIRLY1 is a major organizer of chloroplast nucleoids. *Frontiers in plant science*, 5, 432.
- KUROIWA, T., SUZUKI, T., OGAWA, K. & KAWANO, S. 1981. The chloroplast nucleus: distribution, number, size, and shape, and a model for the multiplication of the chloroplast genome during chloroplast development. *Plant and Cell Physiology*, 22, 381-396.
- LAEMMLI, U. K. 1970. Cleavage of structural proteins during the assembly of the head of bacteriophage T4. *nature*, 227, 680-685.
- LI, H.-M., KANEKO, Y. & KEEGSTRA, K. 1994. Molecular cloning of a chloroplastic protein associated with both the envelope and thylakoid membranes. *Plant molecular biology*, 25, 619-632.
- LINDQUIST, E., ALEZZAWI, M. & ARONSSON, H. 2014. Bioinformatic indications that COPI- and clathrin-based transport systems are not present in chloroplasts: an Arabidopsis model. *PLoS One*, 9, e104423.
- LINDQUIST, E. & ARONSSON, H. 2018. Chloroplast vesicle transport. *Photosynth Res.*
- LINDQUIST, E., SOLYMOSI, K. & ARONSSON, H. 2016. Vesicles Are Persistent Features of Different Plastids. *Traffic*, 17, 1125-38.
- MAJERAN, W., FRISO, G., ASAKURA, Y., QU, X., HUANG, M., PONNALA, L., WATKINS, K. P., BARKAN, A. & VAN WIJK, K. J. 2012. Nucleoid-enriched proteomes in developing plastids and chloroplasts from maize leaves: a new conceptual framework for nucleoid functions. *Plant physiology*, 158, 156-189.
- MANUELL, A. L., QUISPE, J. & MAYFIELD, S. P. 2007. Structure of the chloroplast ribosome: novel domains for translation regulation. *PLoS Biol*, 5, e209.
- MARGULIS, L. 1970. *Origin of eukaryotic cells: Evidence and research implications for a theory of the origin and evolution of microbial, plant and animal cells on the precambrian Earth*, Yale University Press.
- MARTIN, W., STOEBE, B., GOREMYKIN, V., HANSMANN, S., HASEGAWA, M. & KOWALLIK, K. V. 1998. Gene transfer to the nucleus and the evolution of chloroplasts. *Nature Reviews Molecular Cell Biology*, 393, 162.
- MARTIN, W. F., GARG, S. & ZIMORSKI, V. 2015. Endosymbiotic theories for eukaryote origin. *Phil. Trans. R. Soc. B*, 370, 20140330.
- MCFADDEN, G. I. 2001. Primary and secondary endosymbiosis and the origin of plastids. *Journal of Phycology*, 37, 951-959.
- MECHELA, A., SCHWENKERT, S. & SOLL, J. 2019. A brief history of thylakoid biogenesis. *Royal Society Open Biology*, 9, 180237.
- MEURER, J., SCHMID, L. M., STOPPEL, R., LEISTER, D., BRACHMANN, A. & MANAVSKI, N. 2017. PALE CRESS binds to plastid RNAs and facilitates the biogenesis of the 50S ribosomal subunit. *The Plant Journal*, 92, 400-413.

- MORI, H., SUMMER, E. J. & CLINE, K. 2001. Chloroplast TatC plays a direct role in thylakoid  $\Delta$ pH-dependent protein transport. *Febs Letters*, 501, 65-68.
- MORRÉ, D. J., MINNIFIELD, N. & PAULIK, M. 1989. Identification of the 16 C compartment of the endoplasmic reticulum in rat liver and cultured hamster kidney cells. *Biology of the Cell*, 67, 51-60.
- MORRÉ, D. J., SELLDEN, G., SUNDQVIST, C. & SANDELIUS, A. S. 1991. Stromal low temperature compartment derived from the inner membrane of the chloroplast envelope. *Plant Physiol*, 97, 1558-64.
- MOUSLEY, C. J., TYERYAR, K. R., VINCENT-POPE, P. & BANKAITIS, V. A. 2007. The Sec14-superfamily and the regulatory interface between phospholipid metabolism and membrane trafficking. *Biochimica et Biophysica Acta (BBA)-Molecular and Cell Biology of Lipids*, 1771, 727-736.
- MÜHLETHALER, K. 1971. The ultrastructure of plastids. *The Structure and Function of Chloroplasts*, Springer-Verlag, Berlin, 7-34.
- MÜHLETHALER, K. & FREY-WYSSLING, A. 1959. Entwicklung und struktur der proplastiden. *The Journal of Cell Biology*, 6, 507-512.
- NAKAMURA, Y., KANEKO, T., SATO, S., MIMURO, M., MIYASHITA, H., TSUCHIYA, T., SASAMOTO, S., WATANABE, A., KAWASHIMA, K., KISHIDA, Y., KIYOKAWA, C., KOHARA, M., MATSUMOTO, M., MATSUNO, A., NAKAZAKI, N., SHIMPO, S., TAKEUCHI, C., YAMADA, M. & TABATA, S. 2003. Complete genome structure of *Gloeobacter violaceus* PCC 7421, a cyanobacterium that lacks thylakoids (supplement). *DNA Res*, 10, 181-201.
- NICKEL, C., BRYLOK, T. & SCHWENKERT, S. 2016. In vivo radiolabeling of Arabidopsis chloroplast proteins and separation of thylakoid membrane complexes by blue native PAGE. *Plant Proteostasis*. Springer.
- NICKELSEN, J. & ZERGES, W. 2013. Thylakoid biogenesis has joined the new era of bacterial cell biology. *Front Plant Sci*, 4, 458.
- NISHIMURA, K., ASHIDA, H., OGAWA, T. & YOKOTA, A. 2010. A DEAD box protein is required for formation of a hidden break in Arabidopsis chloroplast 23S rRNA. *Plant J*, 63, 766-77.
- OHNISHI, N., ZHANG, L. & SAKAMOTO, W. 2018. VIPP1 Involved in Chloroplast Membrane Integrity Has GTPase Activity in Vitro. *Plant Physiol*, 177, 328-338.
- OLINARES, P. D. B., PONNALA, L. & VAN WIJK, K. J. 2010. Megadalton complexes in the chloroplast stroma of Arabidopsis thaliana characterized by size exclusion chromatography, mass spectrometry, and hierarchical clustering. *Molecular & Cellular Proteomics*, 9, 1594-1615.
- PAIERI, F., TADINI, L., MANAVSKI, N., KLEINE, T., FERRARI, R., MORANDINI, P., PESARESI, P., MEURER, J. & LEISTER, D. 2018. The DEAD-box RNA Helicase RH50 Is a 23S-4.5S rRNA Maturation Factor that Functionally Overlaps with the Plastid Signaling Factor GUN1. *Plant Physiol*, 176, 634-648.
- PAOLILLO, D. J., JR. 1970. The three-dimensional arrangement of intergranal lamellae in chloroplasts. *J Cell Sci*, 6, 243-55.

- PATIL, M. 2018. *Role of putative vesicle trafficking proteins FZL, Synaptotagmin 5.2 and SNARE\_AP in chloroplast development*. *Imu*.
- PATIL, M., SEIFERT, S., SEILER, F., SOLL, J. & SCHWENKERT, S. 2018. FZL is primarily localized to the inner chloroplast membrane however influences thylakoid maintenance. *Plant Mol Biol*, 97, 421-433.
- POGSON, B. J., GANGULY, D. & ALBRECHT-BORTH, V. 2015. Insights into chloroplast biogenesis and development. *Biochimica et Biophysica Acta -Bioenergetics*, 1847, 1017-1024.
- PORRA, R., THOMPSON, W. & KRIEDEMANN, P. 1989. Determination of accurate extinction coefficients and simultaneous equations for assaying chlorophylls a and b extracted with four different solvents: verification of the concentration of chlorophyll standards by atomic absorption spectroscopy. *Biochimica et Biophysica Acta (BBA)-Bioenergetics*, 975, 384-394.
- POWIKROWSKA, M., KHROUCHTCHOVA, A., MARTENS, H. J., ZYGADLO-NIELSEN, A., MELONEK, J., SCHULZ, A., KRUPINSKA, K., RODERMEL, S. & JENSEN, P. E. 2014a. SVR4 (suppressor of variegation 4) and SVR4-like: two proteins with a role in proper organization of the chloroplast genetic machinery. *Physiologia Plantarum*, 150, 477-492.
- POWIKROWSKA, M., OETKE, S., JENSEN, P. E. & KRUPINSKA, K. 2014b. Dynamic composition, shaping and organization of plastid nucleoids. *Frontiers in plant science*, 5, 424.
- PRIBIL, M., LABS, M. & LEISTER, D. 2014. Structure and dynamics of thylakoids in land plants. *J Exp Bot*, 65, 1955-72.
- PULIDO, P., ZAGARI, N., MANAVSKI, N., GAWRONSKI, P., MATTHES, A., SCHARFF, L. B., MEURER, J. & LEISTER, D. 2018. CHLOROPLAST RIBOSOME ASSOCIATED supports translation under stress and interacts with the ribosomal 30S subunit. *Plant physiology*, 177, 1539-1554.
- QIAO, J., MA, C., WIMMELBACHER, M., BÖRNKE, F. & LUO, M. 2011. Two novel proteins, MRL7 and its paralog MRL7-L, have essential but functionally distinct roles in chloroplast development and are involved in plastid gene expression regulation in Arabidopsis. *Plant and cell physiology*, 52, 1017-1030.
- RAST, A., HEINZ, S. & NICKELSEN, J. 2015a. Biogenesis of thylakoid membranes. *Biochimica et Biophysica Acta -Bioenergetics*, 1847, 821-830.
- RAST, A., HEINZ, S. & NICKELSEN, J. 2015b. Biogenesis of thylakoid membranes. *Biochim Biophys Acta*, 1847, 821-30.
- REITER, B., VAMVAKA, E., MARINO, G., KLEINE, T., JAHNS, P., BOLLE, C., LEISTER, D. & RÜHLE, T. 2020. The Arabidopsis Protein CGL20 Is Required for Plastid 50S Ribosome Biogenesis. *Plant Physiol*, 182, 1222-1238.
- RIPPKA, R., WATERBURY, J. & COHEN-BAZIRE, G. 1974. A cyanobacterium which lacks thylakoids. *Archives of Microbiology*, 100, 419-436.
- ROSADO-ALBERIO, J., WEIER, T. E. & STOCKING, C. 1968. Continuity of the chloroplast membrane systems in *Zea mays* L. *Plant physiology*, 43, 1325-1331.

- ROSTON, R. L., GAO, J., MURCHA, M. W., WHELAN, J. & BENNING, C. 2012. TGD1,-2, and-3 proteins involved in lipid trafficking form ATP-binding cassette (ABC) transporter with multiple substrate-binding proteins. *Journal of Biological Chemistry*, 287, 21406-21415.
- RYBERG, M. & SUNDQVIST, C. 1988. The regular ultrastructure of isolated prolamellar bodies depends on the presence of membrane-bound NADPH-protochlorophyllide oxidoreductase. *Physiologia Plantarum*, 73, 218-226.
- SAKAI, A., TAKANO, H. & KUROIWA, T. 2004. Organelle nuclei in higher plants: structure, composition, function, and evolution. *International review of cytology*, 238, 59.
- SAMBROOK, J., FRITSCH, E. F. & MANIATIS, T. 1989. *Molecular cloning: a laboratory manual*, Cold spring harbor laboratory press.
- SATO, N., ALBRIEUX, C., JOYARD, J., DOUCE, R. & KUROIWA, T. 1993. Detection and characterization of a plastid envelope DNA-binding protein which may anchor plastid nucleoids. *The EMBO journal*, 12, 555-561.
- SATO, N., OHSHIMA, K., WATANABE, A., OHTA, N., NISHIYAMA, Y., JOYARD, J. & DOUCE, R. 1998. Molecular characterization of the PEND protein, a novel bZIP protein present in the envelope membrane that is the site of nucleoid replication in developing plastids. *The Plant Cell*, 10, 859-872.
- SCHÄGGER, H. & VON JAGOW, G. 1991. Blue native electrophoresis for isolation of membrane protein complexes in enzymatically active form. *Analytical biochemistry*, 199, 223-231.
- SCHULZ, T. A. & CREUTZ, C. E. 2004. The tricalbin C2 domains: lipid-binding properties of a novel, synaptotagmin-like yeast protein family. *Biochemistry*, 43, 3987-95.
- SCHWEIGER, R. & SCHWENKERT, S. 2014. Protein-protein interactions visualized by bimolecular fluorescence complementation in tobacco protoplasts and leaves. *JoVE (Journal of Visualized Experiments)*, e51327.
- SHIMADA, H., MOCHIZUKI, M., OGURA, K., FROELICH, J. E., OSTERYOUNG, K. W., SHIRANO, Y., SHIBATA, D., MASUDA, S., MORI, K. & TAKAMIYA, K. 2007. Arabidopsis cotyledon-specific chloroplast biogenesis factor CYO1 is a protein disulfide isomerase. *Plant Cell*, 19, 3157-69.
- SHIMONI, E., RAV-HON, O., OHAD, I., BRUMFELD, V. & REICH, Z. 2005. Three-dimensional organization of higher-plant chloroplast thylakoid membranes revealed by electron tomography. *Plant Cell*, 17, 2580-6.
- SOLL, J. 2016. The plastid reticulum reloaded. *Endocytobiosis Cell Research*, 27.
- SOLL, J., SCHULTZ, G., JOYARD, J., DOUCE, R. & BLOCK, M. A. 1985. Localization and synthesis of prenylquinones in isolated outer and inner envelope membranes from spinach chloroplasts. *Arch Biochem Biophys*, 238, 290-9.
- SOLYMOSI, K. & SCHOEFS, B. 2010. Etioplast and etio-chloroplast formation under natural conditions: the dark side of chlorophyll biosynthesis in angiosperms. *Photosynthesis Research*, 105, 143-166.

- STENGEL, A., GUGEL, I. L., HILGER, D., RENGSTL, B., JUNG, H. & NICKELSEN, J. 2012. Initial steps of photosystem II de novo assembly and preloading with manganese take place in biogenesis centers in *Synechocystis*. *Plant Cell*, 24, 660-75.
- STRUGGER, S. 1950. Über den Bau der Proplastiden und Chloroplasten. *Naturwissenschaften*, 37, 166-167.
- SUDHOF, T. C. 2002. Synaptotagmins: why so many? *J Biol Chem*, 277, 7629-32.
- SUDHOF, T. C. 2013. Neurotransmitter release: the last millisecond in the life of a synaptic vesicle. *Neuron*, 80, 675-90.
- SUZUKI, C. K., REP, M., VAN DIJL, J. M., SUDA, K., GRIVELL, L. A. & SCHATZ, G. 1997. ATP-dependent proteases that also chaperone protein biogenesis. *Trends in biochemical sciences*, 22, 118-123.
- TANZ, S. K., KILIAN, J., JOHANSSON, C., APEL, K., SMALL, I., HARTER, K., WANKE, D., POGSON, B. & ALBRECHT, V. 2012. The SCO2 protein disulphide isomerase is required for thylakoid biogenesis and interacts with LHCB1 chlorophyll a/b binding proteins which affects chlorophyll biosynthesis in *Arabidopsis* seedlings. *Plant J*, 69, 743-54.
- TERASAWA, K. & SATO, N. 2009. Plastid localization of the PEND protein is mediated by a noncanonical transit peptide. *The FEBS journal*, 276, 1709-1719.
- TIKKANEN, M., SUORSA, M., GOLLAN, P. J. & ARO, E. M. 2012. Post-genomic insight into thylakoid membrane lateral heterogeneity and redox balance. *FEBS Lett*, 586, 2911-6.
- TILLER, N. & BOCK, R. 2014. The translational apparatus of plastids and its role in plant development. *Molecular plant*, 7, 1105-1120.
- TORABI, S., PLÖCHINGER, M. & MEURER, J. 2014. Localization and topology of thylakoid membrane proteins in land plants. *Bio Protoc*, 4, e1363.
- UNIACKE, J. & ZERGES, W. 2007. Photosystem II assembly and repair are differentially localized in *Chlamydomonas*. *Plant Cell*, 19, 3640-54.
- VON WETTSTEIN, D. 1959. Developmental changes in chloroplasts and their genetic control. *Developmental Cytology*, 123-160.
- VOTHKNECHT, U. C., OTTERS, S., HENNIG, R. & SCHNEIDER, D. 2012. Vipp1: a very important protein in plastids?! *J Exp Bot*, 63, 1699-712.
- VOTHKNECHT, U. C. & SOLL, J. 2005. Chloroplast membrane transport: interplay of prokaryotic and eukaryotic traits. *Gene*, 354, 99-109.
- VOTHKNECHT, U. C. & WESTHOFF, P. 2001. Biogenesis and origin of thylakoid membranes. *Biochimica et Biophysica Acta -Molecular Cell Research*, 1541, 91-101.
- WAEGERMANN, K. & SOLL, J. 1995. Characterization and isolation of the chloroplast protein import machinery. *Methods in cell biology*. Elsevier.

- WAESE, J., FAN, J., PASHA, A., YU, H., FUCILE, G., SHI, R., CUMMING, M., KELLEY, L. A., STERNBERG, M. J. & KRISHNAKUMAR, V. 2017. ePlant: visualizing and exploring multiple levels of data for hypothesis generation in plant biology. *The Plant Cell*, 29, 1806-1821.
- WANG, Q., SULLIVAN, R. W., KIGHT, A., HENRY, R. L., HUANG, J., JONES, A. M. & KORTH, K. L. 2004. Deletion of the chloroplast-localized Thylakoid formation1 gene product in Arabidopsis leads to deficient thylakoid formation and variegated leaves. *Plant Physiol*, 136, 3594-604.
- WATERS, M. T. & LANGDALE, J. A. 2009. The making of a chloroplast. *The EMBO journal*, 28, 2861-2873.
- WESTPHAL, S., HEINS, L., SOLL, J. & VOTHKNECHT, U. C. 2001b. Vipp1 deletion mutant of Synechocystis: a connection between bacterial phage shock and thylakoid biogenesis? *Proc Natl Acad Sci U S A*, 98, 4243-8.
- WESTPHAL, S., SOLL, J. & VOTHKNECHT, U. C. 2001. A vesicle transport system inside chloroplasts. *FEBS letters*, 506, 257-61.
- WESTPHAL, S., SOLL, J. & VOTHKNECHT, U. C. 2003. Evolution of chloroplast vesicle transport. *Plant cell physiology*, 44, 217-222.
- WILLIAMS, P. M. & BARKAN, A. 2003. A chloroplast-localized PPR protein required for plastid ribosome accumulation. *The Plant Journal*, 36, 675-686.
- YAMAGUCHI, K. & SUBRAMANIAN, A. R. 2000. The Plastid Ribosomal Proteins IDENTIFICATION OF ALL THE PROTEINS IN THE 50 S SUBUNIT OF AN ORGANELLE RIBOSOME (CHLOROPLAST). *Journal of Biological Chemistry*, 275, 28466-28482.
- YAMAGUCHI, K. & SUBRAMANIAN, A. R. 2003. Proteomic identification of all plastid-specific ribosomal proteins in higher plant chloroplast 30S ribosomal subunit: PSRP-2 (U1A-type domains), PSRP-3 $\alpha/\beta$  (ycf65 homologue) and PSRP-4 (Thx homologue). *European Journal of Biochemistry*, 270, 190-205.
- YU, F., PARK, S.-S., LIU, X., FOUDEE, A., FU, A., POWIKROWSKA, M., KHROUCHTCHOVA, A., JENSEN, P. E., KRIGER, J. N. & GRAY, G. R. 2011. SUPPRESSOR OF VARIATION4, a new var2 suppressor locus, encodes a pioneer protein that is required for chloroplast biogenesis. *Molecular plant*, 4, 229-240.
- ZAGARI, N., SANDOVAL-IBANEZ, O., SANDAL, N., SU, J., RODRIGUEZ-CONCEPCION, M., STOUGAARD, J., PRIBIL, M., LEISTER, D. & PULIDO, P. 2017. SNOWY COTYLEDON 2 Promotes Chloroplast Development and Has a Role in Leaf Variegation in Both Lotus japonicus and Arabidopsis thaliana. *Mol Plant*, 10, 721-734.
- ZHANG, L., KATO, Y., OTTERS, S., VOTHKNECHT, U. C. & SAKAMOTO, W. 2012. Essential role of VIPP1 in chloroplast envelope maintenance in Arabidopsis. *Plant Cell*, 24, 3695-707.
- ZHOU, Q., ZHOU, P., WANG, A. L., WU, D., ZHAO, M., SUDHOF, T. C. & BRUNGER, A. T. 2017. The primed SNARE-complexin-synaptotagmin complex for neuronal exocytosis. *Nature*, 548, 420-425.

## Acknowledgements

**„Jag har aldrig provat detta förut, så jag är helt säker på att jag ska göra det!”**

**Pippi Långstrump**

When I started studying, I wasn't even aware of the possibility to get a doctorate outside of medicine. Since then, it has been a long and often rocky road to this goal and without companions, I would have had a hard time making it to the end. To this day, only 1% of non-academic children make it this long way in Germany and I am proud to be one of them.

My thanks go to the people who not only gave me inspiration, but also strengthened my faith in myself and supported me in all my endeavours, no matter how unattainable they seemed. First and foremost, I thank my life partner Korbi, who has always stood by my side in this constant madness and has been a light in the darkest days. I thank mom and dad for supporting their "strong character" daughter with love from her first breath and making all roads possible for me. I thank grandma and grandad for still asking me how "school" was when they wanted to hear about my PhD while at the same time telling everyone I was a professor. I would also like to thank the rest of my family and friends for always giving me advice and support. I love you with all my heart.

Big thanks go to my mentors Dr. Michael Heinzmann and Constantin Pelka. Michael taught me very early on that you have to go your own way, because what is common is rarely also the right thing to do. I thank him for being a faithful companion to me since school days, with an open mind and more than good advice. Constantin gave me exactly the right push in exactly the right direction at exactly the right moment. Thanks to him, I have a professional future that I look forward to, a network that makes me feel more than comfortable, and a flock of chickens that gives me a lot of pleasure. In this context, I would also like to express my heartfelt thanks to all my companions from SEA - you are a constant inspiration to me!

The reason I wanted to become a scientist is because of my fascination with the great unsolved mysteries. I therefore thank my idols Prof. Dr. Stephen Hawking for his talent in narrating physics in such a captivating way that I devoured all his books. A big thank you also goes to Sir Dr. Ken Robinson, who introduced me to the innovative and creative side of science and showed me what real talent is. Another great inspiration is Dr. Jane Goodall, who as a woman asserted herself in a real man's world and never made a monkey of herself. Last but not least, I would like to thank Rüdiger Nehberg for his unconventional, impetuous adventurous spirit and his unbroken will to do his own thing, unimpressed by everything, and to achieve great things as an individual.

The time in the lab was educational in many ways and it would have been only half as valuable without my wonderful colleagues and friends. I thank Julia for inspiring lunches, Mel M for sporty breaks in the forest, Manali, Inga and Şebnem for our crazy wedding connection that took us all the way to India, Ahmed and Roberto for the thousands of times they made me laugh, Kerstin and Renuka for Ayurvedic advice, Mel B for “Kranführer Ronny” and the latest shit, Tamy for just about everything, Carina for a perfect haircut, Tim for cookie cutters and cat tips, and Benia for bringing punk to the lab. Furthermore, my thanks go to Li, Petra, Lorenz, Susi, Carsten, Moritz, Tsong, Daniel and Steffen. You all rock! A very big thank you also goes to the LSM Graduate School, Francisca, Nadine, all LSM students and the wonderful LSM student council. I have benefited greatly from being part of this community and I’ll miss all of you.

Thanks also to Bettina and Henning as well as to Chris for experimental tips and hacks. Last but not least, I would like to thank Serena for her support and advice, and Prof. Soll for giving me the opportunity to do a PhD in his lab.